NOTICE

The quality of this microform is heavily dependent upon the quality of the original thesis submitted for microfilming. Every effort has been made to ensure the highest quality of reproduction possible.

If pages are missing, contact the university which granted the degree.

Some pages may have indistinct print especially if the original pages were typed with a poor typewriter ribbon or if the university sent us an inferior photocopy.

Reproduction in full or in part of this microform is governed by the Canadian Copyright Act, R.S.C. 1970, c. C-30, and subsequent amendments.

AVIS

La qualité de cette microforme dépend grandement de la qualité de la thèse soumise au microfilmage. Nous avons tout fait pour assurer une qualité supérieure de reproduction.

S'il manque des pages, veuillez communiquer avec l'université qui a conféré le grade.

La qualité d'impression de certaines pages peut laisser à désirer, surtout si les pages originales ont été dactylographiées à l'aide d'un ruban usé ou si l'université nous a fait parvenir une photocopie de qualité inférieure.

La reproduction, même partielle, de cette microforme est soumise à la Loi canadienne sur le droit d'auteur, SRC 1970, c. C-30, et ses amendements subséquents.

Temperature Dependent Transport Properties of $AlCl_3$ in $SOCl_2$ Solutions - A Non-Aqueous Battery Electrolyte Study

Wendy Pell

A thesis submitted to the School of Graduate Studies and Research in partial fulfilment of the requirements for the degree of Master of Applied Science in the Department of Chemical Engineering University of Ottawa

ISBN 0-315-68054-7

UNIVERSITÉ D'OTTAWA
UNIVERSITY OF OTTAWA

Abstract

This thesis is a physical chemical study of the $AlCl_3/SOCl_2$ system, components of the electrolyte used in $Li/SOCl_2$ batteries. Conductivity, viscosity, and density were determined for $AlCl_3$ concentrations ranging from 0 to 35 weight percent in $SOCl_2$, and over the temperature range -35 to 20°C. The measured conductivity was in the μScm^{-1} range, indicating the solution to be a weak electrolyte. Viscosities ranging from 0.7 cP for pure $SOCl_2$, to 3.0 cP for 4.0M $AlCl_3$ were found, with viscosity increasing with increasing salt concentration. The viscosities were characteristic of molecular liquids. The solution densities for all concentrations considered were approximately 1.7g/ml, and thermal expansivity, α_{TE}, was approximately $1000°K^{-1}$, (5 times greater than α_{TE} of water).

Continuum solvent model theories were found to be inadequate for the concentrated solutions studied due to the high concentration, and incomplete dissociation of the $AlCl_3$ salt. The Batschinski - Hildebrand analysis of viscosity for both pure $SOCl_2$, and the $AlCl_3/SOCl_2$ solutions, indicating that these molecular liquids contain a variety of complexes over the temperature range considered. These molecular complexes exist in equilibrium with dissociation products which account for the solution conductivity.

Experimental results indicate that no abrupt change in the distribution of species in solution occurs, either as a function of solute concentration or temperature. The physical

properties of these solutions were observed to change gradually and smoothly with both solute concentration and temperature indicating that a mechanistic change in the $Li/SOCl_2$ cell operation does not likely occur as a result of changes in bulk electrolyte properties. However, the solutions studied did not contain LiCl, cell reaction products such as SO_2 or S, or proprietary electrolyte additives, making the above conclusion tentative.

Acknowledgements

I would like to thank my supervisor, Dr. W.A. Adams for his input to this project. The support and help of the staff at ESTCO is gratefully acknowledged. To my friends at the University of Ottawa, the members of Team RALOS, thanks for occupying my spare time.

I would also like to acknowledge Keith and the boys, who helped to keep everything in perspective.

Financial support from the School of Graduate Studies, the Faculty of Engineering, and NSERC is gratefully acknowledged.

Glossary of Symbols

A_{Eac}, K Constants in the energy of activation of conductivity analysis

A_{JD} Jones-Dole ion - ion interaction parameter $(moles/l)^{-0.5}$

A_{WS} Wishaw - Stokes fitting parameter

$A_{A\eta}$ Walden analysis constant

å Ionic diameter (m)

B Wishaw - Stokes parameter

B_1 Wishaw - Stokes parameter

B_2 Wishaw - Stokes parameter

B_B Batschinski analysis constant (g/ml cP)

B_{BH} Batschinski - Hildebrand constant $(cP)^{-1}$

B_{JD} Jones - Dole ion - solvent parameter $(moles/l)^{-1}$

B_{WS} Wishaw - Stokes fitting parameter

b Intercept of a linear equation

b' Batschinski analysis constant (ml/g)

b_{OL} Empirical parameter added to improve Debye - Hückel model for conductivity

C_n Rated capacity of a battery (Ah)

C_{WS} Wishaw - Stokes fitting parameter

c Concentration (moles/l)

$c_{w/w}$ Concentration (weight percent $AlCl_3$)

c_o, c_1, c_3,..c_n Coefficients of an nth order polynomial

D_{JD} Jones - Dole higher order interaction parameter $(moles/l)^{-2}$

E_{ac} The energy of activation of conductivity (kcal/mole)

E_{av} The energy of activation of viscosity (kcal/mole)

E_{FO} Fuoss - Onsager parameter

Err^2 Sum of the squared residuals

E_x, E Magnitude of an electric field (V)

e Unit charge (C)

F Wishaw - Stokes parameter

f Mean activity coefficient

$G(x_i)$ Function of the independent variable x

ΔG^* Free energy of activation (kcal/mole)

ΔH^* Enthalpy of activation (kcal/mole)

h Planck's constant

J_{FO} Fuoss - Onsager parameter

K_A Thermodynamic association parameter

L_D Debye length (m)

m Slope of a linear equation

N Avogadro's number (molecules/mole)

N_I Number of ions

n Number of data points to be fit to an equation

n_w Constant determining the deviation from Walden's Rule

P Pressure (atm)

R The gas constant (mole/kcal K)

R^2 Square of the multiple correlation coefficients

Res^2 Sum of the squares of the deviation from the mean of the dependent variable

ΔS^* Entropy of activation (kcal/mole K)

Sig Significance of fit parameter

T Temperature (°K, °C)

u Net ionic velocity (m/s)

u_1 Velocity of an ion in an electric field (m/s)

u_2 Retardation of the velocity of an ion due to the electrophoretic effect (m/s)

V_c Cut-off voltage below which a battery is no longer useful (V).

v Specific volume (ml/g)

v_m Molar volume (ml/mole)

v_o Intrinsic volume, the specific volume a substance in the solid state would have provided that on solidification the molecules preserved all of their degrees of freedom (ml/g)

x, x_i Independent variable

y, y_i Dependent variable

z_i Charge of an ion

α Degree of dissociation

α_{TE} Coefficient of thermal expansivity $(K)^{-1}$

ϵ Dielectric constant

η Solution viscosity (cP)

η_o Solvent viscosity (cP)

η_r Reduced viscosity (η/η_o)

η_* Increment in viscosity associated with coulombic interactions (cP)

η_e Increment in viscosity associated with the size and shape of the ion (cP)

η_a Increment in viscosity associated with molecular alignment (cP)

η_d Increment in viscosity associated with the distortion of the liquid structure (cP)

η_B Increment in viscosity due to the solvent - ion effect (cP)

Θ Debye - Hückel time of relaxation parameter

κ Electrolytic conductivity (S/cm)

Λ Molar conductivity (S cm^2/mole)

Λ_o Molar conductivity at infinite dilution (S cm^2/mole)

λ_o^+, λ_o^- Limiting ionic conductivities (S cm^2/mole)

ρ density (g/ml)

σ Debye - Hückel electrophoretic effect parameter

σ_v^2 variance of a fitted model

ϕ Fluidity ($1/\eta$), $(cP)^{-1}$

Table of Contents

Abstract	i
Acknowledgement	iii
Glossary of Symbols	iv
Table of Contents	viii
List of Tables	xi
List of Figures	xiii
1.0 Introduction	1
1.1 Scope of the Research	1
1.2 Literature Survey	8
2.0 Methodology	15
2.1 Theory of Viscosity	15
2.1.1 Jones - Dole Analysis	15
2.1.2 Energy of Activation Analysis	21
2.1.3 Batschinski - Hildebrand Analysis	25
2.2 Electrolytic Conductance Theory	27
2.2.1 Wishaw Stokes Theory of Conductivity	33
2.3 Method of Data Analysis	36
3.0 Properties of the Materials	40
3.1 Thionyl Chloride	40
3.2 Aluminum Trichloride	41
3.3 The Electrolyte	43
4.0 Experimental	45
4.1 General Techniques	45

4.0 Experimental con't

4.2 Reagent Purification 45

4.2.1 Thionyl Chloride 45

4.2.2 Aluminum Trichloride 46

4.3 Sample Preparation: $AlCl_3/SOCl_2$ 48

4.4 Electrical Conductivity Measurements 50

4.5 Density Measurements 52

4.6 Viscosity Measurements 54

5.0 Results and Discussion 57

5.1 Solution Density 57

5.1.1 Thermal Expansivity 62

5.2 Viscosity Analysis 67

5.2.1 Jones - Dole Analysis of Viscosity 73

5.2.2 Energy of Activation Analysis for Viscosity 83

5.2.3 Batschinski - Hildebrand Analysis of Viscosity 87

5.3 Electrolytic Conductivity 95

5.3.1 Energy of Activation Analysis for Conductivity 106

5.3.2 Wishaw - Stokes Analysis 116

5.4 Solution Composition 122

6.0 Conclusions 128

7.0 Recommendations and Future Research 132

8.0 References 133

Appendices

Appendix A: Theoretical Energy Density 142

Appendix B: Density, Viscosity, and Conductivity Raw Data 143

Appendix C: Raman Spectra of $AlCl_3/SOCl_2$ 146

Appendix D: Glossary of Battery Terminology 151

Appendix E: Abstracts of Work Presented 1988 -1990 153

Appendix F: Error Calculation 157

List of Tables

5.1 Density data fitted to first order polynomial equation, coefficients and fitting parameters as a function of temperature 57

5.2 Density of $SOCl_2$ - $AlCl_3$ solutions and several other compounds 60

5.3 Polynomial fit coefficients and goodness of fit parameters for lnρ vs T. Results used to evaluate coefficient of thermal expansivity 64

5.4 Coefficient of thermal expansivity as a function of the degree of the polynomial expression describing lnρ, and temperature 65

5.5 Second order polynomial fit coefficients and goodness of fit parameters for viscosity as a function of $AlCl_3$ concentration 69

5.6 Viscosity of several solutions as a function of temperature 70

5.7 Viscosity of several solutions as a function of solute concentration at 20°C 71

5.8 Jones - Dole constants and fitting parameters for $AlCl_3$ - $SOCl_2$ solutions over the concentration range 0 to 4.0M, and temperature range -20 to 20°C 75

5.9 Modified Jones - Dole constants and fitting parameters for $AlCl_3$ - $SOCl_2$ 80

5.10 Constants and fitting parameters for the empirical energy of activation of viscosity 86

equation

5.11 Batschinski - Hildebrand coefficients and goodness of fit parameters for the $AlCl_3$ - $SOCl_2$ system as a function of concentration 92

5.12 Fitting constants and parameters for electrolytic conductivity plotted as a function of concentration 97

5.13 Fitting parameters and coefficients for linear plots of $\ln\Lambda$ vs 1/T for $AlCl_3$ concentration ranging from 1.0 to 4.0M 109

5.14 Energy of activation for conductance for various solutions 111

5.15 Constants and fitting parameters for $\ln\eta$ expressed as a function of $\ln\Lambda$ 115

5.16 Best-fit parameters and coefficients obtained for the Wishaw - Stokes analysis of conductivity 119

5.17 Degree of dissociation, α, as a function of temperature 120

5.18 Possible conductive species in $AlCl_3$ - $SOCl_2$ solutions 127

List of Figures

3.1	Proposed structure of liquid $SOCl_2$ based on molecular orbital calculations	42
3.2	Proposed structure of $AlCl_3$ - $SOCl_2$ compounds based on molecular orbital calculations	44
4.1	Vacuum distillation apparatus	47
4.2	Sublimation apparatus	49
4.3	Electrolytic conductivity cell	51
4.4	Density cell	53
4.5	Modified Ostwald viscometer	55
5.1	Density of $AlCl_3/SOCl_2$ solutions as a function of $AlCl_3$ concentration	58
5.2	Viscosity of $AlCl_3$ solutions as a function of percent weight $AlCl_3$	68
5.3	Jones - Dole plot for $AlCl_3$ in $SOCl_2$	74
5.4	$Ln\eta$ vs 1/T for solutions of0 to 4.5M $AlCl_3$ in $SOCl_2$	84
5.5	Energy of activation of viscosity as a function of $AlCl_3$ concentration	85
5.6	Fluidity vs specific volume	89
5.7	Intrinsic volume plotted as a function of $AlCl_3$ concentration	90
5.8	The Batschinski - Hildebrand parameter, B_{BH}, plotted as a function of $AlCl_3$ concentration	91
5.9	Electrolytic conductivity as a function of concentration	96
5.10	Electrolytic conductivity vs concentration	99

for $AlCl_3$ in $SOCl_2$

5.11 Molar conductivity shown as a function of $\sqrt{c}$ for both weak and strong electrolytes 102

5.12 Experimental molar conductivity as a function of $\sqrt{c}$ 104

5.13 Molar conductivity reported from literature as a function of $\sqrt{c}$ 105

5.14 Molar conductivity over concentration range 5×10^{-4} to 4.0M $AlCl_3$ in $SOCl_2$ at 25°C 107

5.15 Energy of activation for conductivity as a function of concentration 110

5.16 $\ln\eta$ plotted as a function of $\ln\Lambda$ 114

5.17 Wishaw - Stokes plot of $\Lambda(\eta/\eta_o)$ as a function of $\sqrt{c}$ for solutions of $AlCl_3$ in $SOCl_2$ 117

1.0 Introduction

1.1 Scope of the Research

Over the past twenty-five years, research into the use of lithium based batteries has flourished as a result of an increasing demand for light-weight, high-performance batteries. Lithium metal is an attractive anode material due to its light weight, high voltage, high electrochemical equivalence (high coulombic output for a given weight of material), ready availability due to high natural abundance, and good conductivity. Since metallic lithium reacts vigorously with water, oxygen and nitrogen, lithium batteries require non-aqueous chemistry, and manufacturing of practical devices, therefore, presents special challenges compared to aqueous based batteries. Other advantages associated with lithium batteries include:

1) High voltage: The voltage of lithium cells varies from 1.5 to 3.9 V depending on the cathode material used. A high cell voltage is an advantage as it can reduce the number of cells required in a battery pack.

2) High energy density: Energy density is defined as the amount of stored electrical energy per unit mass or volume that the system can produce. Obviously, high energy density is preferred. The practical energy density of lithium cells can be as high as 400 to 500 Wh/kg (800 to 900 Wh/l), approximately two to four times better than that of conventional batteries.

3) Operation over a wide temperature range: Lithium cells

are, in general, non-aqueous and as a result can exhibit good performance over a wide temperature range (70 to -40°C). This is an important characteristic as many applications demand reliable non-ambient performance.

4) Good power density: Certain applications demand the delivery of high power. Lithium batteries can be designed with this aspect in mind and are capable of delivering the energy at high current or power.

5) Flat discharge characteristic: Lithium cells can be designed to deliver energy with a flat discharge profile (ie. constant voltage and impedance through most of the discharge cycle). This characteristic is favoured as it ensures that a high percentage of the energy stored in the battery is recoverable. That is, a battery must be capable of delivering current above a certain cut-off voltage, V_c. Should the battery voltage drop below V_c, the energy remaining within the battery is not available to power the application, and is wasted. Lithium batteries are capable of delivering current above the specified cut-off voltage over most of the discharge cycle, so that there is high utilization of the active electrode material. Some lithium cell chemistry involving intercalation does have a sloping voltage discharge profile, eg. Li_xTiS_2 or Li_xMoS_2 cathodes.

6) Superior shelf-life: A requirement of a successful battery is that it remain "charged" even after storage for considerable time. Lithium cells can be stored for long periods

of time even at high temperatures. To date, lithium cells have been stored for up to 5 years at 20°C, and 1 year at 70°C. A ten year storage period at room temperature is projected for the future performance of this battery (Linden, 1984). Implanted pacemaker batteries based on Li/I_2 chemistry can operate for up to 15 years at 37°C (Owens, 1986).

The lithium/thionyl chloride ($Li/SOCl_2$) cell has one of the highest specific energies of any developed primary (non-rechargeable) battery with a theoretical specific energy of 1480 Wh/kg. (Blomgren, 1989; Vallin and Broussely, 1989; Hills and Hampson, 1988). As a result it has been subject to considerable study. Large capacity, low rate (low power) cells have been built that can deliver a practical specific energy of 500 Wh/kg (900 Wh/l), which is 34% of the theoretical specific energy (Linden, 1984). The system has an open circuit voltage of 3.66 V and typically operates in the 3.3 to 3.5 V range. The cut-off voltage is 3.0 V. $Li/SOCl_2$ batteries perform well over a wide temperature range (-40 to 80°C) and are still functional at temperatures as high as 145°C. The maximum operating temperature possible is 186°C, the temperature at which lithium melts (Linden, 1984). The efficiency at low temperatures is somewhat reduced and has been the subject of some investigations (Sibbald, et.al., 1990). In general, these cells are used in low to moderate rate discharges. Discharge and charge rates are generally expressed in terms of capacity, C_n. Batteries are generally designed in terms of a "rated"

capacity, ie. C_{10} = 5 Ah may be interpreted that the cell is capable of delivering 0.5A for 10 h. A cell will not always be operated at the specified rate. Discharges at lower current (lower rate) than is specified will generally take a longer time than that specified, ie. if the battery specified by C_{10} = 5 Ah were discharged at 0.25 A, the discharge period would likely be longer than 20 h. A low rate discharge is < C/3, medium rate, from C/3 to C, and high rate > C. High rate discharges, that is discharges above the rated current, have led to problems that will be discussed in subsequent sections of this thesis. The discharge curve is characteristically flat over the temperature range of operation.

The shelf-life of the $Li/SOCl_2$ cell is quite good; after 3 year storage at 20°C, a loss in capacity of approximately 1 to 2 percent per year could be expected (Linden, 1984). Storage at 70°C leads to a much greater loss in capacity, 30 % in the first year, with smaller losses in subsequent years.

The lithium/thionyl chloride cell consists of a lithium anode, an inert carbon cathode and a non-aqueous electrolyte. Various mechanical designs of $Li/SOCl_2$ cells are in production, including spirally wound ("jelly-roll"), bobbin cells and prismatic cells (Linden, 1984). The electrolyte is composed of thionyl chloride, ($SOCl_2$), lithium chloride, (LiCl), and aluminum trichloride, ($AlCl_3$). Commercial cells also include proprietary additives to improve cell performance. Additives

such as polyvinyl chloride for control of voltage delay, methylethylimidizolium chloride and others were recently discussed by Blomgren and coworkers (1990), and Johnson and Dawson (1990). $SOCl_2$ is both the liquid electrolyte and the active cathode material - the material that undergoes reduction upon the discharge of the battery. As $SOCl_2$ has a very low conductivity, it is necessary to add conductive salts to facilitate Li^+ ion transport. Typically $LiAlCl_4$ (LiCl and $AlCl_3$) is used, both because it is readily soluble in $SOCl_2$, and because it is relatively inexpensive.

The generally accepted reaction occurring in the battery, initially proposed by Gabano in the early 1970's, is:

$$4Li + 2SOCl_2 \rightarrow 4LiCl + S + SO_2 \qquad (1.1)$$

Early studies of this system failed to detect SO_2 in the discharged cell. As a result several, other mechanisms have been proposed including:

$$8Li + 4SOCl_2 \rightarrow 2S + Li_2SO_3 + 6LiCl \qquad (1.2)$$

presented by Auborn et.al. in 1973; and

$$8Li + 4SOCl_2 \rightarrow Li_2S_2O_4 + 6LiCl + S_2Cl_2 \qquad (1.3)$$

presented by Behl et.al. in 1973.

In 1974, Dey and Schlaikjer found infra red spectroscopic evidence of SO_2 in discharged $SOCl_2$ cells, thus discounting the mechanisms proposed by Auborn and coworkers (1973) and Behl and coworkers (1973) (Hills and Hampson, 1988). The actual cell reaction mechanism is believed to be rather complex. It was proposed by Dey in 1976, that the reaction shown in Equation (1.1) occurred via an unstable biradical mechanism in which SO disproportionates to form SO_2 and elemental sulphur. Unfortunately, SO_2 has been detected only at a fraction of the amount predicted by the above discharge reaction. It is now believed that much of the SO_2 is complexed in the electrolyte and it is accepted that the above reaction mechanism does occur over a broad temperature range and over extended depths and rates of discharge. Researchers have unsuccessfully attempted to identify the SO radical species, and theorized that it is a very short lived species (Auborn and Venkatasetty, 1984).

There have been several problems associated with this battery that warrant investigation. The battery capacity at low temperature is somewhat reduced from ambient performance, and as a result 'low' temperature investigations are required. The cell is characterized by a voltage delay phenomenon that is most pronounced during low temperature discharge, after high temperature storage. Cell voltage, at the start of discharge, is lower than expected, and increases slowly with time to the operating voltage. This effect is attributed to the formation of a passivating film at the anode. Material purity was seen to

be a contributing factor to the voltage delay problem. Furthermore, capacity loss at low temperatures after long-term storage at room temperature has been observed (Hills and Hampson, 1988).

Safety has been another aspect of $Li/SOCl_2$ battery design that has received much attention. Cells have been know to vent or explode when subjected to over-discharge or polarity reversal, particularly at low temperatures (below -20°C) (Hills and Hampson, 1988; Auborn and Venkatasetty, 1984). As well, cells have been known to explode or to vent and evolve noxious gases during warm up following low temperature discharge (Donaldson et.al., 1989).

To help solve the problems associated with this system, a more complete understanding of the battery discharge mechanism is required. The battery performance is highly dependent on the electrolyte composition. As a result, more information on the dependence of electrolyte composition on temperature and solute concentration is required. Once a clear understanding of the function and action of all cell components is achieved, improved performance and safety under all conditions will be possible.

The $LiAlCl_4/SOCl_2$ solution is very complex, characterized by the presence of molecular solvent-solute and solvent-solvent interactions, the presence of both LiCl and $AlCl_3$ salts as well as $LiAlCl_4$ in solution, and the presence of ions associated with the above species. This project undertakes to examine the

solution properties of $AlCl_3$ in $SOCl_2$. A study of density, viscosity, and conductivity as a function of both temperature and salt concentration was performed to determine composition dependence of the solution composition. A study of this relatively simple system can lead to a better understanding of the more complex $LiAlCl_4$ solution. By determining the species present in these solutions, and studying the anodic and cathodic reactions one can then interpret the system performance, and hopefully incorporate design changes in practical $Li/SOCl_2$ cells, to improve performance.

1.2 Literature Survey

As stated previously, extensive research on lithium batteries has been conducted over the last 25 years. The use of $SOCl_2$ as a solvent for a lithium battery was patented by Gabano (1969; 1971). Today, nearly every aspect of the $Li/SOCl_2$ cell construction has been considered with various degrees of thoroughness. Several current reviews are available which describe the status of research today (Auborn and Venkatasetty, 1984; Hills and Hampson, 1988; Blomgren, 1989). These articles clearly review the status of each aspect of the cell design. In this literature survey, emphasis will be placed on the low temperature chemistry of the $Li/SOCl_2$ cell with special emphasis on solute properties.

Analysis of both cell components and commercial cells has been undertaken in order to determine safety and performance

characteristics, and also to understand the fundamental chemistry occurring within the cell. Recent analysis of commercial cell performance included low temperature testing (-40°C) of several manufacturers' "D" sized cylindrical cells by Subbarao et.al. (1989), under constant current and constant load conditions. They found the cells exhibited low operating voltage, poor voltage regulation and low capacity at this temperature and reported that cells containing a proprietary catalyst on the cathode, exhibited considerable voltage delay, poor shelf life and no meaningful capacity at -40°C. They found that cells subjected to prolonged voltage reversal were potentially hazardous, and that explosions or cell ventings could occur. Furthermore, cell performance and safety were observed to be a function of the mechanical design of the cell.

Spirally wound "C" and "D" sized cells were tested by Vallin and Broussely (1989). The SAFT cells tested were found to be safe provided normal operating conditions were followed. Cell charging, an abnormal procedure in a non-rechargeable cell, that can, however, occur in a multi-cell battery if the cells have mismatched capacity and cell reversal occurs, was found to be potentially hazardous, especially in the case of partially discharged cells.

Fundamental thermodynamic parameters of commercial (SAFT) "D" sized cells were obtained over temperatures ranging form -10 to 35°C by Bittner et.al.(1989). They obtained the reversible cell potential, E_r, and the temperature dependence

of the reversible cell potential over the above temperature range. The reversible cell potential was found to increase linearly with decreasing temperature over the range considered. No explanation of the increasing cell potential was given.

Researchers at the Electrochemical Science and Technology Centre at the University of Ottawa have also analyzed the thermodynamic properties of commercial "D" sized cells over an extended temperature range (35 to -40°C) (Sibbald et.al., 1990). Using microcalorimetric techniques, the entropy change, ΔS, associated with cell discharge, was calculated from the heat flux for discharge under different resistive loads. The ΔS values exhibited considerable scatter but appeared to be constant from -25 to 25°C (-16.8 ± 1.7 cal/k-eq.). Studies at -40°C consistently produced a lower value of ΔS (approximately -27 cal/k-eq.), indicating that low rate discharge of "D" sized cells may show a change in the reaction mechanism between -25 and -40°C. Further investigation of this region is warranted.

This project is concerned with the solution properties of the $AlCl_3/SOCl_2$ electrolyte. Numerous studies have been published looking at thermodynamic, physical and electrical properties of this system. Interest in pure thionyl chloride has been a concern for a number of years as it is used in the preparation of anhydrous metal chlorides, acyl chlorides, alkyl chlorides and as a reaction medium, as well as in batteries. Solvent purification via distillation was proposed by Friedman and Wetter in 1967.

The early studies of the electrolyte, $AlCl_3$ in $SOCl_2$, were conducted by Long and Bailey in 1963, and Spandau and Brunneck in the early 1950's.(Spandau and Brunneck, 1952; 1955). Concentrations of $AlCl_3$ ranging from 0.1M to 0.75M were studied at room temperature. It was concluded that the main species present was a 1:1 complex of $SOCl_2$ and $AlCl_3$, which was substantially undissociated. Complexation was proposed to occur through the sulphur and oxygen atoms. A quasi or weakly bonded 1:2 adduct was also identified, and is believed to be similar to the 1:1 species, with a second $AlCl_3$ molecule loosely associated.

Interest in the structure of the $SOCl_2$ electrolyte resumed in the 1980's when it was identified as a practical electrolyte for high energy density lithium batteries. In 1981, Salomon published an article reporting the conductivity of $LiAlCl_4$ in $SOCl_2$ at low concentration (between 0.01 and 1.0×10^{-5} mole/l) and ambient temperature (25°C). He also considered the $AlCl_3/SOCl_2$ system independently. He assumed a simple dissociation mechanism for $AlCl_3$ in $SOCl_2$:

$$AlCl_3 + SOCl_2 = SOCl^+ + AlCl_4^- \qquad (1.4)$$

An analysis using Fuoss - Onsager equations was unsuccessful, thus indicating that the distribution of $AlCl_3$ in $SOCl_2$ is much more complex than described by the above equation, even at low concentration. Salomon (1981) concluded that both $AlCl_3$ and

$LiAlCl_4$ in $SOCl_2$ are associated species.

Venkatasetty and Saathoff also published a $LiAlCl_4/SOCl_2$ study in 1981. They studied the $LiAlCl_4/SOCl_2$ system over a concentration range of $3x10^{-4}$M to 2.0M at room temperature. They noted a conductance maximum at 1.8M, and a maximum in equivalent conductance at 0.8M indicating that the solute was weakly dissociated. This behaviour is also characteristic of a low dielectric solvent, $SOCl_2$ has a dielectric constant, ϵ, of 9.25 at 20°C (CRC, E50, 1983-84). Low concentration data were analyzed using the Fuoss-Shedlovsky equation (0.0003 to 0.005M). Fuoss-Krauss analysis was applied to the mid-range conductivity data (0.005 to 0.5M). High concentration data was not analyzed. Viscosity data was analyzed over the entire concentration range via the Jones-Dole, and Energy of Activation theories. The authors concluded that $LiAlCl_4$ in $SOCl_2$ is highly associated, and that the electrolyte can affect mass transport and charge transfer processes during discharge. They found voltammetric evidence of sulfur chlorides and chlorine during discharge. The presence of these compounds was not explained with respect to the generally accepted cell reaction (Equation (1.1)). The authors made no attempt to study the properties of the $AlCl_3/SOCl_2$ solution independently.

A detailed presentation of density, viscosity, and conductivity data of solutions of $AlCl_3$ and $LiAlCl_4$ in $SOCl_2$ with and without the presence of S and SO_2 was published in 1983 by Venkatasetty and Szpak. No analysis of this data was

presented by the authors.

The solution of $LiAlCl_4$ in $SOCl_2$ was further studied by Raman spectroscopy in 1983. Bedford, Corset, Dhamelincourt, Wallant, and Barbier (1983) found evidence of $[Li(SOCl_2)_2]^+[AlCl_4]^-$ ions in solutions of $LiAlCl_4$ in $SOCl_2$, at room temperature. In mixed solvent systems (ie. in the presence of SO_2, a discharge product of the $Li/SOCl_2$) the $[Li(SO_2,SOCl_2]^+[AlCl_4]^-$ ionic species was also identified at room temperature. Again the simplified $AlCl_3/SOCl_2$ system was not studied independently.

Szpak and Venkatasetty (1984) published the transport properties of aluminum chloride - thionyl chloride based electrolytes in 1984. They analyzed the viscosity and conductance data from 1.5 to 4.5 M and -10 to 70°C, (for viscosity), and 0 to 50°C, (for conductivity), using the Jones-Dole, Batschinski-Hildebrand and Energy of Activation methods. They found that conductivity and viscosity were affected by structural changes, and concluded that adduct formation occurred at high solute concentration. Addition of LiCl increased the solution conductivity due to the formation of ion pairs, triple ions, and molecular aggregates. Viscosity analysis characterized the $AlCl_3/SOCl_2$ as a molecular liquid. The temperature effects were not discussed in this paper.

Conductivity of the $LiAlCl_4$ solution over extended concentration (0 to 5 M) and temperature (-20 to 70°C) ranges were studied by Berg, Hjuler, Søndergaard and Bjerrum in 1989.

They calculated a conductivity, temperature, solute concentration surface from the experimental data. They determined that the conductivity maximum was a function of temperature, and that it occurred at lower concentrations for lower temperatures. This group did not consider the $AlCl_3/SOCl_2$ solution and did not analyze the data obtained for the other system in detail.

Room temperature Raman spectra were obtained for $AlCl_3$, and $LiAlCl_4$ - $SOCl_2$ solutions by Mosier-Boss, Szpak, Smith and Nowak in 1989. They identified $SOCl_2$ as a molecular liquid and identified the $SOCl_2$ dimer to be an open chain species, associated through the sulphur and oxygen atoms. Addition of Al_2Cl_6 forms $Cl_3Al{\leftarrow}OSCl_2$, a highly associated molecular species. At high concentration this associated molecular adduct dissociates to form $[Cl_2Al(\leftarrow OSCl_2)_2]^+$ and $AlCl_4^-$. Addition of LiCl destroys the $Cl_3Al{\leftarrow}OSCl_2$ species and results in the formation of $Li(\leftarrow OSCl_2)_2^+$ and $AlCl_4^-$ species.

Although much work has been done on this system, a systematic study, from the perspective of the $Li/SOCl_2$ battery, is needed. Our study involves the experimental determination of density, viscosity and conductivity, over a wide range of temperatures and concentrations, and the analysis of the results using current theories of concentrated electrolyte solutions.

2.0 Methodology

Electrolytic solutions containing solute concentrations greater than approximately 0.5 M are considered to be concentrated. Under these conditions the many theories of dilute electrolyte solution behaviour based on solvent continuum models are not valid. A satisfactory fundamental theory, predicting the physical properties of concentrated solutions, has not been developed. As a result, several empirical methods of analysis were employed to interpret the experimental viscosity and conductivity data. The theories applied to the experimental data are outlined below.

2.1 Theory of Viscosity

2.1.1 Jones-Dole Analysis of Viscosity

Viscosities of electrolyte solutions have been studied for many years (Hildebrand, 1971, 1978, Desnoyers and Perron, 1972; Crudden et.al., 1986; Kacperska, et.al., 1989). In the early part of the century Grüneisen found that the viscosity of very dilute solutions was not linear with concentration. It exhibited a curvature that is now termed the Grüneisen effect. In 1929, Jones and Dole formulated an empirical equation that is the basis for many viscosity analyses today (Robinson and Stokes, 1965).

$$\frac{\eta}{\eta_o} = \eta_r = 1 + A_{JD}\sqrt{C} + B_{JD}C \qquad (2.1)$$

where,

η is the solution viscosity
η_o is the solvent viscosity
η_r is the reduced viscosity, η/η_o
c is the concentration (moles/l)
A_{JD}, B_{JD} are constants

At very low concentration, the second term of Equation (2.1), ($A_{JD}\sqrt{c}$), is the dominant factor governing viscosity - this factor describes the Grüneisen effect. As the solute concentration increases the third term in Equation (2.1), ($B_{JD}c$), gains dominance.

Jones and Dole analyzed this equation in terms of the continuum solvent model of solutions. This model assumes that the solute is in low concentration such that the environment experienced by a solute molecule appears as a continuum of solvent molecules. Based upon this model, Jones and Dole attributed the square root concentration dependence on long-range coulombic forces acting between ions. The coefficient A_{JD} has been calculated theoretically from interionic attraction theory and is dependent on solvent properties, ionic charges and mobilities and on temperature. For uni-univalent electrolytes the Falkenhagen equation may be used to calculate A_{JD} (Kacperska, et.al., 1989; Crudden, et.al., 1986). The Falkenhagen equation is:

$$A_{JD}=\frac{0.2577\Lambda_o}{\eta_o(\epsilon T)^{0.5}\lambda_o^+\lambda_o^-}\left[1-0.6863\left(\frac{\lambda_o^+-\lambda_o^-}{\Lambda_o}\right)^2\right] \qquad (2.2)$$

where,

Λ_o is the molar electrolytic conductivity of the solvent
λ_o^+, λ_o^- are the ionic mobilities
ϵ is the dielectric constant
T is temperature in Kelvin
η_o is the viscosity of the solvent

A_{JD} can also be calculated for non uni-univalent electrolytes, but the resulting equation is necessarily more complicated. As coefficient A_{JD} is evaluated, in this study, from experimental data only it is beyond the scope of this thesis to discuss the theoretical derivation of A_{JD}, the ion-ion parameter, for more complicated electrolyte solutions.

At higher concentrations (>0.002 M and <0.01 M) a linear variation of viscosity with concentration is observed by strong electrolyte solutions. In this region the third term, ($B_{JD}c$), of the Jones-Dole equation, (Equation (2.2)), is dominant. The B_{JD} coefficient of the Jones-Dole equation is determined empirically, and is governed by ion-solvent interactions. Negative B_{JD} coefficients are generally confined to highly associated solvents at low temperatures, and are related to the disturbance of structure which is present in liquids under these conditions. In aqueous solutions there is evidence that the net B_{JD} value (the B_{JD} value of the solution) is the result of ionic contributions. That is, B_{JD} values for pairs of salts

having the same anion and different cations, have constant differences. The division into ionic B_{JD} values has not been attempted for non-aqueous solvents.

Viscosity effects in solution may be attributed to several terms,

$$\eta=\eta_o+\eta_*+\eta_e+\eta_a+\eta_d \qquad (2.3)$$

where,

η is the solution viscosity.

η_o is the solvent viscosity.

η_* is the increment in viscosity associated with coulombic interactions.

η_e is the increment in viscosity associated with the size and shape of the ion.

η_a is the increment in viscosity associated with molecular. alignment.

η_d is the increment in viscosity associated with distortion of the liquid structure.

η_*, the increment in viscosity caused by coulombic interactions ($A_{JD}\sqrt{c}$) is positive. η_e is dependent on both the size and the shape of the ions in solution and is, in general, positive, increasing with increasing ion size. η_a is the result of alignment or orientation of polar molecules by the ionic field, and is generally positive. η_d is the result of the distortion of the solvent structure leading to an increase in fluidity, ϕ, (or a decrease in viscosity) and is negative.

In terms of the Jones Dole analysis:

$$\eta_{\bullet}+\eta_{e}+\eta_{a}+\eta_{d}=\eta_{o}(A_{JD}\sqrt{C}+B_{JD}C) \qquad (2.4)$$

or

$$\eta_{\bullet}=\eta_{o}A_{JD}\sqrt{C}, \quad \eta_{e}+\eta_{a}+\eta_{d}=\eta_{o}B_{JD}C$$

where all symbols have the previously described meaning.

As a result, the B_{JD} coefficient is seen to be the result of the competition between the effects of size and shape, alignment or orientation, and solvent distortion. A negative B_{JD} value indicates that the net effect of shape, orientation and distortion is dominated by the solution distortion effects. In general, negative B_{JD} values characterize highly associated species at low temperature. A negative B_{JD} value may also occur in the case where η_e is small (due to a small surface charge density on an ion, for example quaternary ammonium ions), η_a is small (systems with minimal orientation) and η_d is large as the result of distortion in the immediate neighbourhood of the ion due to the competition between ionic field and bulk structure. Examples of such systems are Cs^+ or I^- in water.

A near zero B_{JD} value is characteristic of intermediate sized ions in solutions, where size and orientation effects are of the same magnitude as the solvent distortion effect. An example of this class of system is ammonia in water.

A large positive B_{JD} is a characteristic of small highly charged cations, such as Li^+, Mg^{++} in aqueous solution. In this

case η_a is large due to the orientation of the water molecules and η_e is large as the charged ion is surrounded by closely bound water molecules. The solution distortion effect, η_d, is small as the hydrated cations are believed to fit well into the tetrahedral water structure. The contribution of each of these effects will be discussed in more detail for the $AlCl_3/SOCl_2$ solutions.

As stated previously, the B_{JD} coefficient is the dominant factor until the solute concentration reaches approximately 0.1M. Above this concentration, viscosity does not show a linear dependence with concentration, and the Jones-Dole equation is generally not valid. As a result, many modifications have been proposed. Many researchers simply add an additional term to the standard Jones Dole equation (Crudden, et.al., 1986; Desnoyers and Perron, 1972):

$$\eta_r = 1 + A_{JD}\sqrt{C} + B_{JD}C + D_{JD}C^2 \qquad (2.5)$$

where,

A_{JD} is the ion - ion interaction parameter
B_{JD} is the ion - solvent interaction parameter
D_{JD} is the higher order interaction parameter

The term D_{JD} is generally positive, and its physical significance is still somewhat obscure. It is believed that this term is related to solute-solute structural interactions (Desnoyers and Perron, 1972). In short, the $D_{JD}C^2$ term of Equation (2.5) must account for all solute - solvent, and

solute - solute interactions that are not included in the A_{JD} and B_{JD} terms of that expression. These interactions include higher order coulombic terms; solute - solvent interactions which are concentration dependent; and higher order solvent - solvent effects. D_{JD} tends to be of the same order of magnitude as A_{JD}. Long-range coulombic forces can be estimated by replacing the standard ionic conductivities in the Falkenhagen equation, Equation (2.2), with actual conductivities at known concentrations. Such a calculation indicates that long-range coulombic forces can contribute significantly to the value of D_{JD}.

At higher solute concentrations, solute - solute interactions are also important. These factors also contribute to the value of D_{JD}. In aqueous solutions, D_{JD} exhibits a strong dependence on the cationic size and is approximately independent of anion size. (Desnoyers and Perron, 1972). Similar studies have not been conducted in non-aqueous solutions. Trends in the value of D_{JD} are often not obvious, indicating that D_{JD} is indeed a mixed parameter and illustrates many effects.

2.1.2 Energy of Activation Analysis

At high concentration, the continuum model of a solute in a solvent is no longer valid. In such a case, data analysis can be carried out by way of the energy of activation of viscosity method (Glasstone, Laidler and Eyring, 1941). The temperature

dependence of viscosity may be used to determine activation energy of viscosity as a function of solute concentration.

In such a case, the Eyring equation may be applied to experimental viscosity data:

$$\eta = \left(\frac{Nh}{v_m}\right)\exp\left(\frac{\Delta G^*}{RT}\right) \qquad (2.6)$$

where,

- η is the solution viscosity
- N is Avogadro's number
- h is Planck's constant
- R is the Gas constant
- T is temperature (Kelvin)
- ΔG^* is the free energy of activation
- v_m is the molar volume

ΔG^* is the minimum value of additional free energy required to bring the system into the intermediate or activated position, at which time viscous flow becomes possible.

This theory is based upon the "hole" concept of solution structure (Frenkel, 1955). In the case of the solid state, the "holes" are defined as those associated with interstices and with vacant sites. In liquids regular vacant sites, and interstices do not exist on the same time scale as in the solid state. Holes, in liquids, can be considered to be more or less widened gaps between molecules in solution. The gaps have neither definite size nor shape, and arise through local fluctuations in molecular kinetic energy. Holes can "move" by disappearing from one site and reappearing at another. It is proposed that molecules in solution jump from one hole to the

next. In formulating this transition, the theory assumes that the molecule must pass through an intermediate or "activated" state of maximum potential. The free energy, described above, corresponds to the smallest amount of work required to make this transition. Substituting,

$$\Delta G^{*}=\Delta H^{*}-T\Delta S^{*} \qquad (2.7)$$

where,

ΔG^{*} is the free energy of activation
ΔH^{*} is the enthalpy of activation
ΔS^{*} is the entropy of activation
T is temperature (Kelvin)

into Equation (2.6) gives,

$$\eta=\left(\frac{Nh}{V_m}\right)\exp\frac{(\Delta H^{*}-T\Delta S^{*})}{RT} \qquad (2.8)$$

which may be reduced to:

$$\eta=A_{Eav}\exp\left(\frac{\Delta H^{*}}{RT}\right)$$

where,

v_m is the molar volume
A_{Eav} is a constant that includes a ΔS^{*} term

Equation (2.8) has the same form as the empirical equation,

$$\eta = A_{Eav} \exp\left(\frac{E_{av}}{RT}\right) \qquad (2.9)$$

where E_{av} is the energy of activation of viscosity.

A_{Eav} is a function of ΔS^*, and indicates an ordering process when molecules pass from an initial to a transition state. The above equations were derived for ideal non - associated liquids and within these restrictions, are in good agreement with experiment (Stokes and Mills, 1965). In associated liquids and solutions containing molecular species, viscous flow involves distortion of liquid structure in addition to that due to normal molecular friction. Structural activation energy is this extra energy needed to promote flow in structured liquids. The structure in an electrolyte solution will depend on both temperature and concentration. Temperature alters structure by the amount of thermal movement; and concentration alters structure by the characteristic ion - solvent interactions that occur as a function of concentration. The amount of entropy change over a temperature or concentration range is dependent on the amount of structure present, and the assumption that ΔS is constant may not be valid. In such a case, a plot of $\ln\eta$ as a function of $(T)^{-1}$ would not yield a straight line.

Many associated electrolyte solutions do however obey the linear law. In such a case, concentration effects may be observed in terms of the energy of activation. An increase in

energy of activation for viscous flow can be explained in terms of ion -ion or ion - solvent interactions. A large change in the activation energy may be an indication of the formation of complex aggregate species.

2.1.3 Batschinski Hildebrand Analysis

Possible relationships between solution viscosity and specific volume have been considered for a long time. In 1913, Batschinski proposed a relationship between viscosity, η, and specific volume, v. This theory is also based upon the hole theory of liquids described briefly in the previous section of this thesis (Batschinski, 1913; Frenkel, 1955). The Batschinski equation is presented below:

$$\eta = \frac{B_B}{(v-b')} \qquad (2.10)$$

where,

η is the solution viscosity
B_B, b' are constants
v is the specific volume

B_B, b' are approximately independent of temperature and pressure. The constant b' is similar to "b" appearing in the Van der Waals' equation, and thus v-b' represents the "free volume" of the liquid. Free volume of a liquid may be described as the volume through which the liquid molecules are free to move, and corresponds to the "volume of holes" in the hole theory of liquids.

The modified Batschinski - Hildebrand equation relates fluidity, ϕ, $(1/\eta)$, to specific excess volume $(v - v_o)$, and to the ratio of unoccupied to occupied volumes, $(v-v_o)/v_o$ (Hildebrand, 1971; 1978).

$$\phi = \frac{B_{BH}(v-v_o)}{v_o} \qquad (2.11)$$

where,

ϕ is fluidity $(cP)^{-1}$
B_{BH} is a constant $(cP)^{-1}$
v is the specific volume (ml/g)
v_o is the intrinsic volume (ml/g)

The intrinsic volume, v_o, is the specific volume of a substance in the solid state, provided that on solidification the molecules preserve all of their degrees of freedom. It is an expression of molecular size and does not imply spherical shape. In general, a liquid can flow freely when expanded in volume by only a few percent over v_o.(Hildebrand, 1971; 1978)

The constant B_{BH} is a property of the liquid and is dependent on molecular size and shape. A large value of B_{BH} is characterized by a solution of high fluidity (low viscosity) and conversely a solution having a small value of B_{BH} has low fluidity and high viscosity. Molecular solutions generally exhibit B_{BH} values in the order of 10 cP^{-1}. A reduction in B_{BH} as a function of solute concentration may indicate the formation of molecular species in a previously non - molecular solution,

or it may indicate the presence of newly formed ionic species which could further reduce the viscosity. Thus, the Batschinski - Hildebrand B_{BH} factor is a measure of a liquids ability to absorb the momentum generating the Newtonian flow, (eg. large B_{BH}, the solution absorbs momentum and continues flowing; small B_{BH}, solution momentum lost).

A discussion of the intrinsic volume and B_{BH} parameter will follow as applied to the $SOCl_2$ solutions of interest.

2.2 Conductance Theory

Conductance theory has been studied for many years, (Fuoss, 1935; 1959; Lind, et.al., 1959; Janz and Tait, 1967; Kay, 1960; Moshetev and Zlatilova, 1982; Salomon and Plichta, 1985) with most theoretical developments applying to the low concentration region. Much of the work is based on the initial studies of Debye and Hückel and later Onsager (Koryta and Dvořák, 1987). The Debye - Hückel theory of electrolyte solution is based on the assumption that the ions in solution are surrounded by ionic atmospheres distributed with radial symmetry about the central ion. There are, on average, more ions of the opposite charge in this ionic atmosphere as a result of the attraction between electrical charges of unlike sign, and the repulsion of charges of like sign. Although the ionic atmosphere is treated as a reality in mathematical discussions, it is actually the result of a time average of a distribution of the ions. The ionic atmosphere will affect the

activities of the ions in solution, and therefore, affect the physical properties of the solution, including conductivity, diffusivity and viscosity. This theory assumes that the passage of an electric current through a solution of electrolyte (ie. conductance) depends on both the concentration of ions present in the solution and on their speed or mobility. In the presence of an ionic atmosphere the conductivity is thus governed by two effects; the ELECTROPHORETIC EFFECT and the TIME - OF - RELAXATION EFFECT.

In a potential gradient of intensity E, a selected ion will move with a velocity, u_1. The velocity is independent of the presence of other ions, and is determined by the limiting mobility, U_o, of the ion constituent. The ion atmosphere, having opposite charge to the ion itself, will tend to move in a reverse direction with a velocity u_2. The velocity u_1 determines the limiting ionic conductance, $\lambda_o^{\pm}$, and the velocity u_2 is the retardation due to the electrophoretic effect. The net velocity of the ion is

$$u = u_1 + u_2 \qquad (2.12)$$

where,

u is the net velocity of the ion

u_1 is the velocity of the ion resulting from the electric field

u_2 is the retardation due to the electrophoretic effect

The velocity retardation due to the electrophoretic effect is a function of the electric field, the ionic charge,

viscosity and the Debye length (or radius of ionic atmosphere). This velocity is given by the expression:

$$u_2 = \frac{z_i e E_x}{6\pi\eta L_D} \qquad (2.13)$$

where,

u_2 is the retarding velocity
z_i is the charge of the central ion
E_x is the electric field
η is viscosity
L_D is the Debye length

For a singly charge ion in an aqueous solution at 25°C experiencing an electric field of 1V/cm, the velocity due to the electrophoretic effect, u_2 is approximately $3 \times 10^{-4}\sqrt{c}$, where c is concentration in moles/l. This corresponds to a decrease in equivalent conductance of:

$$\lambda = N_{Ions} u_2 = 29.9\sqrt{c} \qquad (2.14)$$

where,

λ is the equivalent ionic conductance
N_{Ions} is the number of ions
u_2 is the velocity of retardation due to the electrophoretic effect
c is concentration in moles/l

The other mechanism which affects the equivalent conductance when ionic concentration is increased, is the time of relaxation effect. The effect originates in the time delay (relaxation) phenomena required for the renewal of spherical symmetry of the ionic atmosphere around a central ion moving

under the influence of an applied electric field. If the central ion moves suddenly, it becomes asymmetrically located with respect to the centre of the ionic atmosphere as the ionic atmosphere does not respond spontaneously to the movement. If a central ion is moving steadily, the ionic atmosphere will be under the influence of a permanent distortion, the effect of which is to decrease the velocity of the ion, under a given external coulombic force.

Derivation of these effects was first approximated by Debye and Hückel and later by Onsager. For a univalent ion the equivalent conductance was proposed to be:

$$\Lambda=\Lambda_o-[\theta\Lambda_o+\sigma]\sqrt{c} \qquad (2.15)$$

where,

Λ is the electrolytic molar conductivity
Λ_o is the limiting conductivity
$\theta\Lambda_o\sqrt{c}$ is the time of relaxation effect
$\sigma\sqrt{c}$ is the electrophoretic effect

The first term in the parentheses of Equation (2.15), the Onsager limiting law, has been related to the time of relaxation effect and the second term, to the electrophoretic effect. This expression is based on a number of simplifying assumptions of a physical and mathematical nature, and is strictly valid only as a limiting law and may be expected to hold only for dilute solutions, concentrations less than 0.001 M/l.

Empirical modifications to the Onsager limiting law have been made to model the concentrated solution behaviour of electrolyte solutions. A modified equation is:(Prue and Sherrington, 1961)

$$\Lambda=\Lambda_o-(\Theta\Lambda_o+\sigma)\sqrt{c}+b_{OL}c \qquad (2.16)$$

where b_{OL} is an empirical parameter.

In 1927, Onsager used Equation (2.16) to improve the agreement between experimental and calculated conductances above 0.001M (MacInness, 1961).

Robinson and Stokes (1965) included the concept of finite size of the conducting ion in an expression for conductivity. Their work was based upon the Falkenhagen school, and included a factor of:

$$\frac{1}{1+B\mathring{a}\sqrt{c}} \qquad (2.17)$$

$$where,\quad B\mathring{a} = \frac{50.29\mathring{a}}{(\epsilon T)^{\frac{1}{2}}}$$

where,

å is the ionic diameter
ϵ is the dielectric constant
T is temperature

in the Onsager limiting equation, Equation (2.15), for conductivity:

$$\Lambda=\Lambda_o-\frac{(\theta+\sigma)\sqrt{c}}{1+B\dot{a}\sqrt{c}} \qquad (2.18)$$

This expression was found to reproduce the conductivity of low dielectric solutions poorly (Prue and Sherrington, 1961). As a result, it is not widely used, and modifications to Equation (2.16), such as the addition of a log(c) term, as proposed by Fuoss and Onsager in 1957, are favoured (Lind, et.al., 1958). The Fuoss-Onsager equation is generally applicable to low concentration solutions only. Workers have developed conductivity equations to be used with associated electrolytes, these equations include α, the degree of dissociation. The stardard expressions for associated and unassociated electrolytes as proposed by Fuoss and Onsager for low concentration electrolytes, are presented below: (Kay, 1959)

Unassociated electrolytes:

$$\Lambda=\Lambda_o-S_{FO}\sqrt{c}+E_{FO}c\log c+J_{FO}c \qquad (2.19)$$

Associated electrolytes:

$$\Lambda=\Lambda_o-S_{FO}\sqrt{\alpha c}+E_{FO}(\alpha c)\log(\alpha c)+J_{FO}(\alpha c)-K_A\Lambda f^2(\alpha c) \qquad (2.20)$$

where,

S_{FO}, E_{FO} are known functions of Λ_o, and the solvent properties

J_{FO} is a function of the solvent properties, Λ_o, and the ionic size, å

K_A is the thermodynamic association constant
$= (1 - \alpha)/(\alpha^2 c f^2)$
f is the mean activity coefficient

2.2.1 Wishaw-Stokes Theory of Conductivity

The above expressions model experimental conductivity only at low concentrations (c < 0.01N). An expression for concentrated solutions, based on the Fuoss-Onsager approach was presented by Wishaw and Stokes in 1954. They expressed conductivity as the product of electrophoretic and time of relaxation effects (Della Monica, 1983).

$$\Lambda=\left(\Lambda_o-\frac{B_2\sqrt{C}}{1+B\dot{a}\sqrt{C}}\right)\left(1-\frac{B_1\sqrt{C}}{1+B\dot{a}\sqrt{C}}F\right) \qquad (2.21)$$

where,

$$B_1=\frac{8.2}{(\epsilon T)^{1/2}}$$

$$B_2=\frac{82.5}{\eta_o(\epsilon T)^{1/2}}$$

$$B\dot{a}=\frac{50.29\dot{a}}{(\epsilon T)^{1/2}}$$

$\dot{a}$ *is the ionic diameter* ($\dot{A}$)

$$F=\frac{\exp(0.2929B\dot{a}\sqrt{C})-1}{0.2929B\dot{a}\sqrt{C}}$$

The Wishaw-Stokes equation is based on the Onsager limiting equation, Equation (2.15), but has included the effect of finite ionic size, the ionic diameter concept as suggested

by Robinson and Stokes, and the Falkenhagen evaluation of the relaxation effect (Prue and Sherrington, 1961). They considered the effect of viscosity on conductivity. Viscosity may be interpreted as a measure of the shearing force required to move one layer of solution with respect to another. Flow is resisted by two kinds of intermolecular attractions. The first is attractions due to short- range solvent-solvent and solvent - ion forces, and the second is due to long-range coulombic forces. The effect of the coulombic forces is accounted for in the theory leading up to the development of the Wishaw-Stokes expression, but the effect of short-range forces was not. The effect of the short range forces on conductivity, (ie. a conductivity reduction due to increased viscosity or decreased fluidity) was believed to be relevant. The workers felt justified in including a bulk viscosity term in the conductivity equation. The final form of the Wishaw - Stokes equation is presented below.

$$\Lambda=\left(\Lambda_o-\frac{B_2\sqrt{C}}{1+B\dot{a}\sqrt{C}}\right)\left(\frac{1-B_1\sqrt{C}}{1+B\dot{a}\sqrt{C}}F\right)\frac{\eta_o}{\eta} \qquad (2.22)$$

All parameters have standard meaning as described above.

In general, for very dilute solutions Equation (2.22) is not valid as the coulombic forces will be a major contributor to the viscosity term, and thus in effect will be counted twice. The above equation has been applied successfully to concentrated aqueous solutions; in 1955, Campbell and Kartzmark

used the equation for 8M NH_4NO_3 in H_2O, and in 1958, Campbell and Patterson looked at various sodium salts in water for concentrations as high as 9 M.

Wishaw-Stokes theory applies well to systems in which the ratio of the solution viscosity to the solvent viscosity is small (ie. less than 8). A short-coming of the equation is that while introducing a correction factor which accounts for the change in medium viscosity in the whole conductivity equation (the η_o/η term), it calculates the electrophoretic effect at all concentrations using pure solvent viscosity ($B_2 = 82.5/\eta_o(\epsilon T)^{1/2}$). Recently Della Monica (1983) proposed a modification to the standard Wishaw-Stokes equation. In the modified equation B_2 is determined by putting the viscosity of the solution at different concentrations into the expression for B_2, ($B_2 = 82.5/\eta(\epsilon T)^{1/2}$). In general, this modification improves the performance of the equation for systems in which the viscosity ratio is large. Della Monica (1983) found considerable improvement in the behaviour description of concentrated NaSCN - water solutions.

Molten salt, or liquid melt theory may be applied to concentrated solution conductivity. Detailed structure in these solutions is difficult to determine as ionic mobilities are not easily determined. The "degree of dissociation" cannot be determined easily as for aqueous solutions as there is no inert medium in which the ions migrate. Walden's rule does, however, apply to concentrated solutions in which solute dissociation is

complete (Kortüm and Bockris, p210, 1951).

2.3 Method of Data Analysis

It was necessary to fit the experimental data obtained from density, viscosity and conductivity studies to numerous equations of different order and form. The data correlation was performed using a commercially available PC software package, 'Asystant, The Scientific Number Cruncher' (TM Asyst Software Technologies, Inc., 1988). This program is capable of fitting data to linear, polynomial, logarithmic, exponential and user defined functions.

In the case of a linear fit to the data the program computes the parameters m and b of a function:

$$y=mx+b \qquad (2.23)$$

where,

m is the slope of the linear equation
b is the intercept of the linear equation

that define the best least-squares fit. The program also provides "goodness of fit" parameters, Err^2, R^2, and Sig. Err^2 is the sum of the squared residuals; R^2 is the square of the multiple correlation coefficient, often called the multiple coefficient of determination; and Sig is the significance of fit parameter, computed by applying an F-test to the multiple correlation coefficient, The F-test statistic gives an indication of the global utility of the model.

$$Err^2=\sum_{i=1}^{n} |y_i-(mx_i+b)|^2 \qquad (2.24)$$

where,

y_i is the experimental dependent variable
x_i is the experimental independent variable
$(mx_i + b)$ is the calculated dependent variable
and n is the number of experimental points.

$$R^2=1-\frac{Err^2}{Res^2}, \quad Res^2=\sum_{i=1}^{n} |y_i - \left(\frac{1}{n}\right)\sum_{i=1}^{n} y_i|^2 \qquad (2.25)$$

$$Sig=P_{F_{sig}[n-2,1]}(f_{sig}>F_{sig}), \quad F_{sig}=\frac{R^2(n-2)}{1-R^2} \qquad (2.26)$$

Asystant is also capable of fitting nth order polynomials to (x,y) data by computing the coefficients c_o, c_1, ... c_n that provide the best least-squares fit.

$$y=c_o + c_1x + c_2x^2 +...+ c_nx^n \qquad (2.27)$$

The goodness of fit parameters as described above were also calculated. The polynomial expressions describing these parameters are listed below.

$$Err^2=\sum_{i=1}^{n}|y_i-(c_o+c_1x^1+\ldots+c_mx^m)|^2 \qquad (2.28)$$

$$R^2=1-\frac{Err^2}{Res^2},\quad Res^2=\sum_{i=1}^{n}|y_i-\frac{1}{n}\sum_{i=1}^{n}y_i|^2$$

$$Sig=P_{F_{sig}[n-m-1,m]}(f_{sig}>F_{sig}),\quad F_{sig}=\frac{R^2(n-m-1)}{(1-R^2)m}$$

where y_i is again the experimental value of y, the calculated value of y is given by the expression $(c_o + c_1x^1 +\ldots+c_mx^m)$, n is the total number of experimental points to be fit, and m is the degree of the polynomial expression.

Throughout the analysis of the data it was necessary to fit xy data to equations having non-standard form (eg. the modified Jones Dole equation $\eta_r = 1 + A\sqrt{c} + Bc + Dc^2$). It was possible, using Asystant, for the operator to define a function F(x), and fit the function parameters to give the best least-squares fit to the xy data set. The goodness of fit parameters are again computed.

$$Err^2=\sum_{i=1}^{n}|y_i-G(x_i)|^2 \qquad (2.29)$$

$$R^2=1-\frac{Err^2}{Res^2},\qquad Res^2=\sum_{i=1}^{n}|y_i|^2$$

$$Sig = P_{F_{sig}[n-m,m]}\,(f_{sig} > F_{sig}), \qquad F_{sig} = \frac{R^2(n-m)}{(1-R^2)m}$$

where,

y_i is the experimental value of y
$G(x_i)$ is the calcu'.ated value of y
n is the total number of points to be fit

The method of fit used to determine the function parameters for user defined functions is that presented by Gauss - Newton. The Gauss - Newton method is standard, and a detailed outline of the procedure is presented in the literature (Asystant, 1988).

The variance of the model, σ_v^2, may be estimated from Err^2,

$$\sigma_v^2 = \frac{Err^2}{n-(Number\ of\ estimated\ fitted\ parameters)} \quad (2.30)$$

where, n is the number of experimental points

The estimated value of the variance may be used to check the adequacy of the model, and to provide a measure of the reliability of predictors and estimates. The standard deviation is the square root of the variance.

3.0 Properties of Materials

This project is a physical chemical study of the properties of an inorganic electrolyte which is used commercially in lithium batteries. The electrolyte contains thionyl chloride, lithium salts and proprietary additives. The materials used in this physical chemical study include $SOCl_2$ and $AlCl_3$, two of the three main constituents of the commercial electrolytes used in lithium/thionyl chloride cells. The third main component is LiCl.

3.1 Thionyl Chloride

$SOCl_2$ is a clear colourless liquid at room temperature characterized by a boiling point of 79°C, melting point of -105°C and specific gravity of 1.631 at 10°C. The vapour pressure of liquid $SOCl_2$ at 20°C is approximately 100mm Hg, indicating that it is a high vapour pressure solvent. (CRC Handbook, D198, 1983-84) Thionyl chloride has a relatively low dielectric constant of 9.25, the low value indicates that $SOCl_2$ has limited ionic or polar character (CRC Handbook, E50, 1983-1984). It is characterized by a pungent odour and has an LC50 (rat) of 500 ppm/1h, making it a difficult and dangerous material to study or use commercially (MSDS1, 1990).

It is incompatible with acids, bases, alcohols, metals, amines and water. It readily corrodes many metals including copper, aluminum, iron and many grades of stainless steel. Thionyl chloride will react violently with water resulting in

the production of toxic hydrogen chloride and sulfur dioxide gases. Thionyl chloride decomposes when heated above 140°C and forms chlorine, sulfur dioxide and sulfur monochloride while producing a suffocating odour.

Thionyl chloride exists as a dimer in the anhydrous liquid state. Spectroscopy and theoretical molecular orbital calculations indicate that the complex structure is that of an open chain dimer, with complexation occurring through the oxygen and sulfur atoms (Mosier-Boss, Boss, Gabriel, Szpak, Smith and Nowak, 1989; Mosier-Boss, Szpak, Smith and Nowak, 1989). The possibility of a cyclic structure has been eliminated on the basis of molecular orbital calculations (Mosier-Boss, Boss, Gabriel, Szpak, and Smith, 1989). Figure 3.1 shows the proposed structures. Vibrational spectroscopic assignments are proposed for free and complexed $SOCl_2$ (Mosier-Boss, Boss, Gabriel, Szpak, and Smith, 1989).

Typical impurities found in neat $SOCl_2$ include sulfuryl chloride, SO_2Cl_2, sulphur monochloride, SCl, and sulphur dichloride, SCl_2. Purification by distillation can remove these compounds (Friedman and Wetter, 1967).

Thionyl chloride should be stored in a tightly closed container under nitrogen in a cool dry place way from incompatible materials, and protected from physical damage.

3.2 Aluminum Chloride

$AlCl_3$ is a white or yellowish deliquescent crystalline

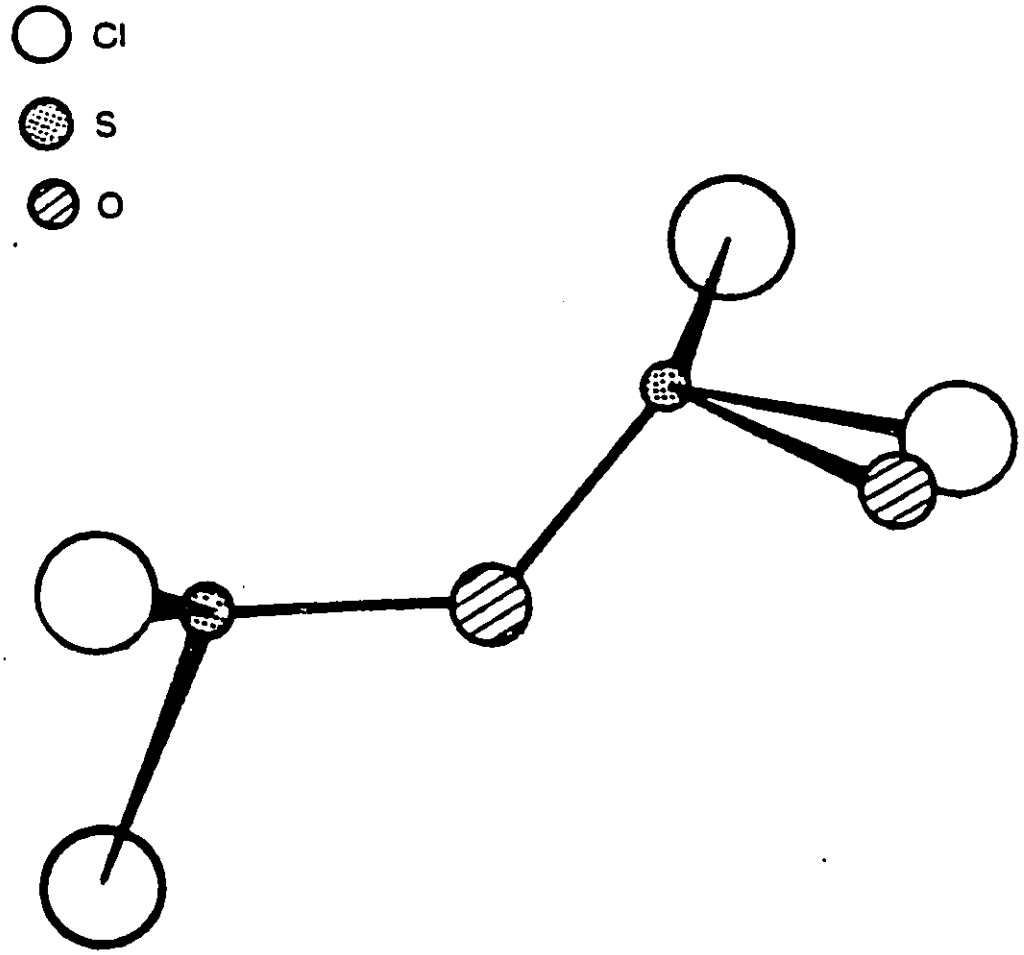

Figure 3.1: Proposed structure of liquid $SOCl_2$ based on molecular orbital calculation (Mosier-Boss, Boss, Gabriel, Szpak, and Smith, 1989).

2powder having a specific gravity of 2.4. $AlCl_3$ is incompatible with water, may react violently and exothermically to form toxic and corrosive hydrogen chloride gas. $AlCl_3$ is a health hazard, and requires the use of a dust mask, gloves and face shield. The toxicity of $AlCl_3$ has been reported as an LD50 (rat) of 3.7g/kg (MSDS2, 1990).

Pure anhydrous aluminum chloride exists as a dimer, Al_2Cl_6. When the solid is vaporized, the dimers persist until approximately 400°C. The molecule is complexed across halide (Cl) bridges. At this temperature the dimer begins to dissociate into two $AlCl_3$ molecules.

$AlCl_3$ should be stored in a tightly closed container under nitrogen in a dry atmosphere.

3.3 The Electrolyte

The $AlCl_3/SOCl_2$ electrolyte was compatible with glass and teflon, but reacted aggressively with most other plastics and metals. As a result, all of the physical chemistry cells (conductivity, density, and viscosity) were constructed from pyrex and Teflon (Reg. TM Dupont).

The $AlCl_3/SOCl_2$ electrolyte is a clear slightly yellowish liquid. Numerous species have tentatively been identified in solution, including dimeric $(SOCl_2)_2$, the $Cl_3Al\text{-}OSCl_2$ molecular adduct and certain ionic species. Figure 3.2 exhibits computer generated structures of the compounds as reported in the literature (Mosier-Boss, Szpak, Smith, and Nowak, 1989).

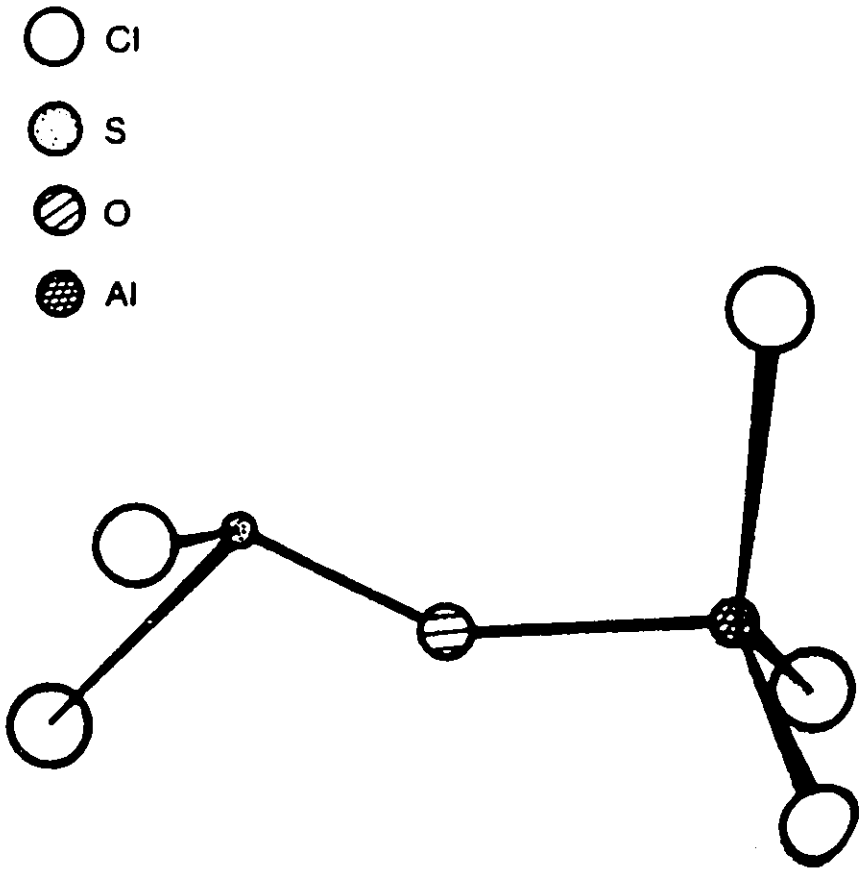

Figure 3.2: Proposed structure of $AlCl_3$ - $SOCl_2$ compounds based on molecular orbital calculations (Mosier-Boss, Szpak, Smith, and Nowak, 1989).

4.0 Experimental

4.1 General Techniques

The use of thionyl chloride, aluminum trichloride and lithium chloride required specialized techniques for sample manipulation. At no time were the thionyl chloride based electrolytes exposed to air, either in sample manipulation or in the measurement of physical properties. Chemical purification, solution preparation and sample storage were conducted in argon atmosphere glove boxes or in sealed reaction chambers. Two glove boxes were required. The first, a stainless steel Dri-lab argon atmosphere glove box was used in the preparation, purification and storage of the chloride salt (aluminum trichloride). The second, a Labconco fibreglass glove box was used for all work involving thionyl chloride including purification, sample preparation, and storage of both the solvent and the solutions. This second box was required due to the corrosive nature of thionyl chloride. The oxygen and moisture content of the boxes was monitored and found to be approximately 1 ppm during the course of this work.

4.2 Reagent Purification

4.2.1 Thionyl Chloride

High grade $SOCl_2$ (Aldrich, 99+ %, bp 79°C, mp -105°C) was refluxed in a sealed environment for one hour under a nitrogen

atmosphere. The clear yellow liquid was then distilled under partial vacuum in a nitrogen atmosphere. The distillation temperature was kept constant at approximately 50°C by regulating the flow of nitrogen. A standard Ace glass distillation apparatus, with a variable flow stopcock as shown in Figure 4.1 was used. Prior to the distillation of the thionyl chloride, the glass apparatus was thoroughly cleaned and flame dried to ensure that new impurities were not introduced. Ground glass joints were not greased as the grease contaminated the purified liquid. A clear colourless liquid was recovered, and a small volume of dark yellow solution remained in the distillation vial. The purified liquid, obtained from middle fractions of the distillation, was stored in a closed container made of dark glass in an argon atmosphere glove box.

The purity of the distillate was verified using NMR spectroscopy (analysis for the presence of hydrogen), and conductivity measurements. The conductivity of the impure $SOCl_2$ was found to be 1.8×10^{-6} S/cm. After distillation, the conductivity was reduced to 1.3×10^{-7} S/cm. The value for conductivity of pure thionyl chloride reported in the literature is $(1.2 \text{ to } 1.4) \times 10^{-7}$ S/cm (Berg, Hjuler, Søndergaard, Bjerrum, 1989).

4.2.2 Aluminum Trichloride

High grade $AlCl_3$ (Aldrich, 99.99%) was purified by

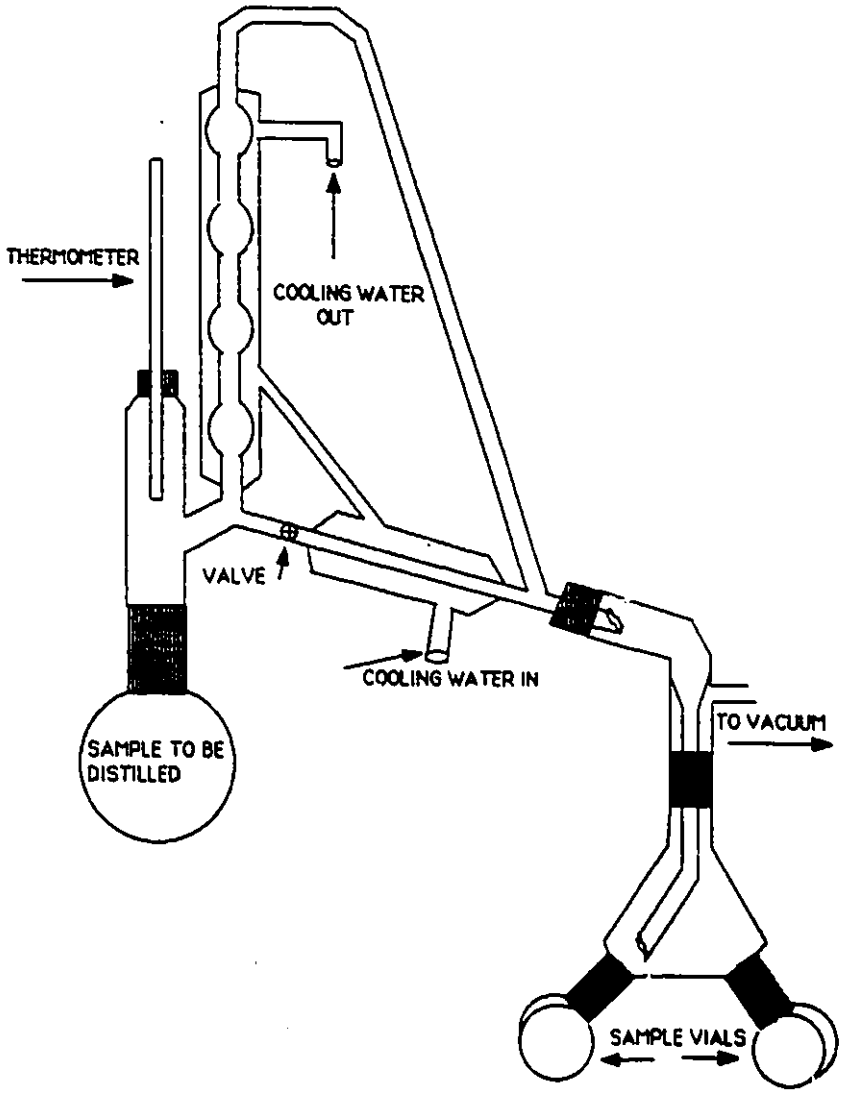

Figure 4.1: Vacuum distillation apparatus, used in the purification of thionyl chloride, $SOCl_2$.

sublimation (solid distillation). The sublimation apparatus was stored in a drying oven containing Dryerite at 110°C. Before the aluminum salt was added to the apparatus, it was flame dried. Approximately twenty grams of off-white $AlCl_3$ powder, weighed on a Mettler PJ300 top-loading balance, were placed in a glass sublimation apparatus in an argon atmosphere Dri-lab glove box. An additional ten percent by weight of sodium chloride (NaCl) was added. The apparatus was removed from the dry box and a vacuum was applied to the closed system. Heat was applied to the apparatus using a bunsen burner. The experimental set up is presented in Figure 4.2. During the heating period, a white solid formed on the sublimation apparatus cold finger. The $AlCl_3$ was removed from the cold finger in an argon atmosphere dry box. Purity of the salt was verified using Raman spectroscopy.

4.3 Sample Preparation: $AlCl_3$/ $SOCl_2$

Samples of $AlCl_3/SOCl_2$ (aluminum trichloride/ thionyl chloride) were prepared at room temperature (20 to 25°C) from purified reagents in an argon atmosphere glove box. Purified alliquots of $AlCl_3$ were weighed, using the Mettler PJ300 balance, and placed into glass sample vials in the Dri-lab glove box. The empty sample vials were stored in a drying oven at 110°C. Once filled, the sample vials were removed from the Dri-lab box and transferred to a second glove box (fibreglass Labconco dry box) in which the $SOCl_2$ was stored. $SOCl_2$ was

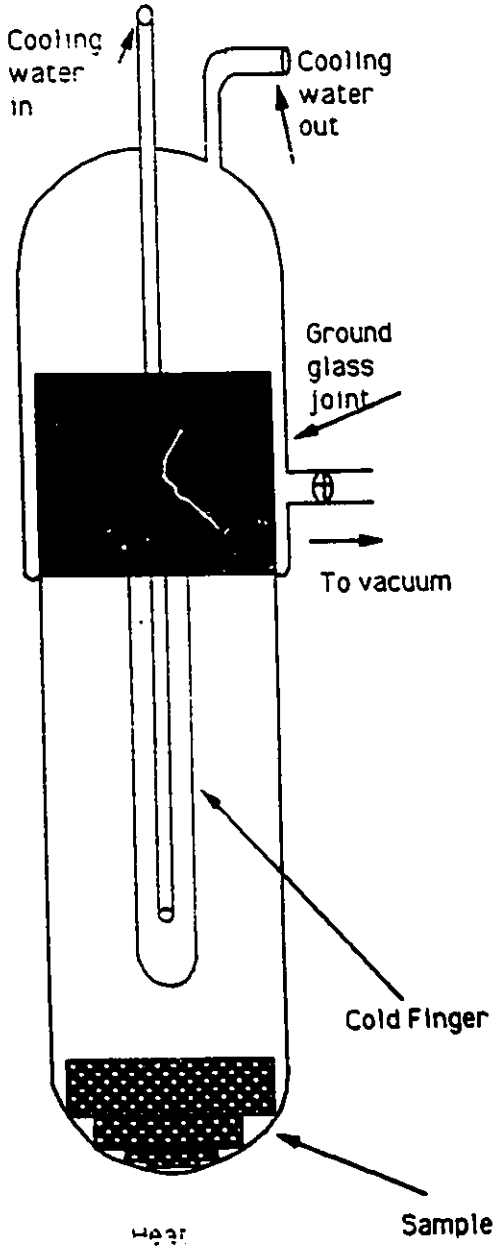

Figure 4.2: Sublimation apparatus, used in the purification of aluminum chloride, $AlCl_3$.

added to form solutions having concentrations between 0 and 35 weight percent $AlCl_3$ in $SOCl_2$. The quantity of $SOCl_2$ was determined by weight using a Sartorius A200S balance. The $SOCl_2$ was weighed outside the Labconco glove box to protect the balance from the thionyl chloride atmosphere. The resulting solutions were stirred to dissolve all $AlCl_3$ powder. Once the solutions were mixed, they were tightly sealed and stored in the glove box until needed.

It was necessary to perform experiments on these solutions quickly as they remained stable for only two to three days. Degradation of solutions was accompanied by a colour change, fresh solutions were clear and slightly yellow in colour, older solutions were cloudy and dark yellow brown in colour. Degradation of solutions was also detected by conductivity. As the solutions aged, the conductivity increased.

4.4 Electrical Conductivity Measurements

Conductivity was determined using a Wayne Kerr Bridge, model: Autobalance Universal Bridge B642, and a glass and platinum conductivity cell as shown in Figure 4.3 (Anantaraman, 1987).

Potassium chloride (KCl) solutions, made from dried KCl and distilled water (having a specific conductance of 2 μS/cm), with concentrations from 0 to 10 weight per cent KCl, were used to determine the cell constant for the conductivity cell. The conductivity of these solutions ranged from 5 to 140 mS/cm.

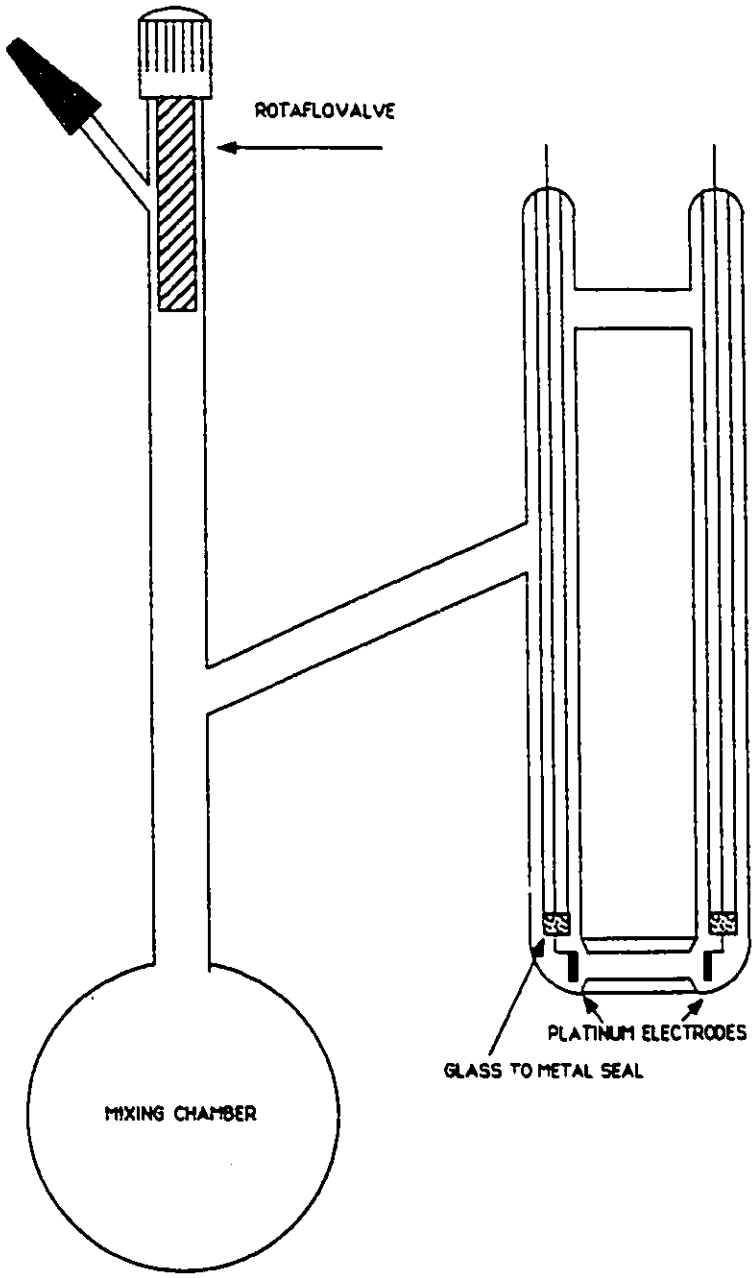

Figure 4.3: Closed vessel conductivity cell.

Data obtained from the literature (CRC Handbook, D247, 1983-84) was fit to a polynomial, using the standard least-squares method, and theoretical conductivity was determined for each concentration. This value was then used to calculate the cell constant, A, in cm^{-1}.

The conductivity cell was cleaned and vacuum-dried, at room temperature, to a constant weight. $AlCl_3$ samples ranging from 0 to 35 weight percent $AlCl_3$ were transferred to the dried conductivity cell in an argon atmosphere Labconco glove box. The conductivity cell was placed in a constant temperature bath and allowed to equilibrate. The constant temperature bath contained either isopropanol at low temperatures, or an inert fluorocarbon solvent, Fluorinert FC77 from 3M, at higher temperatures. Temperature control of 0.1 °C was achieved. The absolute temperature of the bath was determined from a thermometer which had been calibrated in ice water, and in boiling water. Conductivities were determined over the temperature range of -40°C to 25°C. Approximately five measurements were recorded for each sample at each temperature.

4.5 Density Measurements

The density cell was constructed from a 2 ml pipette and a teflon screw cap as shown in Figure 4.4. The cell volume was calibrated using distilled water for temperatures greater than 0°C, and using high grade methanol (BDH, 99.8%) for temperatures less than, or equal to 0°C. The density as a

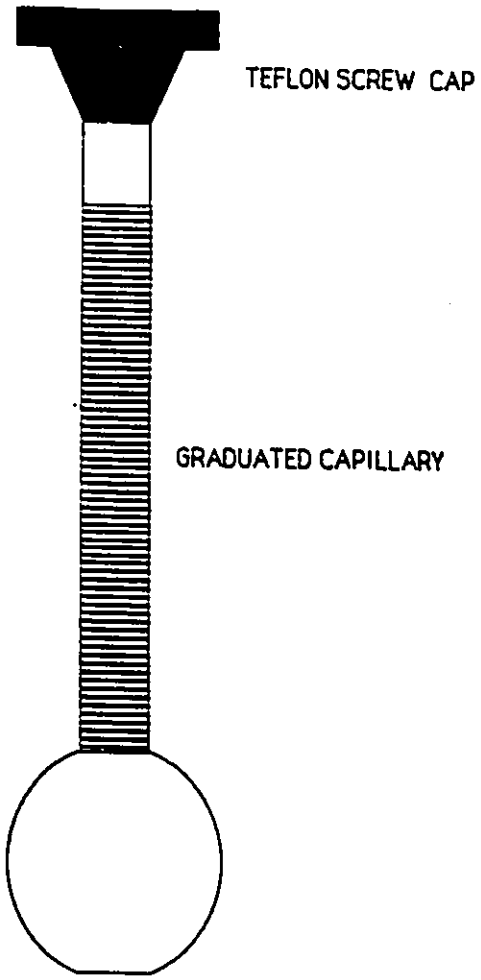

Figure 4.4: Density cell constructed of pyrex glass and teflon.

function of temperature for both pure water and methanol was readily available in the literature (CRC Handbook, F5, 1983-84).

The density cell was vacuum-dried to a constant weight at room temperature. $AlCl_3/SOCl_2$ samples were introduced to the dried density cell via a Hamilton syringe having a Teflon needle, in an argon atmosphere Labconco fibreglass glove box. The dry mass of the cell was determined on a Sartorius A200S analytical balance before the sample was introduced. The filled cell was weighed on the balance then placed in a constant temperature bath (25 to -40°C) inside a double walled glass vessel. The temperature of the bath was controlled to within 0.1°C. The samples were allowed to equilibrate, and several measurements of the uncalibrated volume were recorded. The uncalibrated volume was converted via calibration curves and the density was calculated.

4.6 Viscosity Measurements

A modified Ostwald type viscometer was used to determine the viscosities of solutions (0 to 35 weight percent $AlCl_3$ in $SOCl_2$) over a range of temperatures (20 to -20°C). The viscometer was modified such that it was a closed system with access to the external environment controlled by a roto-flow valve as shown in Figure 4.5 (Anantaraman, 1986; Gee et.al., 1987).

The viscometer was first calibrated with methanol (BDH

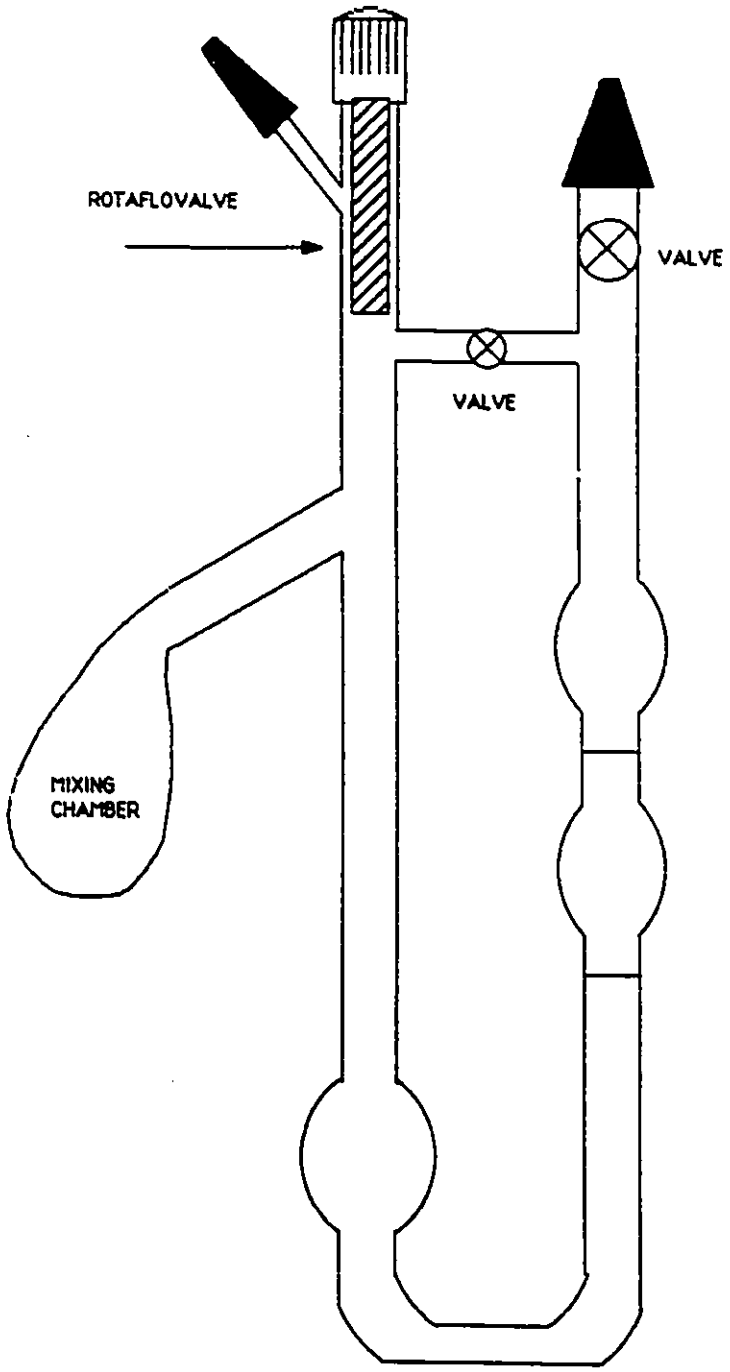

Figure 4.5: Modified Ostwald viscometer used to determine viscosity for $-20^{\circ}C < T < 20^{\circ}C$.

99.8%). Samples were then introduced to the clean, vacuum-dried viscometer and the viscosity of each sample was determined. An average of five measurements at each temperature and concentration was used to determine the viscosity.

The relative viscosity obtained experimentally was transformed into absolute viscosity using the viscosity of methanol available in the literature (CRC Handbook, F41, 1983-84).

5.0 Results and Discussion

Experimental data used to provide Tables and Figures in this thesis is included in Appendix B.

5.1 Solution Density

The density of the $AlCl_3/SOCl_2$ solutions was determined over concentration and temperature ranges (0 to 4 moles/l) and (-20 to 20°C) respectively. The raw data was fit to linear equations using the least squares method.

$$\rho = mc_{w/w} + b \qquad (5.1)$$

where,

ρ is the density (g/ml)
$c_{w/w}$ is the concentration (% w/w $AlCl_3$ / $SOCl_2$)
m is the slope of the linear equation
b is the intercept of the linear equation

This data is presented in Figure 5.1 and Table 5.1 below.

Table 5.1: Density data fitted to a first order polynomial equation, coefficients and fitting parameters as a function of temperature.

Temp (°C)	m (x10^3) (g/ml conc)	b (g/ml)	Err^2	R^2
20.0[1]	2.69±0.06	1.640±0.001	3.24E-4	0.94
10.0±0.1	2.45	1.666	8.61E-5	0.98
0.0	2.71	1.674	2.96E-5	0.99
-20.0	2.92	1.718	6.86E-5	0.95

1: Plot obtained using data from Venkatasetty and Szpak, 1983

Figure 5.1 shows the best fit to the experimental data, and a

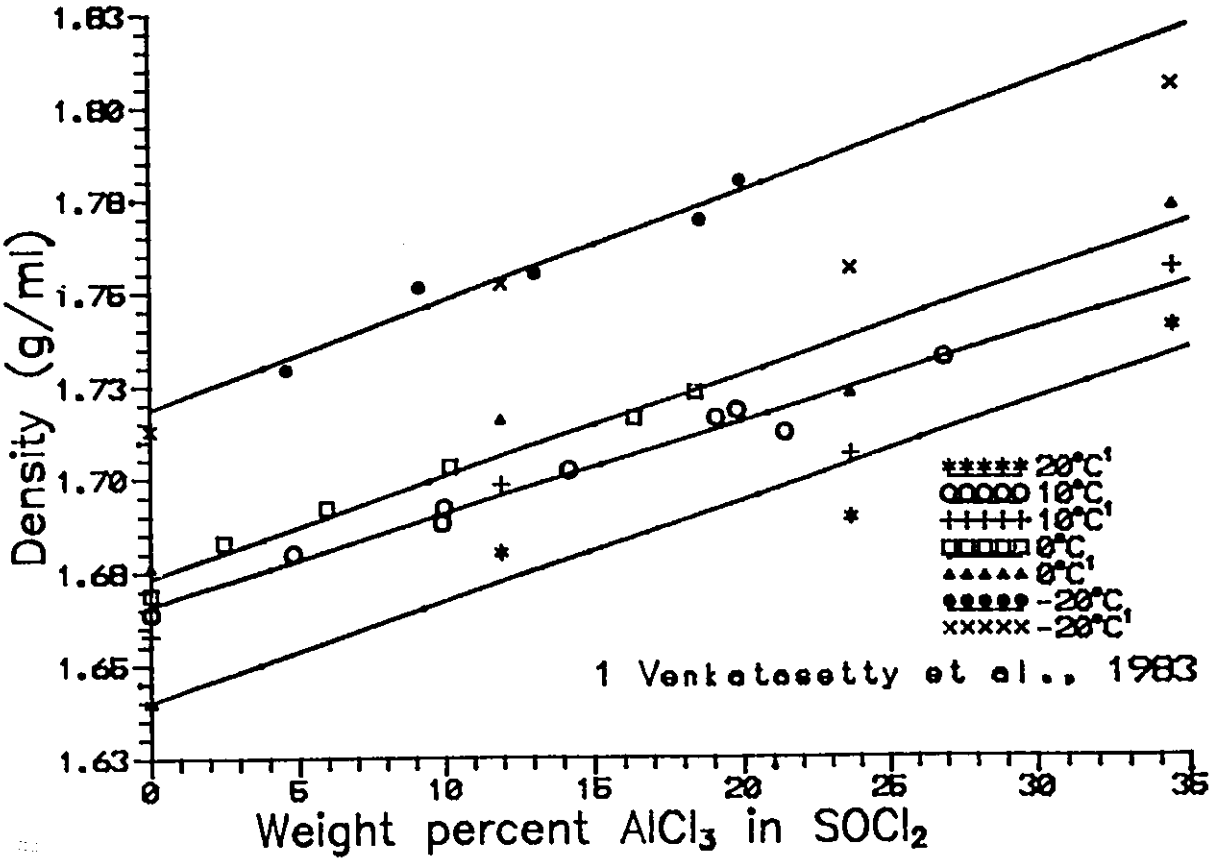

Figure 5.1: Density of $AlCl_3/SOCl_2$ solutions as a function of percent weight $AlCl_3$. Literature data (Venkatasetty and Szpak, 1983) included. First order polynomials obtained in least - squares analysis shown as solid lines.

comparison to the data available in the literature (Venkatasetty and Szpak, 1983). As expected, density is seen to increase with increasing salt concentration, and to increase with decreasing temperature. In general, the experimental data agrees with that of the literature, with the exception of the data at 3.0M (23.67±0.02 weight percent) $AlCl_3$ in $SOCl_2$. The literature density at 3.0M is consistently low for all temperatures studied, 20, 10, 0 and -20°C (Venkatasetty and Szpak, 1983). This is an indication that an anomaly in density occurs at this temperature, or that there exists an error in the literature results. This anomaly is not present in our experimental density results and does not appear in the conductivity or viscosity data, thus indicating the likelihood of an experimental error in the literature results. That the literature data is in poor agreement with our experimental data is not unexpected. The literature data was obtained from density vs temperature plots at three concentrations of $AlCl_3$ in $SOCl_2$, 1.5, 3.0 and 4.5 M. The correlation factor for these plots was reported as 0.99. Also, the literature curves were fit only to data ranging from 70 to -10°C, thus making the low temperature densities a poor estimate.

The density of thionyl chloride and the aluminum chloride solutions is compared to that of other compounds in Table 5.2. Thionyl chloride is a dense liquid (1.64 x the density of water), and at 20°C the concentration of liquid thionyl chloride is approximately 14 mole/l. In the anhydrous liquid

Table 5.2: Density of $SOCl_2$, $AlCl_3$ solutions and several other compounds.

Compound	Density at 20°C (g/ml)
Thionyl chloride	1.640 ± 0.001
10 w/w % $AlCl_3$ in $SOCl_2$	1.667 ± 0.001
20 w/w % $AlCl_3$ in $SOCl_2$	1.694 ± 0.001
30 w/w % $AlCl_3$ in $SOCl_2$	1.721 ± 0.001
sulfuryl chloride[1]	1.6674
water[2]	0.99823
methanol[3]	0.7914
mercury[4]	13.59
10 w/w % KCl in water[5]	1.0633
20 w/w % KCl in water[5]	1.1328
10 w/w % H_2SO_4 in water[6]	1.0661
25 w/w % H_2SO_4 in water[6]	1.1793
50 w/w % H_2SO_4 in water[6]	1.3952
75 w/w % H_2SO_4 in water[6]	1.6692
100 w/w % H_2SO_4 in water[6]	1.8305

1 CRC Handbook, 64th Edition, p B146, 1983-84
2 CRC Handbook, 64th Edition, p F5, 1983-84
3 CRC Handbook, 64th Edition, p C374, 1983-84
4 CRC Handbook, 64th Edition, p F7, 1983-84
5 CRC Handbook, 64th Edition, p D247, 1983-84
6 CRC Handbook, 64th Edition, p D267, 1983-84

state, it exists predominantly as molecular dimers with complexation occurring through the sulphur and oxygen atoms. Liquid water (ρ = 0.998 g/ml at 20°C, 55.4 moles/l) exists as a "quasi - crystalline" structure due to the strong intermolecular forces arising because of hydrogen bonding. Liquid water is, therefore, a highly "structured" liquid -ie.

molecules are ordered with respect to a reference molecule. The presence of some solution structure can be predicted since $SOCl_2$ is a polar molecule. $SOCl_2$ also exhibits considerable structure in the form of the dimeric molecular adducts.

The density of $SOCl_2$ at 20°C is comparable to that of concentrated H_2SO_4 solutions at 20°C (equivalent to approximately 75% H_2SO_4 in water), an electrolyte commonly used in lead - acid batteries. Sulphuric acid (molecular weight approximately 98 g/mole) is highly dissociated in H_2O, forming hydrated hydrogen ions, HSO_4^- and SO_4^{2-}, resulting in a "structured" liquid. Thus, density indicates that thionyl chloride (molecular weight 119 g/mole) solutions should also be "structured".

The density of $SOCl_2$ is slightly lower than that of sulfuryl chloride (SO_2Cl_2), 1.64 g/ml and 1.67g/ml respectively at 20°C. These values correspond to molar densities of 1.37×10^{-2} moles/ml for $SOCl_2$, and 1.23×10^{-2} moles/ml for SO_2Cl_2. As a result $SOCl_2$ based electrolytes have higher molar densities than do the SO_2Cl_2 based electrolytes, and thus the $SOCl_2$ batteries have higher energy densities.

The addition of $AlCl_3$ increases the density of the electrolyte solution. Again molecular species form, with $AlCl_3$ and $SOCl_2$ forming a 1:1 molecular adduct at low concentration, and higher order species as the $AlCl_3$ concentration increases.

The relatively high density of the electrolyte solutions is significant as it is a major contributor to the overall cell

weight. A careful determination of solute concentration is required to maximize the energy and power density of a $SOCl_2$ battery.

5.1.1 Thermal Expansivity

The concentration dependence of thermal expansion of $AlCl_3$ solutions was investigated. Thermal expansivity, α_{TE}, is defined as

$$\alpha_{TE}=\frac{1}{V}\left(\frac{\delta V}{\delta T}\right)_P \qquad (5.2)$$

$$\alpha_{TE}=-\left(\frac{\delta \ln\rho}{\delta T}\right)_P$$

where,

v = volume in ml
T = temperature in ° Kelvin
P = pressure
ρ = density in g/ml

Values of the density, ρ, were interpolated for various concentrations of $AlCl_3$, from the first order polynomials described in Table 5.1. (This is the table of linear fit of density as a function of concentration at 20, 10, 0 and -20°C.) The concentration range studied included solutions having 0 to 30 weight percent $AlCl_3$ in $SOCl_2$, and each of the four temperatures, 20, 10, 0, -20 °C was analyzed. The natural logarithm of density in g/ml was then plotted as a function of temperature, in Kelvin, for all six concentrations of $AlCl_3$. First and second order polynomial equations were fitted to each

of the sets of concentration data.

$$\ln\rho = c_o + c_1 T \qquad (5.3)$$

and

$$\ln\rho = c_o + c_1 T + c_2 T^2 \qquad (5.4)$$

where,

c_o, c_1, and c_2 are the coefficients of the polynomial
T is temperature in Kelvin
ρ is the density, in g/ml

The fitting coefficient and "goodness of fit" parameters are presented in Table 5.3.

The coefficient of thermal expansion, α_{TE}, is given by Equation (5.2) and is:

$$\alpha_{TE} = -c_1 \qquad (first\ order)$$

and

$$\alpha_{TE} = -(c_1 + 2c_2 T) \qquad (second\ order)$$

The value of the coefficient of thermal expansivity obtained at 20°C and -20°C, for first and second order polynomials is presented in Table 5.4. The coefficient of thermal expansion for several other liquids is included in Table 5.4.

Table 5.3: Polynomial fit coefficients and goodness of fit parameters for ln ρ vs T. Results used to evaluate the coefficient of thermal expansivity.

Solution	c_o (±0.002)	c_1 ($\times 10^{-3}$) (±7×10^{-6})	c_2 ($\times 10^{-6}$) (±3×10^{-8})	Err^2 ($\times 10^{-5}$)	R^2	Sig
Pure $SOCl_2$	0.824	-1.119		2.21	0.980	9.9E-3
	0.911	-1.765	1.187	2.20	0.980	1.4E-1
2.5% $AlCl_3$ in $SOCl_2$	0.828	-1.119		1.81	0.984	8.2E-3
	0.957	-2.069	1.743	1.77	0.984	1.3E-1
5.0% $AlCl_3$ in $SOCl_2$	0.839	-1.147		1.62	0.986	7.0E-3
	0.985	-2.218	1.968	1.58	0.987	1.2E-1
10.0% $AlCl_3$ in $SOCl_2$	0.846	-1.140		1.61	0.986	7.0E-3
	1.109	-3.080	3.562	1.46	0.987	1.1E-1
20.0% $AlCl_3$ in $SOCl_2$	0.868	-1.167		1.16	0.990	4.8E-3
	0.341	-4.646	6.389	0.64	0.995	0.7E-1
30.0% $AlCl_3$ in $SOCl_2$	0.890	-1.187		1.23	0.990	5.0E-5
	1.525	-5.872	6.298	0.30	0.998	0.5E-1

The value of the coefficient of thermal expansivity determined from the first order polynomial fit to the lnρ vs 1/T data generally increases as the salt concentration increases (from (1119 ± 7) x 10^{-6} K^{-1} for pure $SOCl_2$, to (1187 ± 7) x 10^{-6} K^{-1} for 30% $AlCl_3$). The scatter observed in the data at 5% and 10% $AlCl_3$ is within the experimental error calculated for this data. The value of approximately 1000 x 10^{-6} K^{-1} for all concentrations considered is, however, quite large.

Table 5.4: Coefficient of thermal expansivity as a function of the degree of the polynomial expression describing lnρ for $AlCl_3/SOCl_2$ solutions.

Solution	Thermal Expansivity $\alpha(x10^6)$ K^{-1} 1st order	Thermal Expansivity $\alpha(x10^6)$ K^{-1} 2nd order, 20°C	Thermal Expansivity $\alpha(x10^6)$ K^{-1} 2nd order, -20°C
$SOCl_2$	1119 ± 7	1070 ± 20	1160 ± 20
2.5% $AlCl_3$	1119	1050	1190
5.0% $AlCl_3$	1147	1070	1220
10.0% $AlCl_3$	1141	990	1280
20.0% $AlCl_3$	1179	900	1410
30.0% $AlCl_3$	1199	830	1520
Water[1]	207		
CCl_4[1]	1236		
Methanol[1]	1199		

1 Perry, p 3-106, 1984

The value of α_{TE} determined at ±20°C from the second order polynomial show two distinct trends. At 20°C, α_{TE} decreases as concentration of $AlCl_3$ increases. At low temperatures, -20°C, α_{TE} increases with increasing salt concentration, indicating that at low temperatures the thermal expansivity can be very important, especially at high salt concentrations.

The value of α_{TE} obtained for all solutions is much higher (app. 6x) than that of water, and similar to that of some organic solvents (eg. methanol and carbon tetrachloride) where intermolecular forces are weaker. In this case the thermal energy is not required to break or lengthen "bonds", thus the

degree of expansion with temperature is higher as there is less resistance to expansion. The relatively large value of α_{TE}, indicates that the "volume change" per degree Kelvin may be quite significant. This factor is of interest as the solution is used in batteries which operate to -40°C where a significant volume change could affect the battery performance. The cell must be carefully designed so that at low temperatures the thermal contraction of the electrolyte does not result in exposed or dry electrodes. If the cathode is exposed then the system has a lower cathodic surface area and the power available at low temperatures would be reduced. In addition, non-uniform electrode stripping during discharge could give rise to safety problems. Thermal expansion is also an important factor to consider during high temperature operation. The electrolyte is located in the porous electrode medium and could expand and break up the active electrode mass. The battery capacity would then be reduced. Thermal expansivity is, in general, more important in rechargeable systems than in non-rechargeable systems where only one discharge is required. A rechargeable system is subject to multiple expansions and contractions as it characteristically has a much longer lifetime.

5.2 Viscosity Analysis

Viscosity can give an insight into the chemical and molecular structure of a liquid. Liquid structure is a time dependent phenomena resulting from the complex chemical and molecular interactions occurring in a solution. An example of liquid structure is found in the observation of water; the structure of liquid water results from hydrogen bond interactions between water molecules. Liquid structure is based on a time-averaged molecular distribution, meaning that observations made on picosecond time-scales would show structure - clearly preferred positions of atoms or molecules with respect to one another. Molecular observations made on a microsecond time scale would show no such definition, the motions and locations of molecules would appear random. A highly structured liquid (eg. water) would have a much higher viscosity than an unstructured liquid (like n-octane), where the molecular orientation is random. Of course, the molecular weight of the solvent is important since the viscosity also increases as the molecular weight increases. Solution viscosity may be correlated with ion - ion, ion - solvent, or solvent - solvent effects (Desnoyers and Perron, 1973). Viscosity can also indicate the presence of ionic or molecular species (Hildebrand, 1971, 1978). The raw data is presented in Figure 5.2. The dependence of liquid structure on the viscosity of $AlCl_3$ in $SOCl_2$ will be considered.

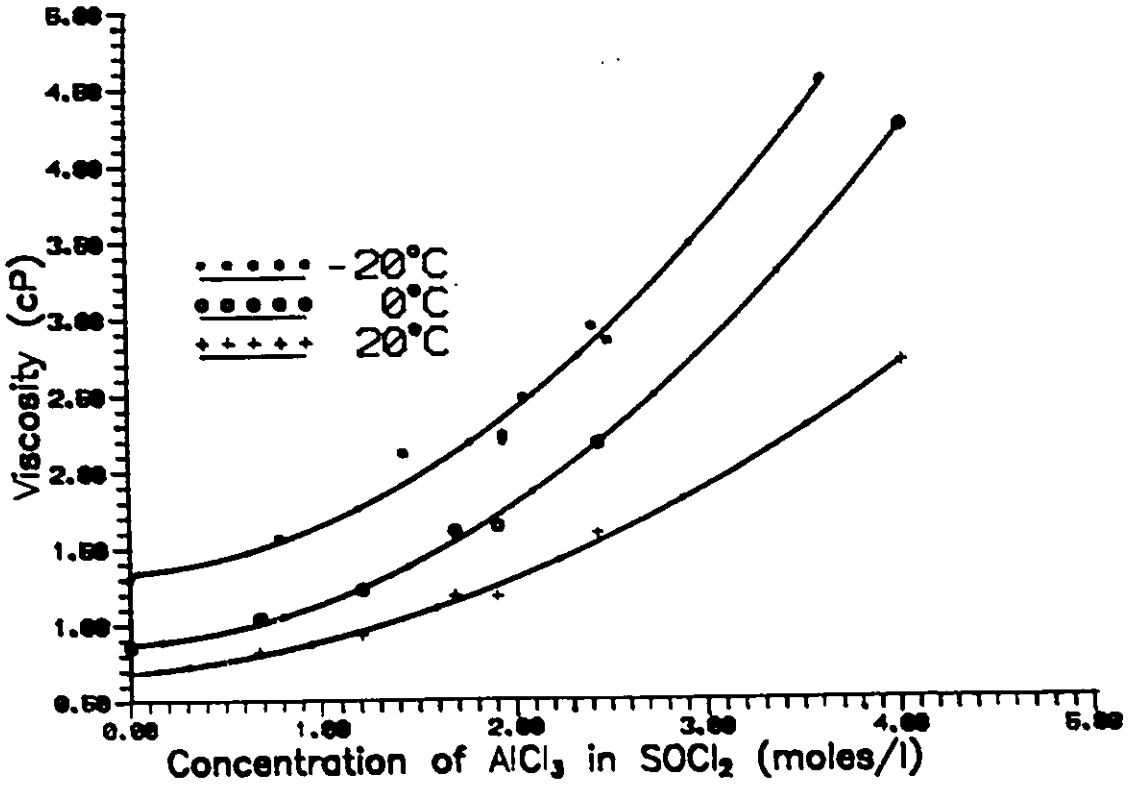

Figure 5.2: Viscosity of $AlCl_3/SOCl_2$ solutions as a function of $AlCl_3$ concentration (moles/l). Second order polynomial equations fit to the experimental data are shown as solid lines.

The viscosity is seen to follow two general trends; firstly, as the salt concentration increases the viscosity of the solution increases; and secondly, as the temperature decreases the viscosity of the solution increases. The viscosity versus concentration data was fitted to a second order polynomial using a least-squares method. The polynomial coefficients and "goodness of fit" parameters obtained are presented in Table 5.5 for the equation:

$$\eta = c_o + c_1 * c + c_2 * c^2 \qquad (5.5)$$

where,

η is the solution viscosity
c_o, c_1, c_2 are fitting parameters
c is the concentration (moles/l)

Table 5.5: Second order polynomial fit coefficients and goodness of fit parameters for viscosity as a function of $AlCl_3$ concentration.

Temp (°C)	c_o (cP)	c_1 (cP/M)	c_2 (cP/M^2)	Err^2	R^2
20.0±0.04	1.33±0.04	0.11±0.04	0.22±0.01	0.0916	0.987
0.0	0.88	0.07	0.19	0.0105	0.999
-20.0	0.68	0.11	0.10	0.0109	0.996

The lower temperature curves, 0 and -20°C, show a more rapid increase in the viscosity, beginning at 2.5 moles/l, than does the 20°C data. Tables 5.6 and 5.7 present the viscosity of

Table 5.6: Viscosity of several liquids as a function of temperature.

Liquid	Viscosity at -20°C (cP)	Viscosity at 0°C (cP)	Viscosity at 20°C (cP)
Pure $SOCl_2$	1.33 ± 0.04	0.88 ± 0.04	0.69 ± 0.04
1.0M $AlCl_3/SOCl_2$	1.65	1.14	0.89
2.0M $AlCl_3/SOCl_2$	2.41	1.78	1.29
4.0M $AlCl_3/SOCl_2$	5.20	4.20	2.67
Water[1]		1.787	1.002
Methanol[1]	1.22 (@-22°C)	0.82	0.597
Ethanol[1]		1.773	1.20
Propanol[1]		3.883	2.256
n-Octane[1]		0.706	0.542
Mercury[1]	1.855	1.685	1.554
SO_2Cl_2[1]	1.45	0.99	0.90

1 CRC Handbook, 64th Edition, p F38 - F42, 1983-84

pure $SOCl_2$, and $AlCl_3/SOCl_2$ solution as compared with that of several other organic, inorganic and aqueous solutions. The viscosity of pure $SOCl_2$ is less than that of pure water, over the full temperature range of our experiments, suggesting that $SOCl_2$ is less structured than water. Although $SOCl_2$ exists as molecular dimers, higher order species are unlikely to form as the dimer is essentially non- polar. Both methanol, and numerous alkanes (eg. n-octane) have a lower viscosity than does $SOCl_2$. As stated previously, viscosity is also a function of molecular weight. Comparing the viscosities of $SOCl_2$

Table 5.7: Viscosity of several solutions as a function of solute concentration at 20°C.

	Visc. at 2.5M ±0.04cP	Visc. at 5 M ±0.04cP	Visc. at 10M ±0.04cP	Visc. at 15M ±0.04cP	Visc. at 20M ±0.04cP
$AlCl_3$ in $SOCl_2$	0.73	0.79	0.97	1.24	1.60
NH_4Cl in water[1]	0.988	0.980	0.968	0.968	0.976
NH_4OH in water[1]	1.034	1.069	1.139	1.205	1.251
KCl in water[1]	0.996	0.994	0.986	0.995	1.010
KOH in water[1]	1.046	1.100	1.231	1.394	1.616

1 CRC Handbook of Chemistry and Physics, p D224-D272, 1983-83

(molecular weight 119 g/mole, η(20°C) 0.7 cP) and methanol (molecular weight 32, η(20°C) 0.6 cP), gives insight into the effects of intermolecular forces and molecular weight on viscosity. As these two species have similar viscosity but a large difference in molecular weight, one can conclude that the intermolecular forces are greater in methanol. Comparing the viscosity of $SOCl_2$ to n-octane (molecular weight 114 g/mole, η(20°C) 0.5 cP), two solvents of similar molecular weight, suggests that the "structure" associated with thionyl chloride is more defined than that in n-octane and that $SOCl_2$ contains associated species.

Of interest is that $SOCl_2$ is less viscous (more fluid) than is sulfuryl chloride (SO_2Cl_2), another inorganic fluid used

as an electrolyte in lithium batteries. Solution viscosity can be related to conductivity: in general, conductivity is inversely proportional to solution viscosity (Fuoss, 1959; Prue and Sherrington, 1961; Della Monica, 1984 . A high viscosity, therefore, results in a lower conductivity, and this factor could have negative effects on battery performance.

The solutions of $AlCl_3$ in $SOCl_2$ above a concentration of 0.5M all have viscosity greater than that of the pure solvent. These solutions, therefore, exhibit greater liquid structure than does the pure solvent, likely as a result of the presence of both molecular adducts and ionic species.

The effect of solute concentration on the viscosity of salt solutions in water obtained from the literature is compared to the effect of solute concentration on $AlCl_3/SOCl_2$ solutions at 20°C. The viscosity of the $AlCl_3$ solution increases as the salt concentration increases similar to the trend evident in the data for potassium and ammonium hydroxide salts in water. Addition of chloride salts to water causes a decrease in the viscosity. The hydroxide salts (and similarly, $AlCl_3$ in $SOCl_2$) increase the solution viscosity as they tend to increase, or leave unchanged, the solution structure. These solutions remain quite structured on the addition of the salts, that is, either solvent-solvent interactions remain intact or they are replaced with stronger solute-solvent interactions. In the case of $AlCl_3$ added to $SOCl_2$, the $AlCl_3$ molecules replace $SOCl_2$ molecules, maintaining the predominantly dimeric

structure of the solution. The chloride salts added to water reduce the viscosity of the solutions as they tend to lead to structure reduction in the liquid, or to a breakdown of intermolecular bonds.

It should be noted that the systems being studied are high concentration systems (0 to 5.0M). This corresponds to a mole ratio of as high as 1:2, $AlCl_3$:$SOCl_2$. This factor will enter into further discussions.

5.2.1 Jones-Dole Analysis of Viscosity Data

A Jones-Dole analysis was performed on the data obtained at 20, 0, and -20°C. The resulting plots are presented in Figure 5.3 and the constants and fitting parameters are presented in Table 5.8. The Jones Dole equation is presented below:

(2.1)

$$\frac{\eta_r - 1}{\sqrt{c}} = A_{JD} + B_{JD}\sqrt{c}$$

where, η_r is the reduced viscosity

c is the concentration (moles/l)

A_{JD} is the ion - ion parameter $(moles/l)^{1/2}$

B_{JD} is the ion - solvent parameter $(moles/l)^{-1}$

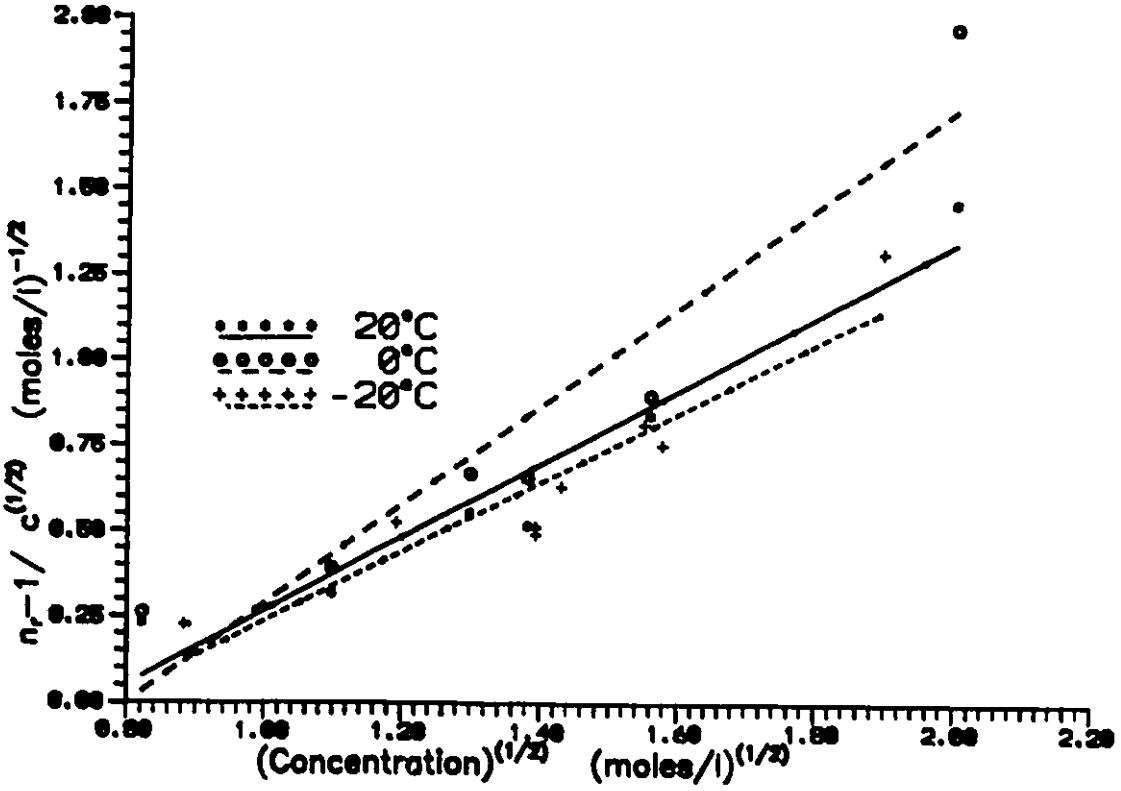

Figure 5.3: Jones - Dole plots for $AlCl_3$ in $SOCl_2$ for concentrations 0 to 4.0 M and temperatures from -20 °C to 20 °C

Table 5.8: Jones-Dole constants and fitting parameters for $AlCl_3$ - $SOCl_2$ over the concentration range 0 to 5 moles/l $AlCl_3$ and temperature range -20 to 20°C

Temp. (°C)	A_{JD} $(l/mole)^{0.5}$	B_{JD} (l/mole)	Err_2	R^2
-20	-0.77±0.04	1.01±0.02	0.0907	.8727
0	-1.16	1.46	0.1549	.9180
20	-0.80	1.07	0.0675	.9323
Literature[1]				
0	-1.0±0.2	1.3±0.1		

1 Szpak and Venkatasetty, 1984

From the information presented in Table 5.8 it is apparent that the results obtained at 0°C for the Jones-Dole analysis are of the same order of magnitude as those reported in the literature, (A, expt -1.16±0.04, lit. -1.0±0.2) and (B, expt 1.46±0.02, lit. 1.3±0.1) and within the experimental error. This agreement, based on the analysis of our data and the literature data, validates our experimental approach.

From the above data it is noted that trends in the value of A_{JD}, the ion-ion parameter, attributed to long-range coulombic forces and B_{JD}, the ion-solvent parameter are not obvious. The Falkenhagen expression for the calculation of A_{JD}, the ionic parameter, for 1:1 electrolytes is presented in the methodology section of this thesis (Equation (2.2)). Equation (2.2) shows that this parameter is coulombic in nature and dependent on the properties of the ions in solution (conductivity, mobility). The parameter B_{JD}, as stated

previously, is empirical. Both of these parameters exhibit a maximum in absolute value at 0°C. The positive value of B_{JD}, that remains relatively constant over the temperature range -20 to 20°C, indicates that the ion - solvent interactions are only weakly concentration dependent. The large positive value indicates that the solution is not highly associated. This is not in agreement with conclusions drawn from a physical analysis of the raw viscosity data, and is an indication of the inadequacies of this model. A decrease in the value of B_{JD} indicates structure breaking character as the value of B_{JD} is strongly correlated to the entropy of solution of the ions. That is, a decrease in B_{JD} has been correlated with decreased solution structure and, therefore, with an increase in solution entropy (randomness). In general, negative values of B_{JD} are found in aqueous systems with ions which exert a "structure breaking" effect on water. Large positive B_{JD} values are found in aqueous systems with ions which are strongly hydrated.

The results obtained for the Jones-Dole B_{JD} coefficient of the non-aqueous $SOCl_2$ system were large and positive over the full temperature range. A positive value was expected as negative values of B_{JD} are generally confined to aqueous systems. The decrease in the B_{JD} value at both higher temperatures (+20°C) and lower temperatures (-20°C) from the intermediate temperature value (0°C), indicates that under these conditions there is some evidence of the structure breaking effect of the $AlCl_3$ ions on the $SOCl_2$ solution. The

value of B_{JD} obtained experimentally at 0°C agrees with that found in the literature, 1.46±0.02 l/mole as compared with 1.3±0.1 l/mole in the literature (Szpak and Venkatasetty, 1984).

The value of the A_{JD} coefficient at 0°C is also in agreement with that found in the literature (expt. -1.16±0.04, lit. -1.0±0.2). The coefficient A_{JD} can however be calculated theoretically, and from theoretical analysis yields a positive value. As stated previously, the A_{JD} parameter was not calculated for the $AlCl_3/SOCl_2$ solution due to the complex nature of the solution. The solute in this solution is only partially dissociated, and complex equilibria exist between the many dissociation products present. Direct calculation of the A_{JD} parameter is possible for more simple systems. Although the theoretical value of A_{JD} is unknown for this system, values for simpler systems are known to be positive and thus, the negative experimental value of A_{JD} does not have physical significance. Furthermore, the value of A_{JD} obtained experimentally is of the same order of magnitude as B_{JD}, generally A_{JD} is much smaller than B_{JD}, as at high concentration the ion-ion (coulombic) interactions are dominated by the solvent-solute interactions (ie. the concentration dependence is generally first or higher order). This discrepancy may be attributed to the high concentration of solute used in this study. The non "real" value of A_{JD} found in this analysis, and in the literature, indicates the limits of the method.

The Jones-Dole model was developed for dilute solutions, in general having concentrations less than 1.0M. It is based upon a continuum model which assumes that the solute molecules are in dilute enough concentration that they are in contact with only solvent molecules - that their environment is a continuum of solvent molecules. In the solutions studied, this assumption is far from valid. The mole ratio of $AlCl_3$ to $SOCl_2$ can be as high as 1:2 for a 30 w/w% solution. At these high concentrations, the solute-solute interactions are significant, which, in effect contradicts the assumption of a continuum model. Furthermore, the Jones-Dole analysis is generally applied to ion - ion solution interactions. Again, this assumption is not valid as the $AlCl_3$ is known to form molecular adducts in solution with $SOCl_2$. Although this model may not be valid for the high concentrations studied, it yields a qualitative insight to the magnitude of the A_{JD} and B_{JD} parameters and can be useful if considered carefully. It is not surprising that the arbitrary separation of ion - ion and ion - solvent interactions proposed by this model fails to adequately account for the complex interactions occurring within the solution.

As previously described, the modified Jones-Dole equation incorporates an additional term, $D_{JD}c^2$. The modified Jones-Dole equation is presented below (Equation (2.5)).

$$\eta_r = \frac{\eta}{\eta_c} = 1 + A_{JD}\sqrt{C} + B_{JD}C + D_{JD}C^2 \qquad (2.5)$$

where,

η_r is the reduced viscosity
η_o is the solvent viscosity
η is the solution viscosity
A_{JD}, B_{JD}, and D_{JD} are the Jones-Dole parameters
c is concentration in moles/l

The additional term, $D_{JD}c^2$, is believed to account for higher terms of ion-solvent and ion-ion interactions. As with the simplified Jones-Dole method of analysis, the A_{JD} parameter is attributed to first order coulombic ion-ion interactions. Parameter B_{JD} is again an empirical factor believed to account for first order ion-solvent interactions. The addition of the higher order c^2 term improves the model considerably. This is apparent in both the fit to the data, and also in the value obtained for parameter A_{JD}, the ion - ion parameter. The value of R^2 is improved from approximately 90% to 99%, thus indicating that the data is better described by the modified model. The results obtained for the modified model are presented in Table 5.9. The A_{JD} parameter is generally small and positive, and thus, could have physical significance. A_{JD} is positive as the theoretical derivation defines only non-zero values. This parameter is generally small as it accounts for coulombic ion-ion interactions. The contribution to viscosity of these interactions is most important at very low concentration. At all other concentrations its effect is minimal and the coefficient is expected to be small.

Furthermore, analysis of the modified Jones-Dole equation

Table 5.9: Constants and fitting parameters for the modified Jones-Dole equation for $AlCl_3/SOCl_2$ solutions over the concentrations 0 to 4.0 M, and temperatures -20 to 20°C.

Temp. (°C)	A_{JD} $(M)^{-0.5}$	B_{JD} $(M)^{-1}$	D_{JD} $(M)^{-2}$	Err^2	R^2
-20	0.35±0.02	-0.25±0.01	0.209±0.005	0.053	0.9859
0	0.19	-0.09	0.242	0.012	0.9997
20	-0.07	0.23	0.134	C.023	0.9993

gives rise to several trends; the ion-ion parameter, A_{JD}, decreases (from 0.35 to -0.07) as temperature increases from -20 to 20°C. The constant A_{JD} is a function of solvent properties, ionic charges and mobilities, and temperature. As A_{JD} is inversely proportional to temperature it is expected to increase with a decrease in temperature.

Parameter B_{JD}, the ion - solvent term increases as temperature increases; at lower temperatures it is negative, and at higher temperatures it becomes relatively large and positive. This indicates an increase in the ion - solvent interactions as temperature decreases, and that the low temperature ionic species act as structure breakers. It is also an indication that the solution is highly associated. The structure breaking capacity of the added salt is reduced at higher temperatures as the solution structure is sufficiently broken by thermal agitation that the effect of the added ions is minimal.

The viscosity of a particular solution may be interpreted as the result of solute effects acting in the solvent. Solution

viscosity may be divided into the effect of the solvent, η_o, the effect of ion-ion interactions (coulombic), η_*, and the viscosity effects due to solvent-ion interactions (the B_{JD} factor effects), η_B. Thus,

$$\eta=\eta_o+\eta_*+\eta_B \qquad (5.6)$$
$$=\eta_o(1+A_{JD}\sqrt{C}+B_{JD}C)$$

In the Jones-Dole analysis, η_* is the coulombic effect $\eta_o A_{JD} c^{0.5}$. The solvent - ion effect, η_B, is $\eta_o B_{JD} c$. The viscosity B_{JD} value may be interpreted in terms of the competition of several ion - solvent terms. The competing factors include viscosity change due to size (including a mass effect) and shape of the ion (generally positive, and increasing with increasing ion size), η_e; viscosity change due to alignment or orientation of polar molecules by the electrostatic field (again positive), η_a; and the viscosity change associated with the distortion of the solvent structure leading to an increase in fluidity (negative, decrease in viscosity), η_d.

$$\eta_B=\eta_e+\eta_a+\eta_d=\eta_o B_{JD} C \qquad (2.4)$$

A large negative η_d results in a negative value for the B_{JD} parameter in the Jones-Dole equation. Thus the low temperature negative B_{JD} is the result of a large distortion term. As temperature increases, the distortion term also decreases as there is less competition between the electrostatic field and

the reduced solvent structure. The contribution of size and shape to factor B_{JD} remains relatively constant over temperature, and the alignment factor decreases slowly as temperature increases. The net effect is, however, for the B_{JD} factor to increase.

Coefficient D_{JD}, accounting for the higher order ion - ion and ion - solvent interactions, as well as changes arising from the dependence of the solute - solvent interactions on concentration, did not exhibit a clear trend over the temperature range considered. The value of D_{JD} remained fairly constant, relatively large and positive (0.15 to 0.25 ± 0.01). The positive value of D_{JD} is in agreement with general results reported in the literature (Desnoyers and Perron, 1972). The relatively constant value for D_{JD} indicates that there are no major changes in the solute - solvent interactions as a function of concentration at the different temperatures considered. That D_{JD} is relatively large, indicates under the concentration range considered (up to 4.5M), that the higher order interactions are significant.

The modified Jones-Dole analysis is still not a good model for this high concentration system. The A_{JD} value becomes negative at higher temperature, indicating that the model does not have physical significance under these conditions. As well, A_{JD} is of the same order of magnitude as B_{JD}, an in general should be much smaller. At high concentration the long-range ion - ion coulombic interactions are not as important as are

the ion - solvent interactions. Although an improvement over the unmodified model, it is still based on continuum theory of ion - ion interactions.

5.2.2 Energy of Activation Analysis of Viscosity Data

An analysis of the energy of activation for viscous flow was undertaken as the $AlCl_3/SOCl_2$ system was studied over a high concentration range. Activation theory has been proven successful at higher concentrations (Glasstone et al., 1941). Plots of $\ln\eta$ vs. 1/T were obtained for several concentrations, ranging from pure $SOCl_2$ to 4.0M $AlCl_3$ in $SOCl_2$, and are presented in Figure 5.4. A first order polynomial was fit using the least squares method to each set of concentration data. The results of these fits were used to determine E_{av} based on the equation:

$$\ln\eta = \frac{E_{av}}{R}\left(\frac{1}{T}\right) + A_{Eav} \qquad (2.9)$$

where,

E_{av} is the energy of activation (kcal/mole)
R is the gas constant (kcal/molel K)
T is temperature (K)
A_{Eav} is a constant

and are presented in Table 5.10 below.

Figure 5.5 shows plots of E_{av} vs concentration for the $AlCl_3$-$SOCl_2$ solutions studied. This theory is based upon the

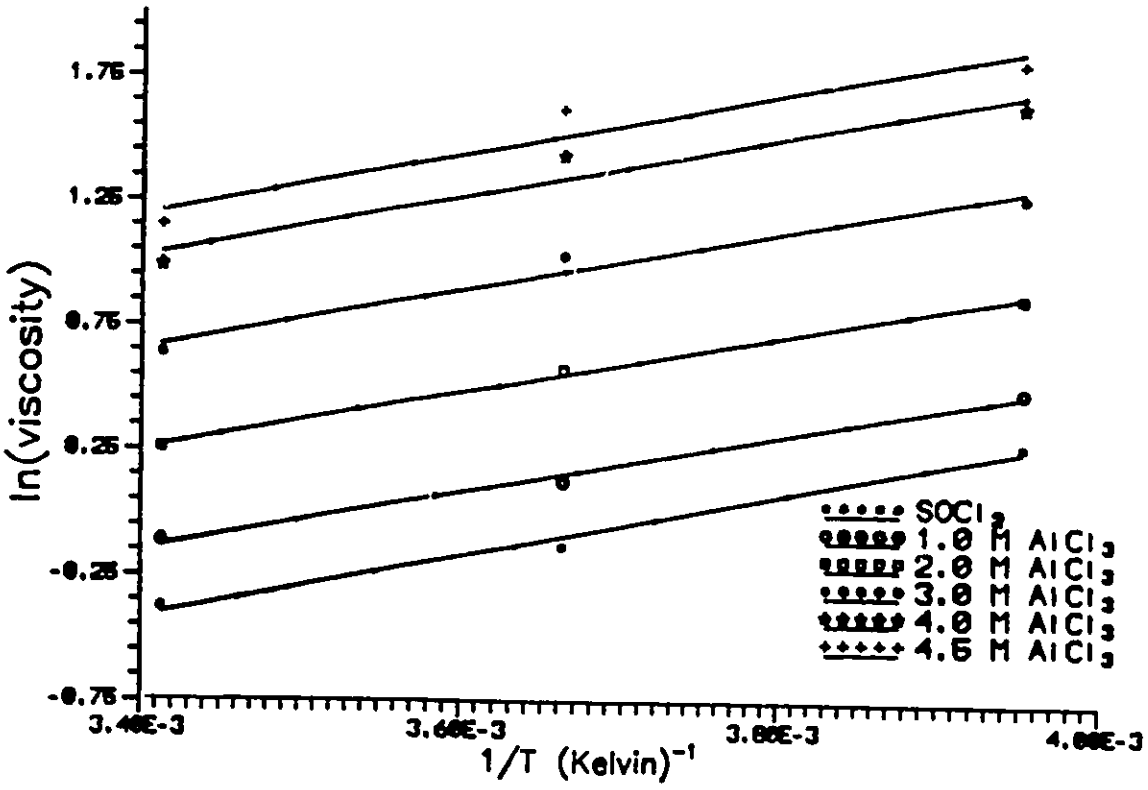

Figure 5.4: $\ln\eta$ vs 1/T for solutions of 0 to 4.5 M $AlCl_3$ in $SOCl_2$.

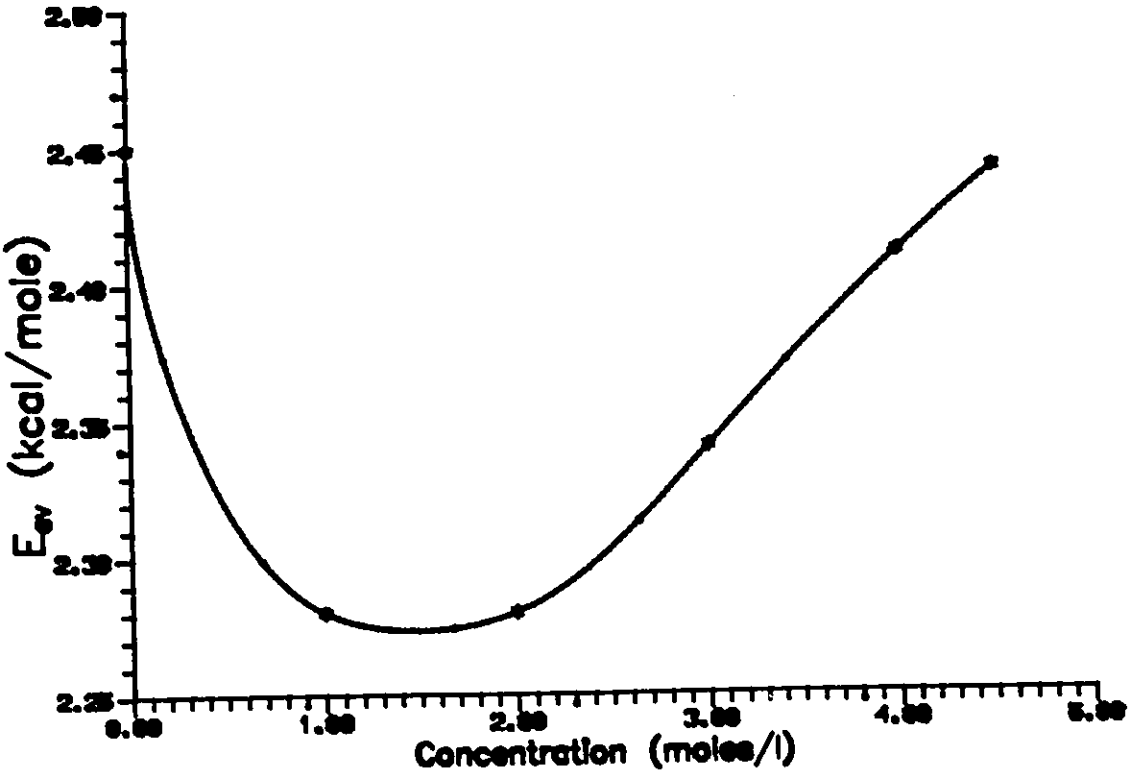

Figure 5.5: Energy of activation of viscosity as a function of $AlCl_3$ concentration.

Table 5.10: Constants and fitting parameters for the empirical Energy of Activation of viscosity equation.

Conc moles/l	E_{av}/R ($x10^{-3}$) K	E_{av} kcal/mol	A_{Eav}	Err^2	R^2
0.0	1.23±0.13	2.45±0.05	-4.61±0.01	2.5E-3	.98
1.0	1.15	2.28	-4.0439	1.2E-3	.99
2.0	1.15	2.28	-3.6435	5.9E-4	.99
3.0	1.18	2.34	-3.3491	5.9E-3	.97
4.0	1.21	2.41	-3.1018	1.3E-2	.94
4.5	1.23	2.44	-2.9884	1.7E-2	.93
1.5[1]		2.11			
3.0[2]		2.34			
4.5[3]		3.27			

1) 1.5M $AlCl_3$, 0.5M S, 0.5M SO_2, in $SOCl_2$ (Szpak and Venkatasetty, 1984)
2) 3.0M $AlCl_3$, 0.5M S, 0.5M SO_2, in $SOCl_2$ (Szpak and Venkatasetty, 1984)
3) 4.5M $AlCl_3$, 0.5M S, 0.5M SO_2, in $SOCl_2$ (Szpak and Venkatasetty, 1984)

hole theory of liquids described in the methodology section of this thesis. The energy of activation can be interpreted as the energy the molecules require to reorganize - ie. where a reorganization is equivalent to flow of the liquid. The reorganization is believed to occur by one of two mechanisms. "Jump distance theory" predicts that molecules can "jump" or "hop" from an occupied hole to an unoccupied hole, and that only the molecule that is jumping is affected. The energy of activation is the energy required to complete this jump. A second mechanism assumes that every molecule in the solution is involved in the rate determining reorganization which allows the molecules to move. In this case, the energy of activation is the energy required to allow all of the molecules to

reorganize. A rise in E_{av} is observed as the $AlCl_3$ concentration is increased from 1.0 M to 4.5M, indicating that more energy is required to reorganize the molecules as the salt concentration increases. This rise in E_{av} can be attributed to the increase in higher order molecular and ionic species in solution. In general, our results are in qualitative agreement with results reported by Szpak and Venkatasetty (1984) for a similar system, ($SOCl_2$, 0.5M S, 0.5M SO_2, $AlCl_3$). For very high $AlCl_3$ concentrations (4.5 M) our results show a less abrupt change with concentration in E_{av} than is reported in the literature. This indicates that the electrolyte free from discharge products (our study) is less concentration dependent than is the system simulating a partially discharged electrolyte that would contain SO_2 and S ($SOCl_2$, $AlCl_3$, 0.5M S, 0.5M SO_2).

Our experimental results indicate that kinetic rate limiting processes present at low concentrations are also present at higher concentrations and that increasing the salt concentration does not lead to an abrupt change in the kinetic processes occurring in solution. The slight minimum, followed by an increase in E_{av}, is an indication that solution composition does exhibit some concentration dependence, likely at higher concentrations higher order molecular adducts begin to form.

5.2.3 Batschinski-Hildebrand Analysis of Viscosity Data

The Batschinski-Hildebrand equation relates fluidity, ϕ,

$(1/\eta)$ to the ratio of unoccupied volume or free volume, $(v-v_o)$, to occupied volume, (v_o).

$$\phi = \frac{B_{BH}(v-v_o)}{v_o} = B_{BH}\frac{v}{v_o} - B_{BH} \qquad (2.11)$$

The parameter B_{BH} is a property of the liquid measuring its ability to absorb momentum generating the Newtonian flow. The value of B_{BH} is dependent on molecular size and shape and yields qualitative information on molecular structure. The constant v_o, the intrinsic volume, is defined as the volume the solution would occupy if it were a solid, provided that all the degrees of freedom present in the liquid were preserved. Mathematically, the intrinsic volume is defined as:

$$v_o = \lim_{\phi \to 0}(v) \qquad (5.7)$$

Table 5.11 lists the B_{BH} values and intrinsic volume obtained for the $AlCl_3/SOCl_2$ system as a function of $AlCl_3$ concentration.

Fluidity is plotted as a function of specific volume in Figure 5.6. Figures 5.7 and 5.8 show intrinsic volume and the Batschinski-Hildebrand B_{BH} parameter plotted as a function of concentration (moles/l). The order of magnitude of the experimental results agrees with those found in the literature (B_{BH} approximately 10, v_o approximately 0.5). The value of 10 for B_{BH} is characteristic of a molecular liquid, thus results

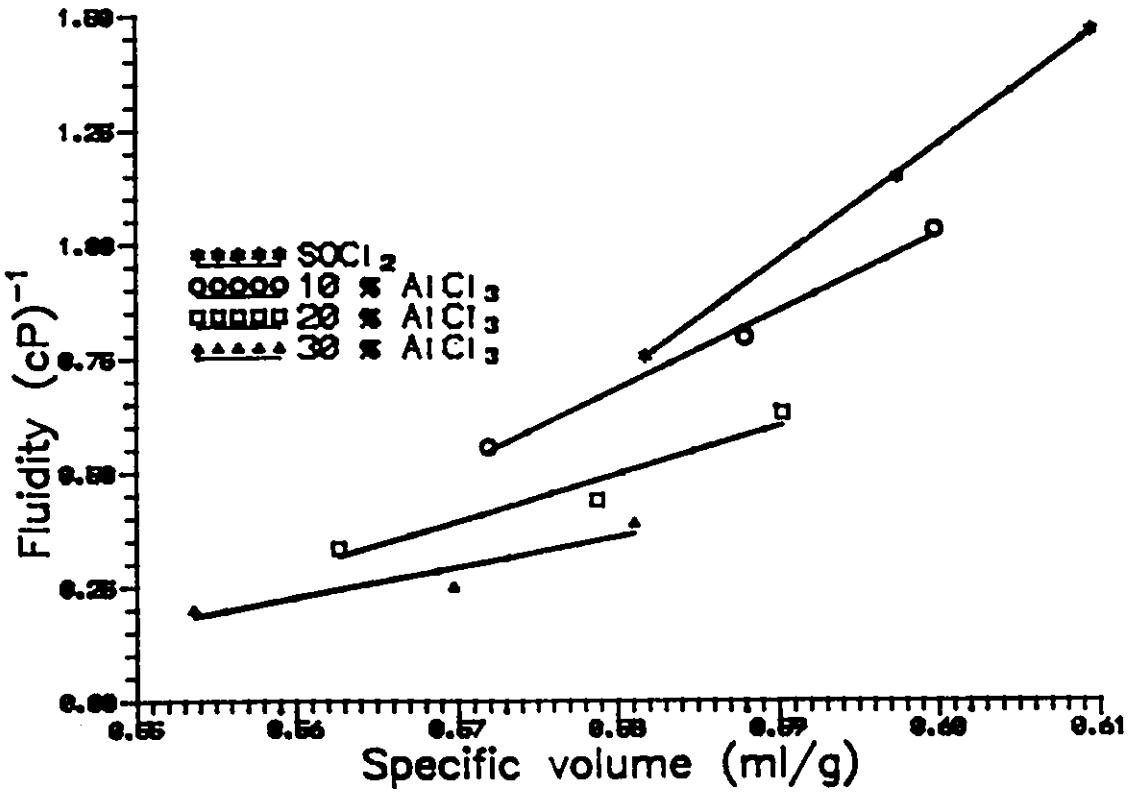

Figure 5.6: Fluidity vs specific volume for the $AlCl_3/SOCl_2$ solutions containing various $AlCl_3$ concentrations. First order polynomial equations fitted to the experimental data are shown as solid lines.

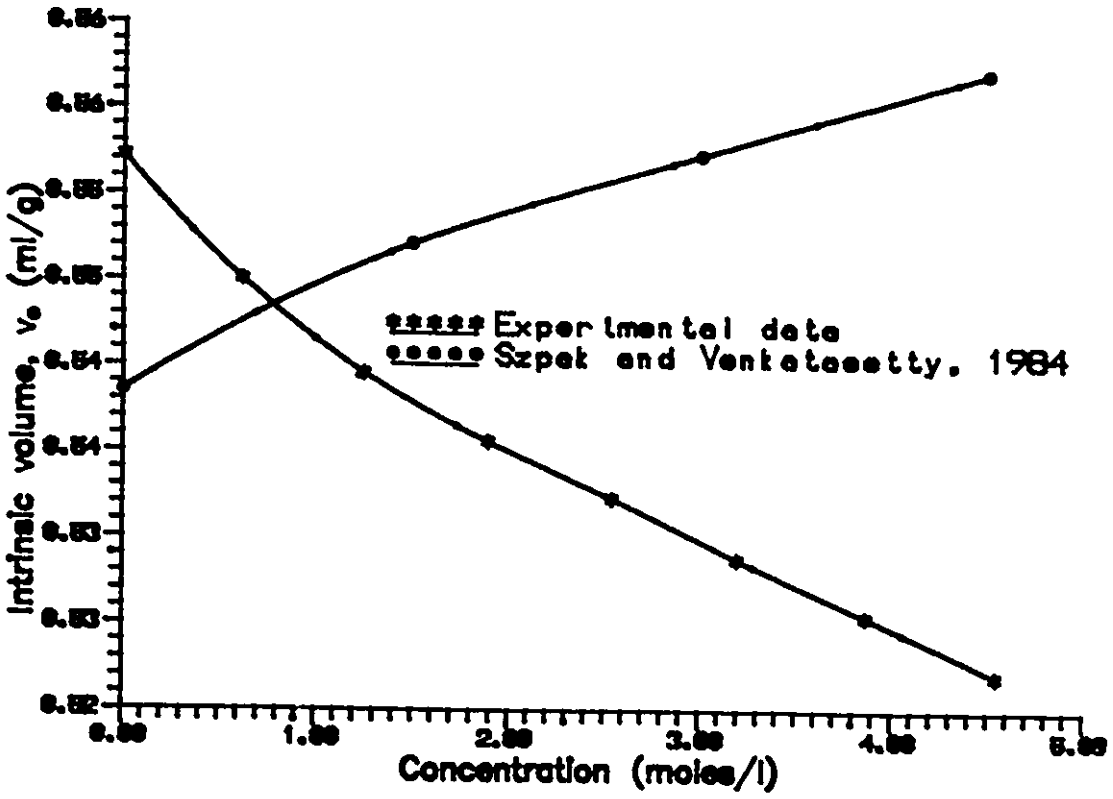

Figure 5.7: Intrinsic volume for the $AlCl_3/SOCl_2$ system plotted as a function of $AlCl_3$ concentration.

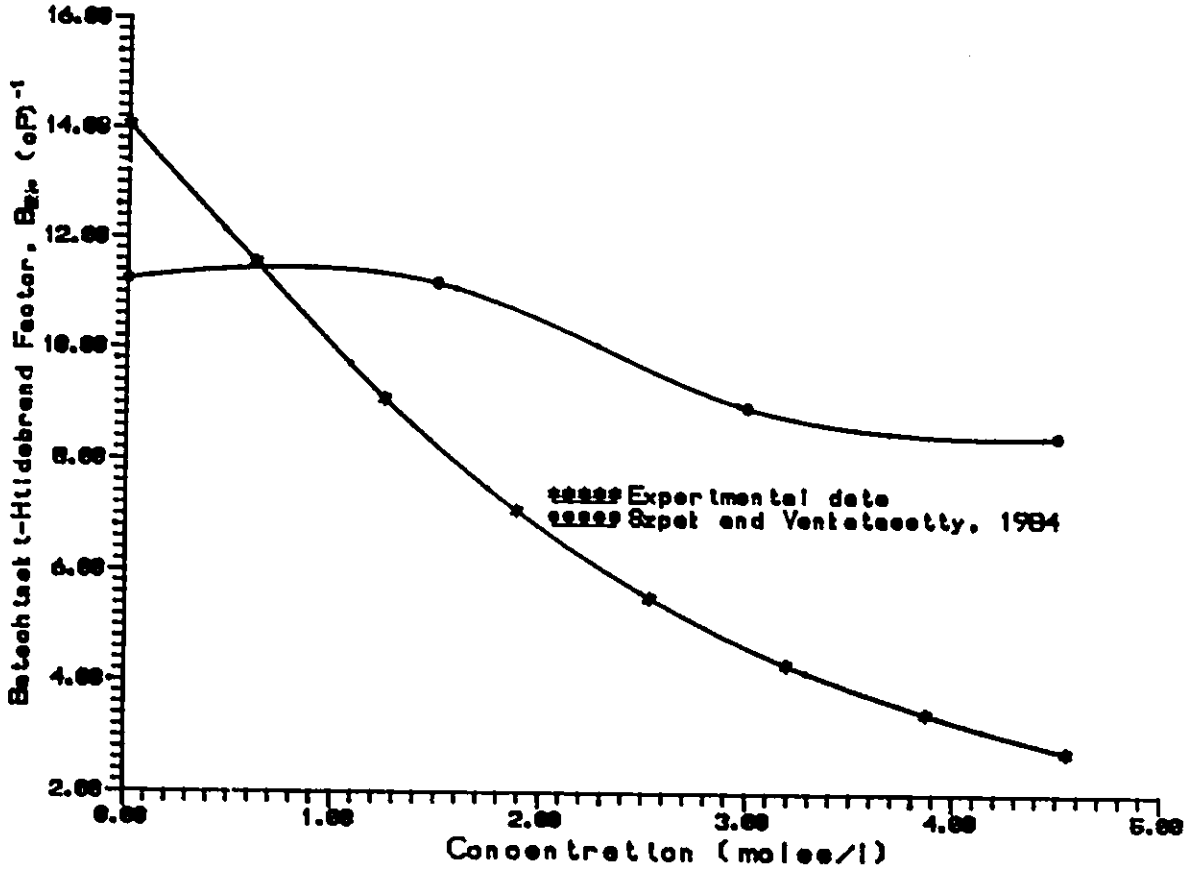

Figure 5.8: The Batschinski - Hildebrand parameter, B_{BH}, plotted as a function of $AlCl_3$ concentration.

Table 5.11: Batschinski-Hildebrand coefficients and goodness of fit parameters for the $AlCl_3/SOCl_2$ system as a function of concentration.

Weight % $AlCl_3$	Conc. moles/l	B_{BH} $(cP)^{-1}$	v_o (ml/g)	Err^2	R^2
0	0	14.05±0.01	0.5523±0.0004	7.03E-5	0.999
5	0.62	11.55	0.5450	8.98E-6	0.999
10	1.25	9.08	0.5395	7.44E-4	0.993
15	1.89	7.07	0.5356	2.12E-3	0.969
20	2.54	5.52	0.5323	2.96E-3	0.933
25	3.20	4.32	0.5288	2.94E-3	0.897
30	3.87	3.45	0.5255	2.94E-3	0.869
35	4.55	2.77	0.5221	2.01E-3	0.842
	0[1]	11.24	0.5385		
	1.5[1]	11.16	0.5471		
	3.0[1]	8.95	0.5523		
	4.5[1]	8.44	0.5572		
	C_3H_8[2]	18.6	61.0ml/mole		
	CCl_4[2]	17.4	88.3ml/mole		

1 Szpak and Venkatasetty, 1984
2 Hildebrand, 1971; 1978

obtained indicate $SOCl_2$, and the $SOCl_2/AlCl_3$ solutions are molecular liquids. This is in agreement with spectroscopic studies which show $SOCl_2$ to be a dimerized liquid and the solution to form $AlCl_3$ - $SOCl_2$ molecular adducts. The addition of $AlCl_3$ reduces the B_{BH} value from that of pure $SOCl_2$. Assuming a relatively constant value of v_o, a decrease in B_{BH} corresponds to a decrease in fluidity, ϕ, and an increase in viscosity.

This is expected as the more concentrated the $AlCl_3/SOCl_2$ solution, the higher the viscosity, and hence the lower the B_{BH} value. The change in B_{BH} may also be attributed to the $AlCl_3$ salt modifying the $SOCl_2$ - $SOCl_2$ dimerized structure to form the $AlCl_3$ - $SOCl_2$ molecular adduct.

The reduction of B_{BH} can also be an indication of the presence of newly formed ionic species. The B_{BH} values gradually decrease as the solute concentration is increased. The change is gradual, thus indicating that any change in solution composition is also gradual. Thus there is no evidence of an abrupt change in the species distribution at a particular solute composition, rather the distribution is a continuous smooth function of solute concentration.

The value of the intrinsic volume was also seen to decrease as a function of concentration. This is an indication that the solution containing the molecular adduct has a smaller volume than the dimerized solvent species. This fact is reflected in the density of solutions, where $SOCl_2$ has a lower density than does $AlCl_3$. The values obtained experimentally do not agree with those in the literature, except in order of magnitude. Results obtained by Szpak and Venkatasetty (1984), indicate an increasing intrinsic volume with increasing salt concentration. Intuitively this relationship seems incorrect. The salt solutions have higher density, and hence should be characterized by a lower intrinsic volume. Furthermore, the addition of the salt leads to dissociation to charged species

which has the effect of increasing the closeness of molecular packing through electrostriction, and hence to a decrease in the specific and intrinsic volumes (Frenkel, 1955). Electrostriction is the process whereby an ion or solute molecule in solution electrostatically attracts the solvent molecules into a space that was originally occupied by fewer molecules before the addition of the solute. Szpak and Venkatasetty (1984) do not attempt to explain why they obtained an increasing intrinsic volume for the $AlCl_3/SOCl_2$ solutions.

The Batschinski - Hildebrand analysis gives no indication of an anomaly occurring between 0 and 1.0M $AlCl_3$ as was evident in the energy of activation analysis. A low concentration analysis would be of interest to examine the region between 0 and 1.0 M $AlCl_3$, however, the concentration of the battery electrolyte is always much greater than 1.0 M $AlCl_3$, typically 1.8M, making this region not critical in the context of this study.

5.3 Electrolytic Conductivity

The general form of an electrolytic conductivity (κ,Scm-1) - concentration curve for both weak and strong electrolyte solutions is presented in Figure 5.9 (Brown, 1984). Over a large concentration range both weak and strong electrolyte solutions show a maximum in electrolytic conductivity. Often, however, the maximum is not observed experimentally as solution saturation occurs at a concentration below that of the maximum. In such a case, only the left most portion of Figure 5.9 is observed. For strong electrolytes the characteristic shape of Figure 5.9 is the result of competing effects of concentration of charge carriers, and ionic interference, or decreasing ionic mobility. As concentration increases, the number of ions in solution increases, resulting in a positive contribution to conductivity; the ionic mobility, however, decreases, and therefore, contributes a negative effect to the solution conductivity. The observed conductivity is the result of competition between these factors.

The $AlCl_3/SOCl_2$ solutions are weak electrolyte solutions characterized by conductivity in the μScm^{-1} range, and small dissociation constants for the dissolution of the solute molecules into ions. The electrolytic conductivity versus concentration curve is governed by the competing effects of concentration, the degree of ionisation, and the mobility of ions. As with strong electrolytes, as the concentration increases, the total number of solute molecules in a given

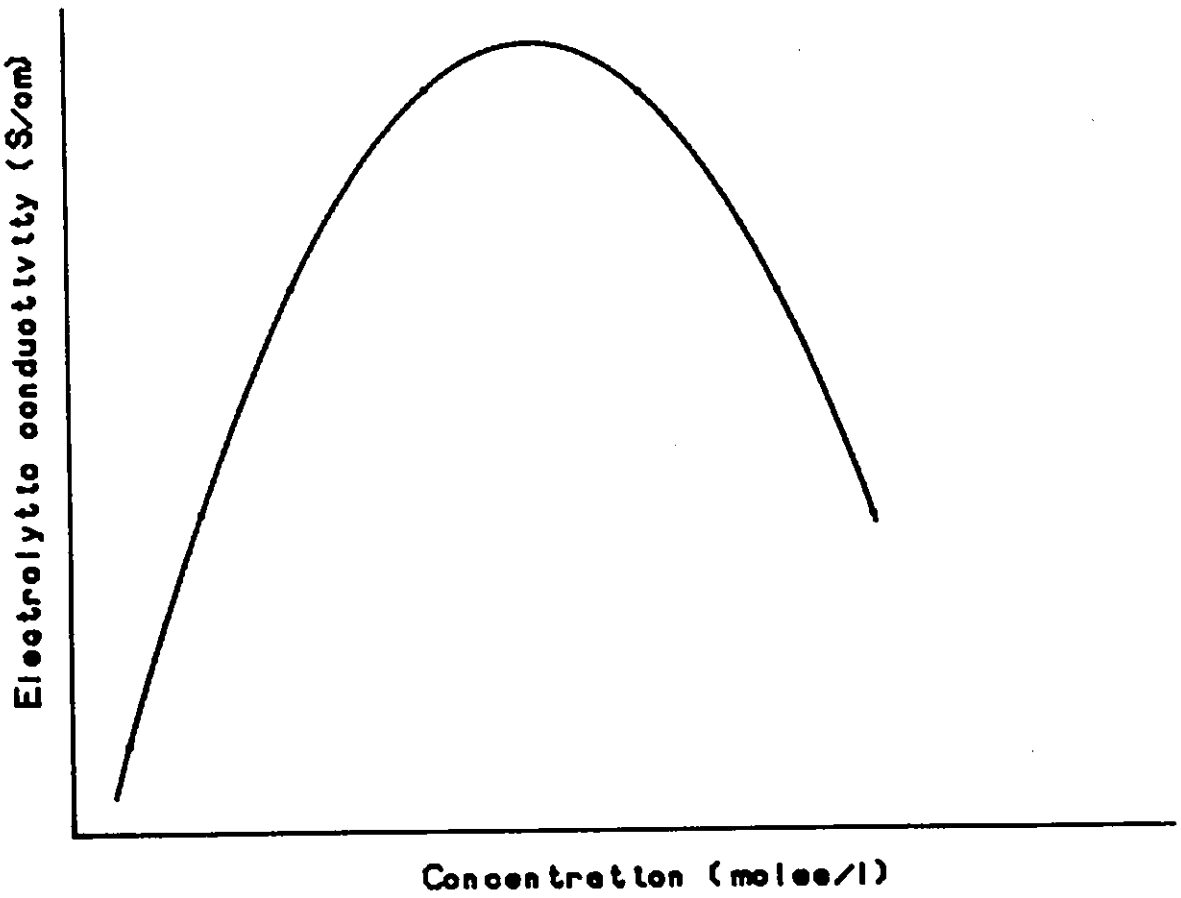

Figure 5.9: The general shape of an electrolytic conductivity - concentration curve for both weak and strong electrolytes.

volume of solution increases, resulting in a positive contribution to conductivity, the mobility of ions in solution, however, decreases (a negative effect). An increase in the total number of solute molecules present results in a decrease in the degree of ionisation of the weak electrolyte solution. This factor contributes to a decrease in conductivity. The net result of these effects is an increasing electrolytic conductivity for low concentration, and at higher concentration the ionisation and mobility factors gain dominance, and conductivity decreases with increasing concentration.

Table 5.12: Fitting constants and parameters for electrolytic conductivity as a function of concentration for $AlCl_3/SOCl_2$ from 0 to 4.0 M.

$\kappa = c_1$[concentration] + c_0; concentration = moles/l

Temp. (°C)	c_0 (Scm^{-1}) $x10^{-6}$	c_1 (Sl/cm mol) $x10^{-6}$	Err^2	R^2	Sig
25	2 ± 20	198 ± 8	1.23E4	0.930	3.57E-2
10	-37	144	3.25E4	0.846	3.37E-3
0	-17	102	3.81E3	0.935	3.73E-4
-33.9	-26	99	3.06E1	0.997	3.74E-2

The experimental results obtained agree in general with those available in the literature - ranging from (10 to 600 μScm^{-1}) over the concentration and temperature ranges considered; (0 to 4.5 M) and (-35 to 25°C) respectively. A linear curve was fit to the experimental data, representing the

left portion of Figure 5.9 The results of this fit are exhibited in Table 5.12 and Figure 5.10.

The curves described in Figure 5.10, and Table 5.12 do not represent the physical significance of the conductivity data over all concentration ranges as indicated by the negative value of c_0, the intercept. Physically, c_0 is the electrolytic conductivity of the pure solvent, $SOCl_2$, and should be a small, but positive value. For thionyl chloride the electrolytic conductivity is very low, approximately (0.04 to 0.14)μScm^{-1} (less than 0.31 % of the conductivity of 0.36 M $AlCl_3$ solution at -34°C, the least concentrated solution studied).

The scatter of the data and the resulting negative value of the intercept may be the result of several factors. The electrolytic conductivity of the solutions was found to be very sensitive to impurities introduced in either the solute or the solvent, or to solution contamination due to the environment during preparation, due to the use of plastics during preparation and due to solution aging. The decomposition of $SOCl_2$ in the presence of water may have accounted for this degradation. The decomposition products of $SOCl_2$, in the presence of water are:

$$\begin{aligned} SOCl_2 + 2H_2O \rightarrow 4H^+ + SO_3^{2-} + 2Cl^- \\ \rightarrow HCl(g) + SO_2(g) + H_2O \end{aligned} \qquad (5.8)$$

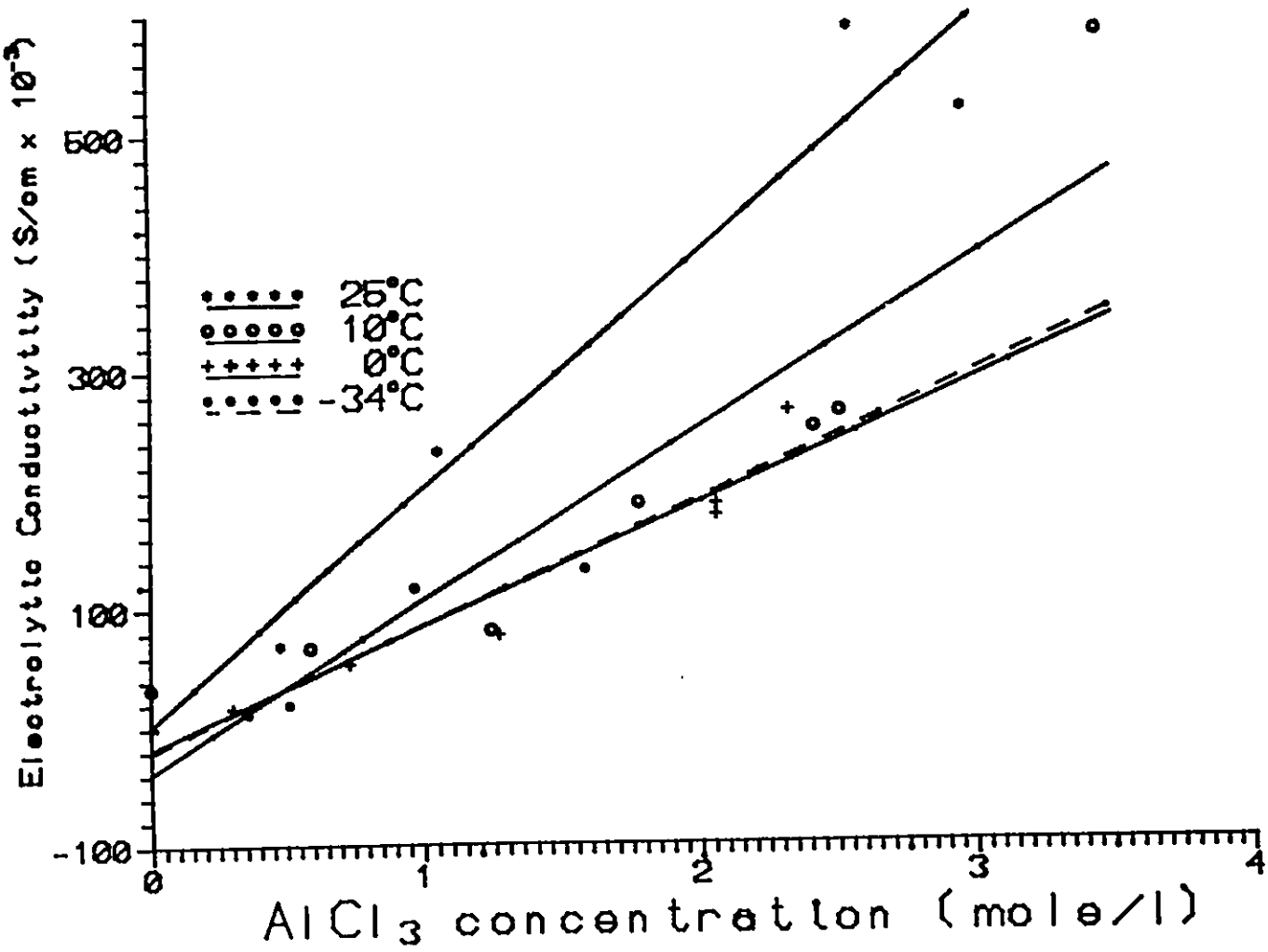

Figure 5.10: Electrolytic conductivity vs concentration for $AlCl_3$ in $SOCl_2$. First order polynomial equations shown as solid lines.

and on warming $SO_2(g)$ and HCl(g) are evolved. In the presence of $AlCl_3$ and water, $SOCl_2$ is readily decomposed, again forming SO_2 and HCl. Aluminum trichloride is readily hydrated in the presence of water.

$$AlCl_3 \cdot xH_2O + xSOCl_2 \rightarrow AlCl_3 + xSO_2(g) + 2xHCl \qquad (5.9)$$

Proton NMR spectroscopy indicates that the $AlCl_3$ solute forms complexes with excess water present. A complex equilibria is established with $AlCl_3$ and H_2O forming $Al(OH)Cl_2$, $Al(OH)_2Cl$ and a small amount of $Al(OH)_3$ (Hong et al., 1989).

Solutions prepared in an argon atmosphere glove box and stored in glass, platinum and teflon cells under argon exhibited a variation in conductivity over a period of 24 hours. The aged solution had higher conductivity than the fresh solutions. Assuming the increased conductivity was the result of the degradation of $SOCl_2$ in the presence of water, the increased conductivity results from the formation of HCl, H^+, and Cl^-. These small ions have high mobility when compared with the larger charged species in purified $AlCl_3/SOCl_2$ solutions.

At low concentrations and temperatures, the Wayne-Kerr bridge (conductivity meter) was operating at its sensitivity limit. This could have been remedied by redesigning the conductivity cell - larger electrode area and smaller separation between electrodes would yield a cell capable of measuring lower conductivities. This was not a suitable solution as the closed system cell was not commercially

available, and having a cell custom built was not practical due to time constraints.

The conductivity of the $AlCl_3/SOCl_2$ solutions is similar to that of double distilled water. The solution conductivity range from (10 to 200)μScm^{-1}, and that of double distilled water was measured in the laboratory to be 3 μScm^{-1}.

As stated previously, in the concentration range considered it is the left most region of Figure 5.9 that is under investigation. This is the region where the concentration effect is dominant over the ionisation effect and that conductivity is seen to increase with increased solute concentration.

Of general interest is the molar conductivity, defined as the electrolytic conductivity divided by concentration.

$$\Lambda = \frac{\kappa(Scm^{-1})}{c(mole/cm^{-3})} = \frac{Scm^2}{mole} \qquad (5.10)$$

where,

Λ is the molar conductivity
κ is the electrolytic conductivity
c is molar concentration

A plot of molar conductivity, Λ, as a function of $c^{0.5}$ or 1/c (c = concentration) yields characteristic curves for both weak and strong electrolyte solutions (see Figure 5.11). For strong electrolytes, the molar conductivity reaches a maximum at zero salt concentration, Λ_0. For weak electrolytes, molar conductivity increases exponentially as concentration

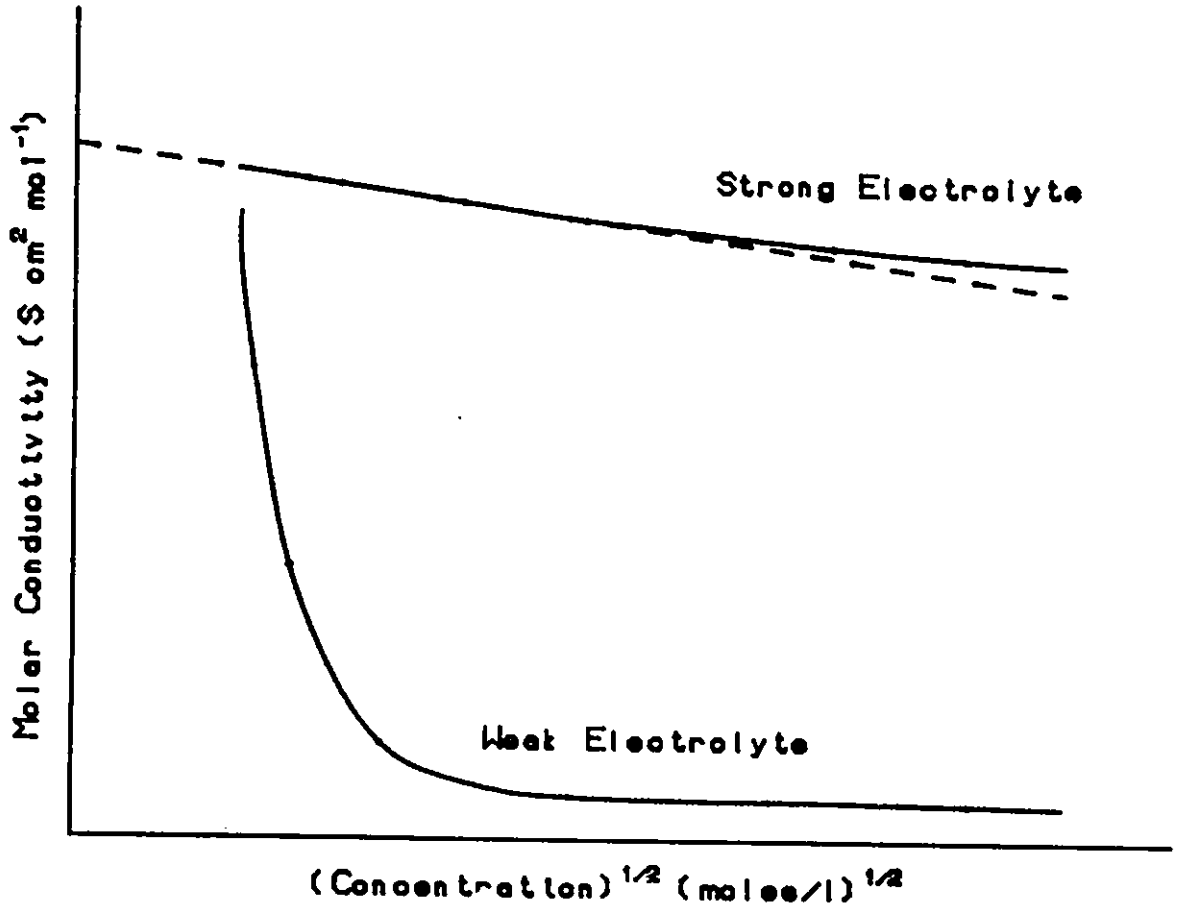

Figure 5.11: Molar conductivity shown as a function of $\sqrt{c}$

decreases. Λ_0, the molar concentration at infinite dilution or zero concentration can be calculated for weak electrolyte solutions provided the molar ionic conductivities are known.

The characteristic plots of electrolytic and molar conductivities for both many weak and strong electrolytes may be obtained from the literature. Lithium chloride in water is a strong electrolyte, with electrolytic conductivity ranging from 10 to 170 mS/cm. A maximum in electrolytic conductivity is observed at 5.8 M. The molar conductivity is approximately linear with respect to the square root of concentration in the region of 0.12 M to 8.3 M (CRC, p D239, 1983-84). The molar conductivity ranges from 86 S cm^2/mole (0.12 M) to 17.5 S cm^2/mole (8.3 M). Acetic acid, a weak electrolyte in water, also exhibits the characteristic curves shown in Figures 5.9 and 5.11. The maximum in electrolytic conductivity achieved for acetic acid is 1.7 mS/cm, this maximum occurred for concentrations between 2 and 4 M. The molar conductivity was found to be highest at low concentrations (3.6 S cm^2/mole at 0.08 M), and decreases exponentially with the square root of concentration. At high concentrations, molar conductivity of acetic acid is relatively constant (0.1 S cm^2/mole for concentrations between 2.6 and 3.2 M) (CRC, p D225, 1983 - 1984).

Plots of the molar conductivity as a function of the square root of concentration are presented in Figures 5.12 and 5.13 for experimental and literature data (Venkatasetty and

5.13 for experimental and literature data (Venkatasetty and Szpak, 1983) in the high concentration range. The experimental data resulted in relatively constant, though slightly decreasing, molar conductivity over the concentration range considered for each temperature. It is believed that the results obtained represent the molar conductivity of the right most portion of Figure 5.11.

The literature data exhibits a maximum at 3.0 M for all temperatures. Molar conductivity at 1.5 and 4.5 M is relatively constant and shows a slight decrease with increasing concentration, similar to the experimental data. The anomaly at 3.0 M may be the result of an error throughout the literature analysis due to the way in which the data was presented (fit as a function of temperature for three different concentrations), or due to experimental error. This anomaly was also present in both density and viscosity measurements as well, and is likely an artifact. The literature and experimental data are the same order of magnitude. In general, for both literature and experimental data, conductivity decreases as temperature decreases, and the relatively constant values of molar conductivity obtained indicate that we are considering the high

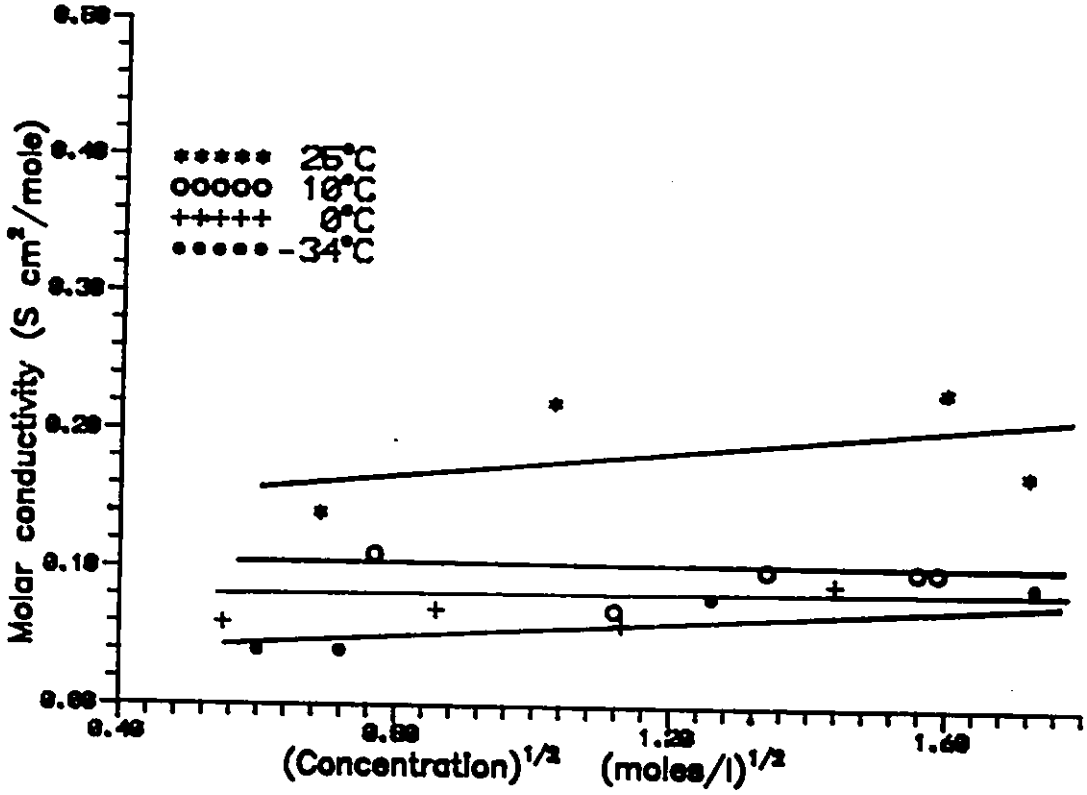

Figure 5.12: Experimental molar conductivity as a function of $\sqrt{c}$ for $AlCl_3$ in $SOCl_2$.

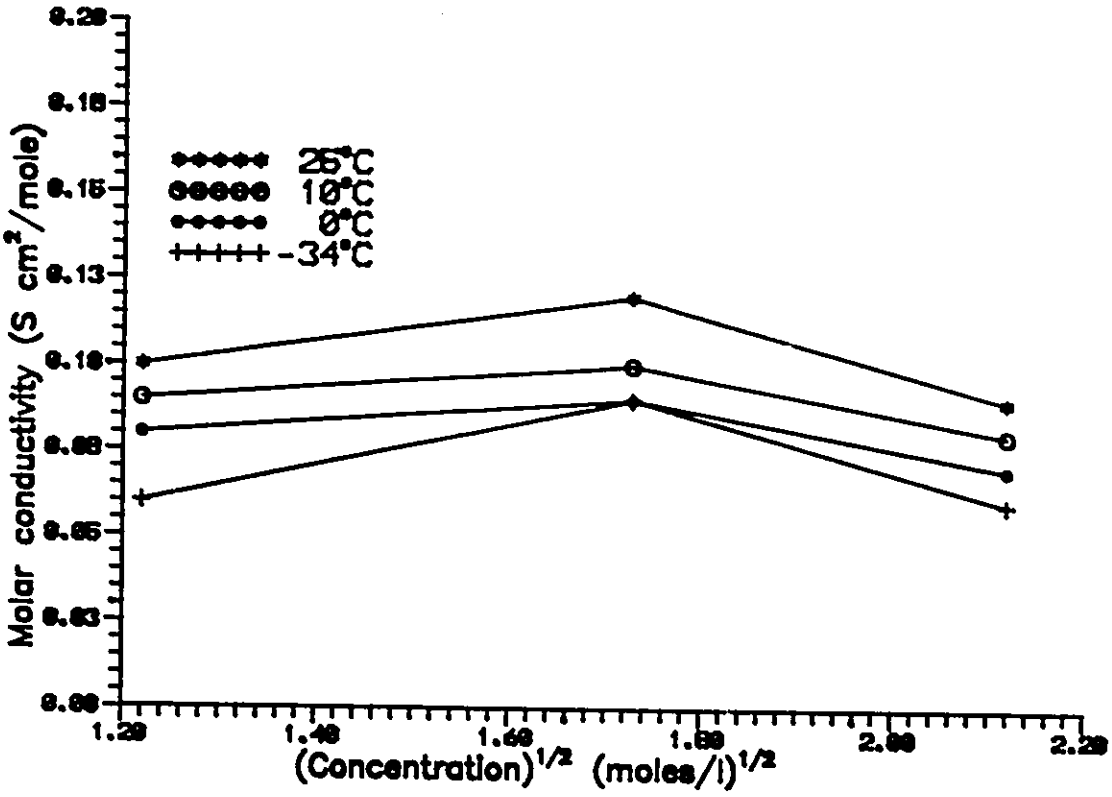

Figure 5.13: Molar conductivity reported in the literature (Venkatasetty and Szpak, 1983) as a function of $\sqrt{c}$ for $AlCl_3$ in $SOCl_2$

concentration region of Figure 5.11.

Figure 5.14 shows molar conductivity of the $AlCl_3/SOCl_2$ solution at 25°C, including data obtained from Salomon's low concentration study (1981). With molar conductivity plotted on this larger scale it becomes apparent that the experimental data and the literature data (Szpak and Venkatasetty, 1984) are in qualitative agreement. Also, as suspected, the experimental data and Salomon's data describe the correct shape of the molar conductivity verses square root of concentration curve for a weak electrolyte, as exhibited in Figures 5.11 and 5.14. The $AlCl_3/SOCl_2$ solution is a weak electrolyte solution characterized by a low concentration of ions in solution. At very low concentration (less than 0.1M) the conductivity increases, the degree of ionisation and the ionic mobilities are very high. The result is a large positive value for molar conductivity for solutions with low solute concentrations.

5.3.1 Energy of Activation for Conductance

Similar to the analysis of the energy of activation of viscosity, the energy of activation for conductance can be calculated. Assuming that conductances is controlled by a diffusional process governed by a rate limiting step, then it may be represented by Equation (5.11).

$$\Lambda = A_{Eac} e^{-\frac{E_{ac}}{RT}} \qquad (5.11)$$

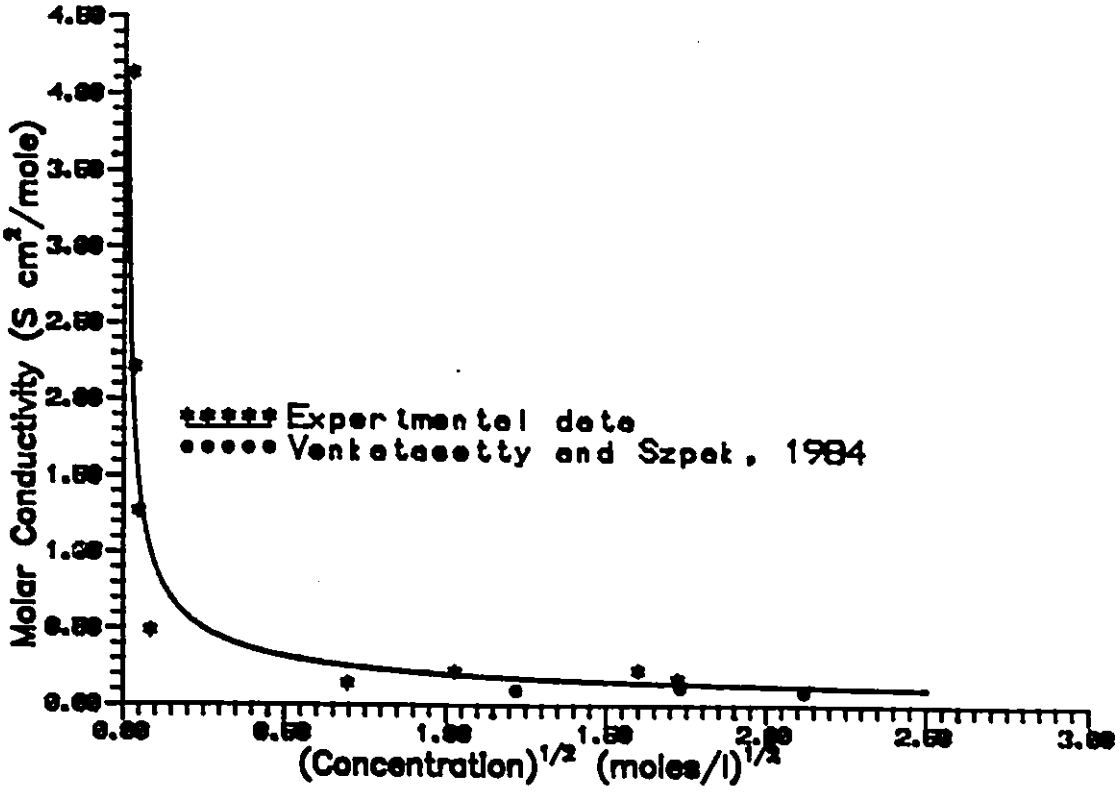

Figure 5.14: Molar conductivity over the concentration range 5×10^{-4} to 4M $AlCl_3$ in $SOCl_2$ at 25°C. Low concentration data determined by Salomon (1981).

or

$$\ln\Lambda = -\frac{E_{ac}}{R}\left(\frac{1}{T}\right) + K$$

where,

A_{Eac} and K are constants, and $K = \ln(A_{Eac})$
Λ is the molar conductivity (S cm^2/mole)
E_{ac} is the energy of activation for conductivity
R is the gas constant (1.98717 cal K^{-1} mol^{-1})
T is temperature in Kelvin

The natural logarithm of molar conductivity was plotted as a function of inverse temperature for concentrations ranging from 1.0 to 4.5 M for both experimental and literature data. The experimental values of the molar conductivity were obtained by first calculating values of the electrolytic conductivity from curves defined in Table 5.12, then calculating the molar conductivity corresponding to this value of electrolytic conductivity. Five different concentrations of $AlCl_3$ salt in $SOCl_2$ were considered. The natural logarithm of molar conductivity was then calculated and plotted as a function of inverse temperature for each of the five concentrations. A linear (first order) polynomial was fit to each set of concentration data using the least-squares method. The results of these fittings are presented in Table 5.13 below.

The value of E_{ac} was calculated from the slope of curves described in Table 5.13, E_{ac} = -slope x R, where R is the gas constant. The activation energy for conductance is presented

Table 5.13: Fitting parameters and coefficients for linear plots of lnΛ vs 1/T for $AlCl_3$ concentration ranging from 1.0 to 4.5 M $AlCl_3$

$$\ln\Lambda = c_0 + c_1(1/T)$$

Concentration $AlCl_3$ in $SOCl_2$	c_o (±0.13)	c_1 (K) (±0.04E3)	Err^2	R^2	Sig
1.0M	1.51	-1.02E3	0.186	0.678	0.1769
2.0	1.07	-8.67E2	0.133	0.682	0.1740
3.0	0.90	-8.11E2	0.122	0.672	0.1806
4.0	0.89	-8.06E2	0.114	0.684	0.1731
4.5	0.86	-7.95E2	0.113	0.680	0.1755
Literature[1]					
1.5	-0.39	-5.74E2	1.40E-5	0.999	5.60E-5
3.0	-1.47	-2.24E2	1.26E-2	0.605	2.22E-1
4.5	-0.91	-4.64E2	2.00E-2	0.803	1.04E-1

1 Szpak and Venkatasetty, 1984

in Table 5.14 and Figure 5.15.

For experimental data, the energy of activation is seen to decrease with increasing concentration. This general trend is also observed for the value of E_{ac} calculated from the data available in the literature. The anomaly in the literature calculated value of E_{ac} exists at 3.0 M, and the E_{ac} is a minimum at this concentration. The value of E_{ac} for the $SOCl_2/AlCl_3$ solutions (1 to 2 kcal/mole) is considerably lower than that of a typical aqueous solution (3.36 kcal/mole)(Kortüm and Bockris, 1951).

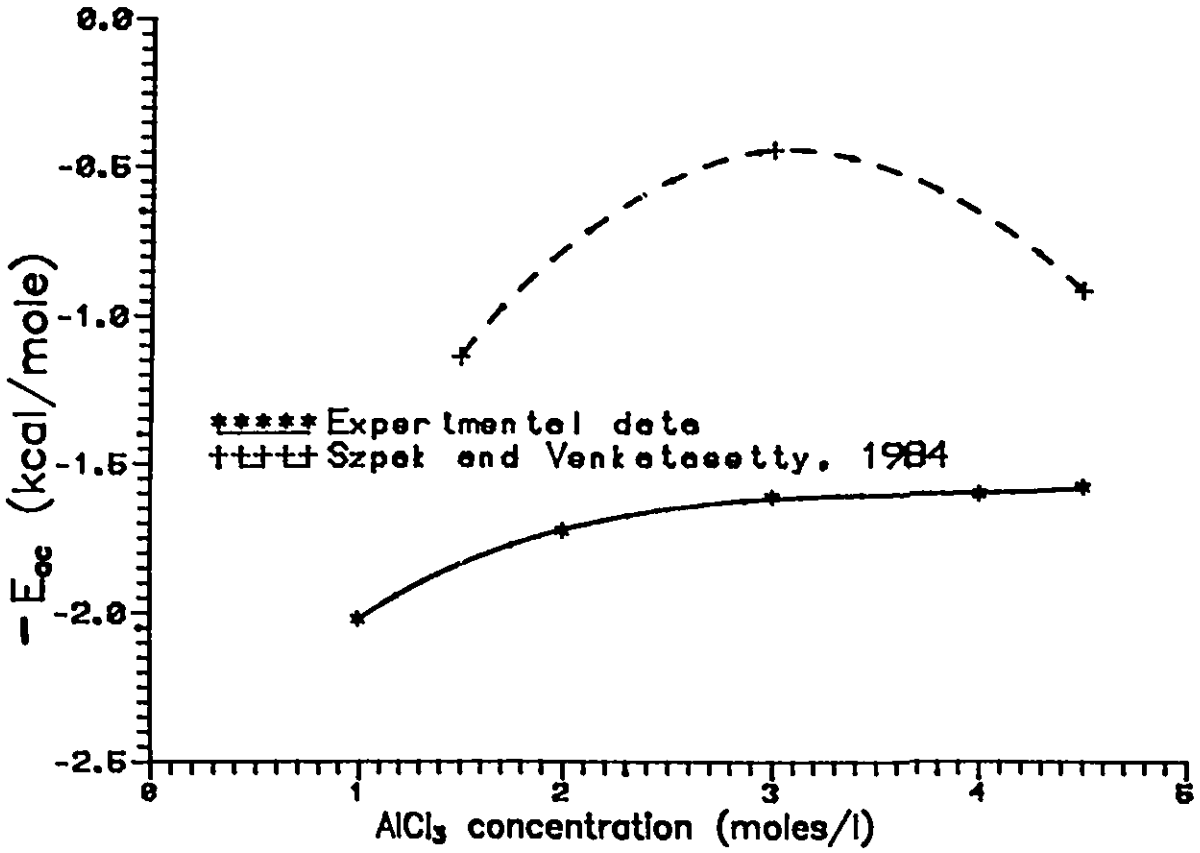

Figure 5.15: Energy of activation for conductivity as a function of $AlCl_3$ concentration.

Table 5.14: Energy of Activation for conductance for various solutions

$AlCl_3/SOCl_2$	
Concentration (moles/l)	$\lvert E_{ac} \rvert$ (kcal/mole)
1.0	2.02 ± 0.08
2.0	1.72
3.0	1.61
4.0	1.60
4.5	1.58
Literature[1]	
1.5 [1]	1.141
3.0 [1]	0.446
4.5 [1]	0.921
Aqueous solutions[2]	3.36
$SOCl_2$+.5MS+.5MSO_2 +X$MLiAlCl_4$ [3]	
1.5 [3]	1.5
3.0 [3]	2.4
4.5 [3]	3.9

1Szpak and Venkatasetty, 1984
2Kortüm and Bockris, 1951
3 Szpak and Venkatasetty, 1984

The more conductive $LiAlCl_4$ solution has activation energies higher than that of the $AlCl_3$ solution, and similar to that of an aqueous system. Furthermore, the activation energy for the $LiAlCl_4$ system is observed to increase with increasing salt concentration.

As both experimental and literature data yield the

E_{ac} decreasing with increasing concentration, this trend must be explained. An increase in E_{ac} with concentration could be a result of strong ion - ion and ion - solvent interactions leading to the formation of complex aggregates. A decrease in E_{ac} with increasing concentration can then be the result of a breakdown of large complexes which interfere with the solution conductance. As concentration increases, the degree of association also increases, thus there are fewer ionic species present and more non - ionic species. In this case the ionic mobility increases and E_{ac} decreases. In the electrolyte simulating a partially discharged cell, containing S, SO_2, and $LiAlCl_4$, the E_{ac} increases with concentration. This electrolyte behaves more as a strong electrolyte than does our experimental system. As a result, E_{ac} increases with increasing salt concentration, corresponding to an increase in the number of ions present in solution, and a decrease in mobility.

The product of molar conductivity and viscosity has been found to be independent of temperature for some electrolyte solutions.

$$\Lambda\eta = CONSTANT \qquad (5.12)$$

This relationship is known as Walden's rule (Walden, 1906) and is based on the assumptions that the conductive ion is spherical, and the effective ionic radius is constant (Stokes law, Kortüm and Bockris, p134-137, 1951).

Often, however, Walden's rule is not obeyed and the

product of molar conductivity and viscosity decreases as temperature increases. In systems where energy of activation for viscosity is greater than for conductivity, there exists a relationship (Szpak and Venkatasetty, 1984),

$$\Lambda^{n_w}\eta = A_{\Lambda\eta} \qquad (5.13)$$

where,

$A_{\Lambda\eta}$ is a constant
n_w is a constant

Plotting $\ln\eta$ vs $\ln\Lambda$ can be a useful way to determine n_w, as rearranging Equation (5.13) gives:

$$\ln\eta = -n_w \ln\Lambda + \ln(A_{\Lambda\eta}) \qquad (5.14)$$

The value of n_w, which is always greater than one, gives an indication of the validity of Walden's rule.

Viscosity and molar conductivity were determined as a function of temperature from Tables 5.10 and 5.13, for -35, -20, -10, 0, 10, 20°C. $\ln\eta$ was plotted as a function of $\ln\Lambda$ in Figure 5.16. Table 5.15 shows values of $-n_w$ and $\ln(A_{\Lambda\eta})$, as well as fitting parameters obtained for these fits.

It is also interesting to study the product of $\Lambda\eta$. At the lowest concentration considered this product decreases from 139$Scm^2cP/mole$ at -35°C to 125$Scm^2cP/mole$ at 20°C,

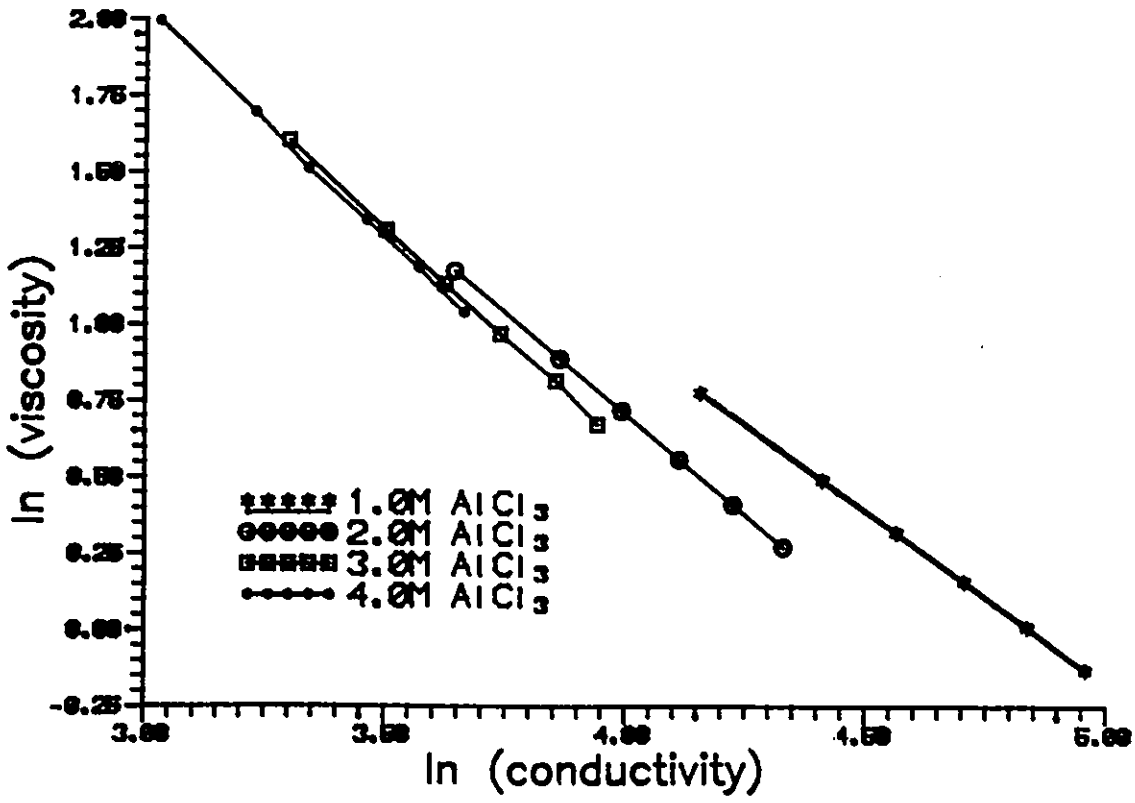

Figure 5.16: Natural logarithm of viscosity plotted as a function of the natural logarithm of molar conductivity for 1.0 to 4.5 M $AlCl_3$ in $SOCl_2$. First order polynomials shown as solid lines.

Table 5.15: Constants and fitting parameters for $\ln\eta$ expressed as a first order polynomial of $\ln\Lambda$.

Concentration $AlCl_3/SOCl_2$	$\ln(A_{\Lambda\eta})$ (±0.002)	$-n_w$ (±0.001)	Err^2	R_2
1.0M	5.473	-1.130	2.55E-8	1.0
2.0	5.999	-1.323	8.30E-8	1.0
3.0	6.363	-1.442	8.80E-5	0.9997
4.0	6.546	-1.502	1.08E-5	0.9999
4.5	6.701	-1.548	8.51E-9	1.0

a decrease of 10%; and at 4.5M, the product decreases from 164 cP mS/cm^3 to 116 cP mS/cm^3, a decrease of 35%. At all concentrations considered, the rate of decrease of viscosity with increasing temperature is greater than the rate of increase of conductivity. This is an indication that viscous flow is governed by large molecular species, and that conductivity is governed by the smaller ionic species.

The results in Table 5.15 indicate that even at the lowest concentration (1.0M), Walden's rule is invalid, indicating the possible presence of a solvation sheath surrounding the ions in solution. As the concentration of the solute increases, the value of n_w increases from (1.130 to 1.548) ± 0.001. Thus, the solution that most closely approximates the conditions of Walden's rule occurs at low concentration of $AlCl_3$, where n_w is closest to one. As the concentration increases, the value of n_w increases, and deviation from Walden conditions increases. There is evidence, therefore, that the effective ionic radius

is not constant, that either the distribution of species in solution changes, that the degree of association is concentration dependent, and different ions act as the charge carriers, or that the solvation sheath changes.

5.3.2 Wishaw - Stokes Analysis

As an extension of Onsager theory Wishaw and Stokes (1954) developed an equation to describe the conductivity of concentrated electrolyte solutions.

$$\Lambda=\left(\Lambda_o-\frac{B_2\sqrt{C}}{1+B\mathring{a}\sqrt{C}}\right)\left(1-\frac{B_1\sqrt{C}}{1+B\mathring{a}\sqrt{C}}F\right)\frac{\eta_o}{\eta} \qquad (2.22)$$

where the first term in Equation (2.22) is attributed to the electrophoretic effect, and the second term to the relaxation effect. The experimental results were plotted as $\Lambda(\eta/\eta_o)$ as a function of $\sqrt{c}$ in Figure 5.17, for each of 25, 10, 0 and -33.9°C.

$$\Lambda\frac{\eta}{\eta_o}=A_{WS}-\frac{B_{WS}\sqrt{C}}{1+C_{WS}\sqrt{C}}+\frac{D_{WS}(\sqrt{C})^2}{(1+C_{WS}\sqrt{C})^2} \qquad (5.15)$$

where,

$A_{WS} = \Lambda_o$ (the limiting conductivity) (5.16)
$B_{WS} = B_2 + B_1F\Lambda_o$
$C_{WS} = B\mathring{a}$
$D_{WS} = B_1B_2F$

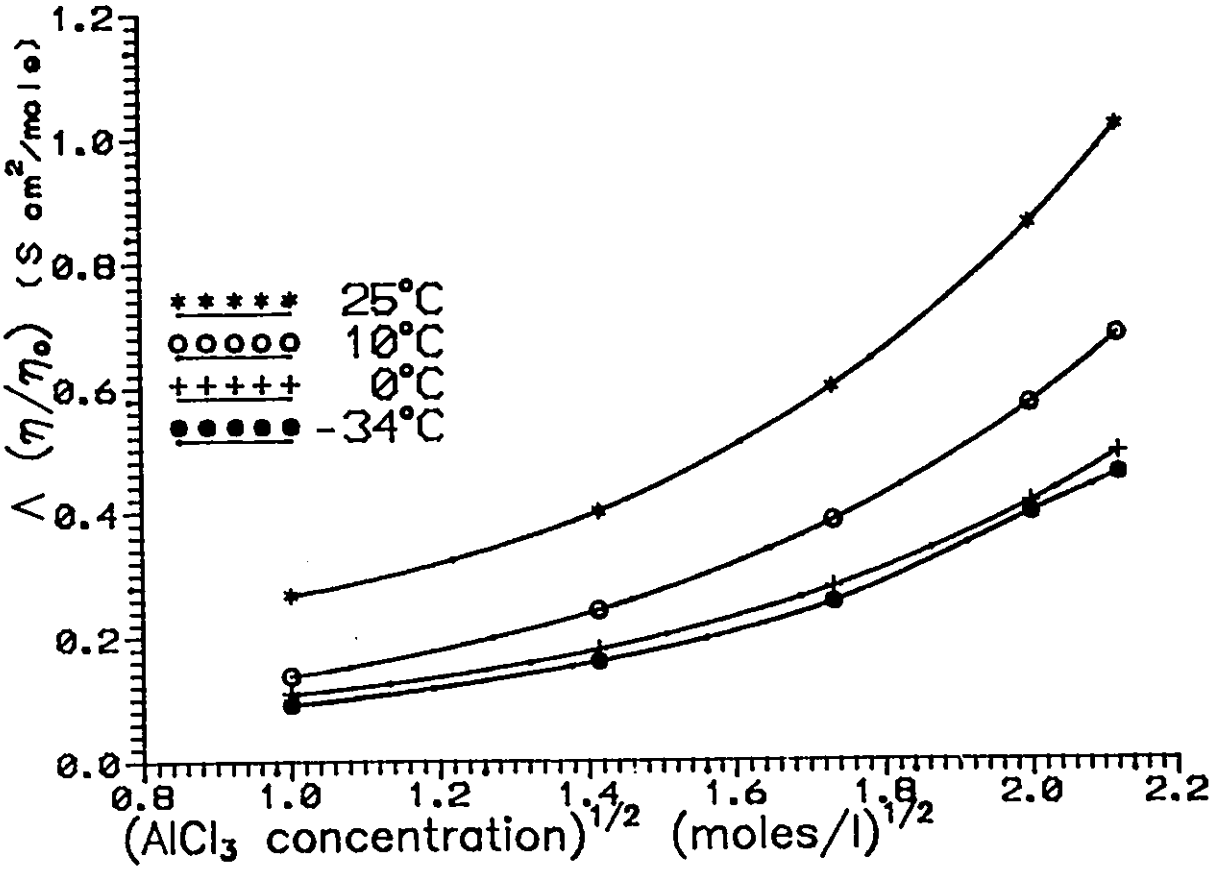

Figure 5.17: Wishaw - Stokes plot of $\Lambda(\eta/\eta_o)$ as a function of $\sqrt{c}$ for solutions of $AlCl_3$ in $SOCl_2$.

The data was then fit to an equation of the form shown in Equation (5.15). Estimates of (A_{WS},B_{WS},C_{WS},D_{WS}) were input to the Gauss-Newton fitting routine based on estimates from Equation (2.21) (in methodology section) and Equation (5.16). The best-fit parameters are reported in Table 5.16. The limiting or infinite dilution value of conductivity is seen to increase with increasing temperature, similar to the trend observed in molar conductivity. The constants A_{WS}, B_{WS}, C_{WS}, and D_{WS} were then used to calculate the Wishaw-Stokes constants B_2, B_1, and Bå. A negative value of Bå was obtained for all temperatures, Bå became increasingly negative as the temperature decreased. The value of Bå should, based on the theoretical derivation, be a positive number, therefore indicating that the model is not valid for these solutions. Furthermore, the values determined for B_1F, and B_2 are complex, and therefore, do not have physical significance. The value of Λ_o, the molar conductivity at infinite dilution, parameter A_{WS} in this analysis, is also and indication of the failure of the Wishaw - Stokes model to adequately describe this system. Λ_o calculated from the Wishaw - Stokes equation ranges from (0.51 to 0.16) ± 0.01 S cm^2/mole. This value is much too low, the molar conductivity at 5 x 10^{-4} moles/l and 25°C is 4.1 S cm^2/mole (Salomon, 1981). The value at infinite dilution should be greater than this value.

The Wishaw-Stokes equation applies best to solutions with a low viscosity ratio (η/η_o) and is generally applied to aqueous solutions of dissociated electrolytes. The viscosity

Table 5.16: Best-fit parameters and coefficients obtained for Wishaw - Stokes analysis of the conductivity and viscosity of $AlCl_3$ in $SOCl_2$

Temperature (°C)	A_{WS} ±0.01	B_{WS} ±0.01	C_{WS} ±0.01	D_{WS} ±0.01	Err^2	R^2
25.0	0.51	0.58	-0.05	0.33	3.05E-4	0.999
10.0	0.26	0.32	-0.07	0.19	8.05E-5	0.999
0.0	0.18	0.19	-0.10	0.11	2.60E-5	0.999
-33.9	0.16	0.19	-0.09	0.12	9.43E-3	0.998

ratio considered for the thionyl chloride solutions varied from approximately 1 at 1M $AlCl_3$ for all temperatures considered, to approximately 5 at 4.5M $AlCl_3$. The relatively large value of the viscosity ratio indicates that the calculation of the electrophoretic effect ($B_2 = 82.5/\eta_o(\varepsilon T)^{1/2}$) based on the solvent viscosity is not valid. Furthermore, the direct correlation of conductivity to salt concentration is also not valid, as it assumes complete dissociation of the solute. That the model does not result in physically meaningful results, indicates that the solution contains associated species, such as the $AlCl_3$-$SOCl_2$ adduct. It also indicates that the degree of dissociation is quite small. A crude indication of the degree of dissociation is found from classical ionic theory of Arrhenius. Arrhenius proposed that the degree of dissociation, α, may be predicted by the formula shown in Equation (5.17).

$$\alpha = \frac{\Lambda}{\Lambda_o} \qquad (5.17)$$

where,

α is the degree of dissociation
Λ is the molar conductivity
Λ_o is the limiting molar conductivity

The experimental data, and the value of the limiting conductivity determined from the Wishaw-Stokes equation were used to calculate the degree of dissociation. The results are presented in Table 5.17 for 1.0 and 4.5M solutions. The values for α reported in this table are high, the actual degree of dissociation is much lower. This is due to the uncertainty in Λ_o which could be much larger than our estimate (eg. by comparison, the limiting molar conductivity was estimated in this work to be 0.5 to 0.1 S cm^2/mole, but the low concentration value available in the literature was 4 Scm^2/mole (Salomon, 1981)).

Table 5.17: Degree of dissociation, α, as a function of temperature, for $AlCl_3$ in $SOCl_2$ at 1.0 and 4.5 M $AlCl_3$ using data obtained from the Wishaw - Stokes analysis.

Temperature	1.0M $AlCl_3$	4.5M $AlCl_3$
25 °C	0.32 ± 0.01	0.31 ± 0.01
10	0.42	0.54
0	0.47	0.55
-33.9	0.46	0.58

The Arrhenius expression is strictly valid for systems in which the activity coefficient is unity, and assumes that at a given temperature the ionic mobilities are constant and independent of concentration of salt. The above results are not, therefore, quantitatively valid, they do indicate, however, that the solute is only partially dissociated, and that the Wishaw-Stokes equation is not valid.

The modified Wishaw-Stokes equation calculates the electrophoretic effect based on the solution viscosity (not the solvent viscosity). The modified equation was also developed for dissociated electrolytes and its application to this problem is limited. Furthermore, the parameters, B_1 and B_2 appear in Onsager's limiting law, and å, the ionic radius, is derived from the Debye Hückel theory. Both of these theories are based upon the continuum model - the solute molecules are suspended in a continuum of solvent molecules. Therefore, these theories are not applicable to this complex, highly associated, concentrated electrolyte.

5.4 Solution Composition

Thionyl chloride forms dimers and higher order oligomers in the anhydrous state. The higher order species generally form at low temperatures. As indicated by the low conductivity, (10^{-9} Scm^{-1}), thionyl chloride exists predominantly as a molecular species, with low self-ionisation. In the bulk solution, a series of complex equilibria exist (Mosier-Boss, Szpak, Smith, Nowak, 1989).

$$(SOCl_2)_n \rightleftharpoons (SOCl_2)_{n-1}, \quad n=2,3,4... \tag{5.18}$$

Studies have indicated that self-ionisation is very low (Spandau and Brunneck, 1952; 1955). The self-ionisation reaction is shown below,

$$SOCl_2 \rightleftharpoons SOCl^+ + Cl^- \qquad k = 10^{-4} \tag{5.19}$$

Thus, neat $SOCl_2$, is a complex mixture of $SOCl_2$, $(SOCl_2)_n$, $SOCl^+$, and Cl^-. Complex self-ionisation equilibria exist for the molecular species, which tend to favour the neutral species rather than the ionic species. The addition of $AlCl_3$ further complicates the equilibria present in $SOCl_2$. In excess $SOCl_2$, the 1:1 molecular adduct forms (Szpak and Venkatasetty, 1984; Mosier-Boss, Szpak, Smith and Nowak, 1989).

$$SOCl_2 + AlCl_3 \rightleftharpoons Cl_3Al(\leftarrow OSCl_2) \tag{5.20}$$

At high $AlCl_3$ concentrations the 1:2 molecular adduct has been identified (Szpak and Venkatasetty, 1984).

$$SOCl_2 + 2AlCl_3 \rightarrow (2Cl_3Al)(-OSCl_2) \qquad (5.21)$$

and

$$Cl_3Al(-OSCl_2) + AlCl_3 \rightarrow (2Cl_3Al)(-OSCl_2) \qquad (5.22)$$

The 1:2 molecular adduct is believed to exist as the 1:1 molecular adduct, with a second $AlCl_3$ molecule loosely bonded to the structure. Higher order species are likely present at very high $AlCl_3$ concentrations, but are not the predominant species.

$$\begin{aligned} mAlCl_3 + SOCl_2 &\rightleftharpoons SOCl_2 \cdot mAlCl_3 \\ SOCl_2 \cdot (m-1)AlCl_3 + AlCl_3 &\rightleftharpoons SOCl_2 \cdot mAlCl_3 \end{aligned} \qquad (5.23)$$

Salomon suggested that the charge carrying species resulted from the dissociation of the 1:1 molecular adduct (Salomon, 1981).

$$Cl_3Al(-OSCl_2) \rightleftharpoons AlCl_4^- + SOCl^+ \qquad (1.4)$$

Long and Bailey (1963) had calculated the equilibrium constant for Equation (1.4) in excess $SOCl_2$ to be 10^{-4}, the same order of magnitude as the equilibrium constant for the self-dissociation of $SOCl_2$. Salomon found that this mechanism did not adequately

describe the measured conductivity, and suggested that higher order species contributed to the conductivity, even at very low solute concentration. The low value of the dissociation constant for the 1:1 molecular species indicates that it is not sufficient to account for the increase in conductivity.

In the presence of excess Cl^- ion, (ie. from self-dissociation of $AlCl_3$), Szpak and Venkatasetty (1984) proposed that the 1:1 molecular ion formed $AlCl_4^-$ and $SOCl_2$:

$$Cl_3Al(\leftarrow OSCl_2) + Cl^- \rightleftharpoons AlCl_4^- + SOCl_2 \qquad (5.24)$$

As the concentration of $AlCl_3$ increases, the acidity of the solution increases and higher molecular and ionic species form ($Al_2Cl_7^-$, $Al_3Cl_{10}^-$, $mCl_3Al(\leftarrow OSCl_2)$). Spectroscopic evidence of $AlCl_4^-$ has been reported (Mosier-Boss, Boss, Gabriel,Szpak, Smith, and Nowak, 1989). To date, physical evidence of the $SOCl^+$ ionic species has not been presented.

As stated previously, at high $AlCl_3$ concentration, the 1:2 and higher order molecular species become more important. A series of complex equilibria exist. For example:

$$2Cl_3Al(\leftarrow OSCl_2) \rightleftharpoons Cl_2SO{\rightarrow}(AlCl_3)_2 + SOCl_2 \qquad (5.25)$$

$$2Cl_3Al(\leftarrow OSCl_2) \rightleftharpoons Cl_7Al_2^- + SOCl^+ \qquad (5.26)$$

$$3Cl_3Al(\leftarrow OSCl_2) \rightleftharpoons Cl_{10}Al_3^- + SOCl^+ \qquad (5.27)$$

Other researchers have noted the appearance of new Raman spectroscopic bands between 2 and 3M $AlCl_3$ in $SOCl_2$, and increase in conductivity in this region (Mosier-Boss, Szpak, Smith and Nowak, 1989; 1989). They have attributed both of these phenomena to the formation of a large molecular ion:

$$2\,[Cl_2Al(\text{-}OSCl_2)] \rightleftharpoons [Cl_2Al(\text{-}OSCl_2)_2]^+ + AlCl_4^- \qquad (5.28)$$

The above internal exchange reaction occurs in the presence of excess $SOCl_2$. At low $AlCl_3$ concentration the extent of this reaction is limited by the low dielectric constant of the solvent. The dielectric constant is proportional to capacitance; preliminary studies indicate that there is no increase in capacitance, and therefore, in the dielectric constant, as the $AlCl_3$ concentration increases. The assumption that the dielectric constant is uniform for all solutions studied, is valid. At high $AlCl_3$ concentration (>2.0M) the extent of this reaction is dominated by the "donor" properties of $SOCl_2$ (Mosier-Boss, Szpak, Smith and Nowak, 1989). $SOCl_2$ is a very weak donor, so that the extent of the above reaction is very small, even at high $AlCl_3$ concentration. Although the proposed $[Cl_2Al(\text{-}OSCl_2)_2]^+$ species gains dominance at high $AlCl_3$ concentration it is present over the full $AlCl_3$ concentration range, 1 to 5 M $AlCl_3/SOCl_2$ as observed by Raman spectroscopy in this study and by others (Mosier-Boss, Boss, Gabriel, Szpak, Smith and Nowak, 1989). Furthermore, our results indicate a gradual rise in conductivity with increasing solute

concentration, and do not indicate a rapid increase between 2 and 3 M as suggested by others (Mosier-Boss, Boss, Gabriel, Szpak, Smith, and Nowak, 1989). Raman spectroscopy performed at the University of Ottawa, indicates that at 20°C the species distribution in solution changes gradually over the concentration range 2 to 30 weight percent $AlCl_3$ (Hill, 1990).

Table 5.18 presents a list of the possible conductive species as described in the above discussion. Molecular weight and estimated ionic radii are included. The estimates assume that the ions are spherical, with the radii being the maximum atomic separation (ionic diameter) divided by 2. Structures and atomic separations proposed by Mosier-Boss, Szpak, Smith and Nowak (1989) were used. Furthermore, the solvation sheath was not included in this analysis.

The conductivity, even at low $AlCl_3$ concentration, is considerably greater than that of pure $SOCl_2$. In pure $SOCl_2$, the conductive species result from self-ionisation of $SOCl_2$ as shown in Equation (5.19). In dilute $AlCl_3$ solutions, the conductive species result from a number of equilibrium reactions occurring in solution. The mechanism of Equation (1.4) is not sufficient to account for the conductivity of the solutions, the equilibrium constant of this reaction is 10^{-4}, the same order of magnitude as self-dissociation of $SOCl_2$. As a result, it is likely that the conductivity associated with these ions will be considerably lower than that measured. It is very likely that the ionic species in Equation (5.24)

Table 5.18: Possible conductive species in $AlCl_3/SOCl_2$ solutions.

Conductive Species	Molecular Weight (g/mole)	Ionic Radius (Å)
$SOCl^+$	83.4	1.8
Cl^-	35.5	1.5
$AlCl_4^-$	168.9	3.0
$Al_2Cl_7^-$	302.1	4.0
$Al_3Cl_{10}^-$	435.4	6.0
$[Cl_2Al(-OSCl_2)_2]^+$	335.7	4.5
$SOCl_2 \cdot SOCl^+$	202.4	3.5
$(SOCl_2)_2 \cdot SOCl^+$	321.4	5.5
$(SOCl_2)_3 \cdot SOCl^+$	440.4	7.5

contribute significantly to the conductivity of the solution - the $AlCl_4^-$ ion has been identified in solution.

The presence of molecular adducts further complicates the character of the solutions as outlined in Equations (5.20), (5.21), (5.22), and (5.23). Furthermore, these adducts exist in complex equilibria relationships with a number of ionic species. In general, the larger ion species, such as $Cl_7Al_2^-$, $Cl_{10}Al_3^-$, will have lower mobility than the smaller ions, such as $SOCl^+$. As a result, it is likely that the contribution to conductivity of the very large ions is minimal.

6.0 Conclusions

1) Theories based upon the continuum solvent model (eg. Jones - Dole and Wishaw - Stokes) provide little insight into the solution structure of this system as they are not valid at the high concentrations used in this study. Negative values of the Jones - Dole A_{JD} parameter were obtained, as were imaginary values for the Wishaw - Stokes, B_1 and B_2 parameters. These results are not physically meaningful and indicate that the theory is invalid under high concentration conditions.

2) The models based on the "hole theory" of liquids describe this system better than do the continuum theory models. Viscosity analysis based on this model identified both pure $SOCl_2$ and $AlCl_3$ solutions as molecular liquids. The analysis indicated that the addition of $AlCl_3$ resulted in the formation of new ionic and molecular species.

3) Conductivity theory identified the solutions as classic weak electrolytes. The κ vs c, and Λ vs $\sqrt{c}$ plots are examples of weak electrolyte plots.

4) Thionyl chloride and aluminum trichloride in thionyl chloride exist predominantly as molecular liquids as indicated by low conductivity, high density and relatively high viscosity, especially for the salt solutions.

5) Thionyl chloride has very low conductivity, the conductive species form upon self-ionisation of $SOCl_2$.

6) Analysis of the viscosity data using the modified

Jones - Dole method, indicated that on addition of $AlCl_3$ to pure $SOCl_2$, one of the two $SOCl_2$ molecules in the dimerized species was replaced with an $AlCl_3$ molecule. Specifically, the relatively constant value of B_{JD}, the Jones - Dole ion - solvent parameter, is consistent with the presence of the $AlCl_3/SOCl_2$ molecular adduct.

7) Walden's rule does not apply to this system. Deviations from the assumptions of spherical ions, and constant effective radius, increase as the salt concentration increases. Our results indicate that the viscosity is governed by large negatively charged or uncharged species, and that the conductivity is governed by smaller solvated positive species. It is likely that the conductive ion is a function of solution composition, and that the solvation sheath is also not constant with changing composition. A change in the solvation sheath is equivalent to a change in the effective ionic radius.

8) The dissociation of the 1:1 molecular adduct (Equation (1.4)) can not account for the increased conductivity. We propose that the conductivity of the $AlCl_3$ solutions be attributed to many weak dissociative reactions.

9) We propose, based upon our Raman spectra, that $[Cl_2Al(\text{-}OSCl_2)_2]^+$ and $AlCl_4^-$ species exist, and that they contribute to the conductivity, over the full concentration range considered.

10) We interpret our experimental results to indicate that an abrupt change in the species distribution does not occur,

either as a function of $AlCl_3$ concentration or temperature. Thus, mechanistic changes as a result of $AlCl_3/SOCl_2$ interaction are not responsible for low temperature safety problems in $Li/SOCl_2$ cells.

11) The large value obtained for the coefficient of thermal expansivity for all $SOCl_2$ based electrolytes indicates that solvent contraction on cooling could result in uneven consumption of the lithium anode in $Li/SOCl_2$ cells, and therefore lead to battery failure, and/or safety problems.

7.0 Recommendations and Future Research

The $AlCl_3/SOCl_2$ system studied in this thesis is only the first step to understanding the electrolyte characteristics of the $Li/SOCl_2$ battery as a function of temperature and salt concentration. This work provides a basis for further studies that would eventually lead to practical design improvements. A complete analysis of the low temperature - concentration composition surface for $LiAlCl_4$ in $SOCl_2$ is proposed as a topic for future research. Reagent purification, and solution preparation would follow the methods outlined in this thesis. The experimental apparatus and procedures would also remain the same.

The effect of additives, such as PVC, suggested by Blomgren et.al. (1990), on the physical properties of the solution could be considered. Both sulphur and sulphur dioxide could be added to the electrolytes being studied to simulate electrolyte composition of partially discharged cells. Increasing the quantity of SO_2 or S in the electrolyte would simulate an increasingly discharged cell.

Finally, mixed solvents such as $SOCl_2/SO_2Cl_2$, have recently been seen to improve low temperature performance (Abraham and Alamgir, 1987). A complete study of this system, including additives (PVC) and discharge products (S, SO_2) would provide an interesting comparison to the $SOCl_2/LiAlCl_4$ system.

8.0 References

Abraham, K.M., M. Alamgir, "Lithium - Inorganic Electrolyte Cells Exhibiting Improved Low Temperature Performance", JECS, 134, 258, (1987).

Anantaraman, A.V., "Thermodynamics of Solvent Mmixtures I. Density and Viscosity of Binary Mixtures of N-methyl-pyrrolidinone Tetrahydrafuran and Propylene Carbonate-acetonitrile", Can. J. Chem., 64, 46, (1986).

Anantaraman, A.V., Canadian Patent 1,222,286 (1987).

Asyst Software Technologies, Inc. "Asystant, the Scientific Number Cruncher", (1988).

Auborn, J.J., K.W. French, S.I. Lieberman, V.K. Shah, A. Heller, "Lithium Anode Cells Operating at Room Temperature in Inorganic Electrolytic Solutions", JECS, 120, 1613, (1973).

Auborn, J.J., H.V. Venkatasetty, "Chapter 5: Lithium Battery Technology", Sponsored by the Electrochemical Society, John Wiley and Sons, New York, (1984).

Batschinski, A.J., Z. Phys. Chem., 84, 643, (1913).

Bedfer, Y., J. Corset, M.C. Dhamelincourt, F. Wallart, P. Barbier, "Raman Spectroscopic Studies of the Structure of Electrolytes Used in the Li/$SOCl_2$ Battery", J. Power Sources, 9, 267, (1983).

Behl, W.K., J.A. Christopulos, M. Ramirez, S. Gilman, "Lithium Inorganic Electrolyte Cells Utilizing Solvent Reduction", JECS, 120, 1619, (1973).

Berg, R.W., H.A. Hjuler, A.P.L. Søndergaard, N.J. Bjerrum, "Conductivity of Thionyl Chloride - Lithium Tetrachloro-aluminate Solutions", JECS, 136, 323, (1989).

Bittner, H.F., B.J. Carter, S.W. Donley, M.V. Quinzio, "Thermodynamic Measurements on the Li/$SOCl_2$ Couple", J. Power Sources, 26, 441, (1989).

Blomgren, G.E., "Advances in Primary Lithium Liquid Cathode Batteries", J. Power Sources, 25, 51, (1989).

Blomgren, G.E., J.C. Bailey, J.W. Bailey, D.W. Kalisz, "Very High Rate, High Energy Lithium Thionyl Chloride Cells for Coupled Systems", JECS Extended Fall Abstracts, No. 137, 203, (1990).

Brown, G.I., "Introduction to Physical Chemistry, 3rd Edition",

Longman Group Limited, Essex, England, (1984).

Campbell, A.N., E.M. Kartzmark, "The Electrical Conductance of Strong Electrolytes: A test of the Stokes' equation", Can. J. Chem, 33, 887, (1955).

Campbell, A.N., W.G. Paterson, "The Conductance of Aqueous Solutions of Lithium Chlorate at 25.00°C and at 131.8°C", Can. J. Chem., 36, 1004, (1958).

Crudden, J., G.M. Delaney, D. Feakins, P.J. O'Reilly, W.E. Waghorne, K.G. Lawrence, "The Viscosity and Structure of Solutions", J. Chem. Soc., Faraday Trans. I, 82, 2195, (1986).

CRC Handbook of Chemistry and Physics, 64th Edition, (1983-1984).

Della Monica, M., "Conductance Equation for Concentrated Electrolyte Solutions", Electrochimica Acta, 29, 159, (1984).

Desnoyers, J.E., G. Perron, "The Viscosity of Aqueous Solutions of Alkali and Tetra-alkylammonium Halides at 25°C", J. Sol. Chemistry, 1, 199, (1972).

Dey, A.N., S. Schlaikjer, "Proceedings of the 26th Power Sources Symposium", Atalantic City, New Jersey, April, (1984).

Dey, A.N., "Experimental Optimaization of Li/$SOCl_2$ Primary Cells With Respect to the Electrolyte and Cathode Compositions", JECS, 123, 1262, (1976).

Donaldson, G.J., J. Anderson, C. Hayes, T. Patraboy, J. White, Power Sources, 12, 451, (1989).

Frenkel, J., "Kinetic Theory of Liquids", Dover Publications, Inc., New York, (1955).

Friedman, L., W.P. Wetter, "Purification of Thionyl Chloride", J. Chem. Soc.(A) Part I, 36, (1967).

Fuoss, R.M., "Solution of the Conductance Equation", JACS, 57, 48, (1935).

Fuoss, R.m., "Conductance of Dilute Solutions of 1-1 Electrolytes", JACS, 81, 2659, (1959).

Gabano, J.P., French Patent 1,583,804 (1969).

Gabano, J,P., French Patent 2,079,744 (1971).

Gee, N., G.V. Freeman, A.V. Anantaraman, "Comment on The Thermodynamics of Solvent Mixtures. I. Density and Viscosity of Binary Mixtures of N-methylpyrrolinone - tetrahydrafuran and

Propylene Carbonate - acetonitrile, Can. J. Chem., 65, 456, (1987).

Glasstone, S., K.J. Laidlet, H. Eyring, "The Theory of Rate Processes", McGraw Hill Book Co. Inc., New York, (1941).

Hildebrand, J.H., "Motions of Molecules in Liquids: Viscosity and Diffusivity", Science, 174, 490, (1971).

Hildebrand, J.H, "Theories and Facts about Liquids", Faraday Discuss. Chem. Soc., 66, 151, (1978).

Hill, I.R., Personal Communication, (1990).

Hills, A.J., N.A. Hampson, "The Li-$SOCl_2$ Cell - A review", J. Power Sources, 24, 253, (1988).

Hong, C.M., K. Ma, W.Z. Yang, "NMR Spectra of H-Species in $SOCl_2$ Electrolytes (extended abstract)", J. Power Sources, 26, 415, (1989).

Janz, G.J., M.J. Tait, "Application of the Fuoss - Onsager Theory to Conductance Data for Sodium and Potassium Iodide Solutions in Various Solvents", Can. J. Chem., 45, 1101, (1967).

Johnson, C.J., S. Dawson, "Calorimetry of 25Ah Lithium/Thionyl

Chloride Cells", JECS, Extended Fall Abstracts, No 15, 22, (1990).

Kacperska, A., S. Taniewska-Gsinska, A. Bald, A. Szejgis, "Influence of Ionic Association on the B Coefficient of the Jones - Dole Equation for NaI in Water-t-Butyl Alcohol Mixtures at 26ºC", J. Chem. Soc., Faraday Trans. I, 85, 4147, (1989).

Kay, R.L., "An Application of the Fuoss-Onsager Conductance Theory to the Alkali Halides in Several Solvents", JACS, 82, 2099, (1960).

Kortüm, G., J.O'M. Bockris, "Textbook of Electrochemistry, V1", Elesevier Publishing Co, New York, (1951).

Koryta, J., J. Dvořák, "Principles of Electrochemistry", John Wiley and Sons, Toronto, (1987).

Lind, J.E. Jr., J.J. Zwolenik, R.M. Fuoss, "Calibration of Conductance Cells at 25ºC With Aqueous Solutions of Potassium Chloride", JACS, 81, 1557, (1959).

Linden, D., "Handbook of Batteries", McGraw-Hill, New York, (1984).

Long, D.A., R.T. Bailey, "Spectroscopic Studies of Solvent

Systems", Trans. Faraday Soc., 59, 594, (1963).

Moshtev, R.V., P. Zlatilova, "Conductance of LiBr Solutions in Acetonitrile in the Presence of Sulphur Dioxide", Electrochimica Acta, 27, 1107, (1982).

Mosier-Boss, P.A., R.D. Boss, C.J. Gabriel, S. Szpak, J.J. Smith, R.J. Nowak, "Raman and Infrared Spectroscopy of the $AlCl_3$-$SOCl_2$ System", J. Chem. Soc., Faraday Trans. I, 85, 11, (1989).

Mosier-Boss, P.A., S. Szpak, J.J. Smith, R.J. Nowak, "LiCl-$AlCl_3$-$SOCl_2$ System. Structures, Species, and Equilibria", JECS, 136, 1282, (1989).

Mosier-Boss, P.A., S. Szpak, J.J. Smith, R.J. Nowak, "Electroreduction of $SOCl_2$, 1.$AlCl_3$-$SOCl_2$ System on Pt Electrode", JECS, 136, 2455, (1989).

MSDS1, $SOCl_2$, Sigma-Aldrich Corporation, Milwaukee, Wi, (1990).

MSDS2, $AlCl_3$, BDH Chemicals Canada, Limited, Toronto, (1990).

Owens, B., "Batteries for Implantable Biomedical Devices", Plenum Press, New York, (1986).

Perry, R.H., D. Green, "Perry's Chemical Engineers' Handbook, 6th Edition", McGraw-Hill Book Co., New York, (1984).

Robinson, R.A., R.H. Stokes, "Electrolyte Solutions", Butterworths, London, (1965).

Salomon, M., "Conductivities in Thionyl Chloride", JECS, 128, 233, (1981).

Salomon, M., E.J. Plichta, "Conductivities of 1:1 Electrolytes in Mixed Aprotic Solvents - II.Dimethoxyethane Mixtures with Propylene Carbonate and 4-butyrolactone", Electrochimica Acta, 30, 113, (1985).

Sibbald, A.M., V.S. Donepudi, I.R. Hill, W.A. Adams, G.J. Donaldson, "Microcalorimetric Studies on Lithium-Thionyl Chloride Cells: Temperature Effects Between 25ºC and -40ºC", Submitted to J. App. Electrochem., (1990).

Spandau, H., E. Brunneck, Z. Anorg. Chem., 270, 201, (1952).

Spandau, H., E. Brunneck, Z. Anorg. Chem, 278, 17, (1955).

Stokes, R.H., R. Mills, "The International Encyclopedia of Physical Chemistry and Chemical Physics: Viscosity of Electrolytes and Related Properties", Pergamon Press, New York,

(1965).

Subbarao, S., F. Deligiannis, D.H. Shen, G. Halpert, "Low Temperature Testing of Li-$SOCl_2$ Cells", J. Power Sources, 26, 211, (1989).

Szpak, S., H.V. Venkatasetty, "Transport Properties of Aluminum Chloride - Thionyl Chloride - Based Electrolytes", JECS, 131, 961, (1984).

Vallin, D., M. Broussely, "Safety Test Results of Lithium Thionyl Chloride Wound Type Cells", J. Power Sources, 26, 201, (1989).

Venkatasetty, H.V., D.J. Saathoff, "Properties of $LiAlCl_4$-$SOCl_2$ Solutions for Li/$SOCl_2$ Battery", JECS, 128, 773, (1981).

Venkatasetty, H.V., S. Szpak, "Properties of $SOCl_2$ - Based Electrolytes. 1.Conductivity, Viscosity and Density", J. Chem. Eng. Data, 28, 47, (1983).

Wishaw, B.F., R.H. Stokes, "Diffusion Coefficients and Conductances of Electrolyte Solutions", JACS, 76, 2065, (1954).

Walden, P., Z. Physik Chem., 55, 207, (1906).

Appendix A

Theoretical Energy Density

1. The total mass of the battery includes active material only, lithium and thionyl chloride.
2. Two moles of lithium reacts with one mole of thionyl chloride, and 2 moles of electrons are transferred.
3. The mass associated with one mole of lithium is 6.9g, of two moles of lithium, 13.8g, and the mass associated with one mole of thionyl chloride is 119.0g. The total mass is 132.8g.
4. The amp-hour capacity associated with this amount of reactants is:

charge of two electrons x Avogadro's number

= $2 \times 1.6 \times 10^{-19}$ C/electron x 6.022×10^{23} electrons/mole

= 1.9×10^{5} C/mole

= 1.9×10^{5} A s x 1h/3600s

= 53.5 Ah

5. The theoretical energy density is:

(amp-hour capacity x voltage)/mass

= 53.5 Ah x 3.66V/.1328 kg

= 1475 Wh/kg

6. The theoretical energy density of the Li/thionyl chloride system is 1475 Wh/kg.

Appendix B

Experimental Data

Density data for $AlCl_3$ in $SOCl_2$

T = 10°C		T = 0°C		T =-20°C	
Wt % $AlCl_3$ ±0.02	ρ (g/ml) ±0.0002	Wt % $AlCl_3$ ±0.02	ρ (g/ml) ±0.0001.	Wt % $AlCl_3$ ±0.02	ρ (g/ml) ±0.0002
0.00	1.6645	0.00	1.6703	4.58	1.7293
4.75	1.6802	2.47	1.6830	9.12	1.7513
9.91	1.6887	5.95	1.6916	13.07	1.7550
9.97	1.6922	10.18	1.7027	19.91	1.7797
14.19	1.7023	16.36	1.7155	18.56	1.7692
19.13	1.7161	18.40	1.7224		
19.89	1.7184				
21.40	1.7116				
26.94	1.7320				

Appendix B con't.

Viscosity data for $AlCl_3$ in $SOCl_2$

T =-20°C		T = 0°C		T = 20°C	
Wt % $AlCl_3$ ±0.02	η (cP) ±0.004	Wt % $AlCl_3$ ±0.02	η (cP) ±0.004	Wt % $AlCl_3$ ±0.02	η (cP) ±0.004
0.00	1.299	0.00	0.857	0.00	0.688
6.29	1.560	5.45	1.042	5.45	0.819
11.37	2.112	9.67	1.227	9.67	0.930
15.42	2.187	13.43	1.601	13.43	1.183
15.42	2.225	15.16	1.635	15.16	1.173
16.24	2.471	19.21	2.177	19.21	1.589
19.01	2.937	31.11	4.241	31.11	2.698
19.63	2.838				
28.08	4.536				

Appendix B con't.

Conductivity data for $AlCl_3$ in $SOCl_2$

T = 25°C		T = 10°C	
Wt % $AlCl_3$ (±0.02)	Λ (S cm^{-1}) (±5)	Wt % $AlCl_3$ (±0.02)	Λ (S cm^{-1}) (±5)
3.96	69	0.00	34
8.55	232	4.75	68
20.08	586	9.97	81
23.20	517	14.19	187
		19.13	250
		19.89	263
		26.94	581

T = 0°C		T = -33.9°C	
Wt % $AlCl_3$ (±0.02)	Λ (S cm^{-1}) (±5)	Wt % $AlCl_3$ (±0.02)	Λ (S cm^{-1}) (±5)
0.00	1	2.90	13
2.47	17	4.04	21
5.95	55	7.84	117
10.18	78	12.64	132
16.36	176		
16.36	186		
18.40	264		

Appendix C

Raman Spectra of $AlCl_3$ in $SOCl_2$

Concentration of $AlCl_3$ 5.8 and 26.4%

Raman Spectra: 5.8% w/w AlCl3 in SOCl2

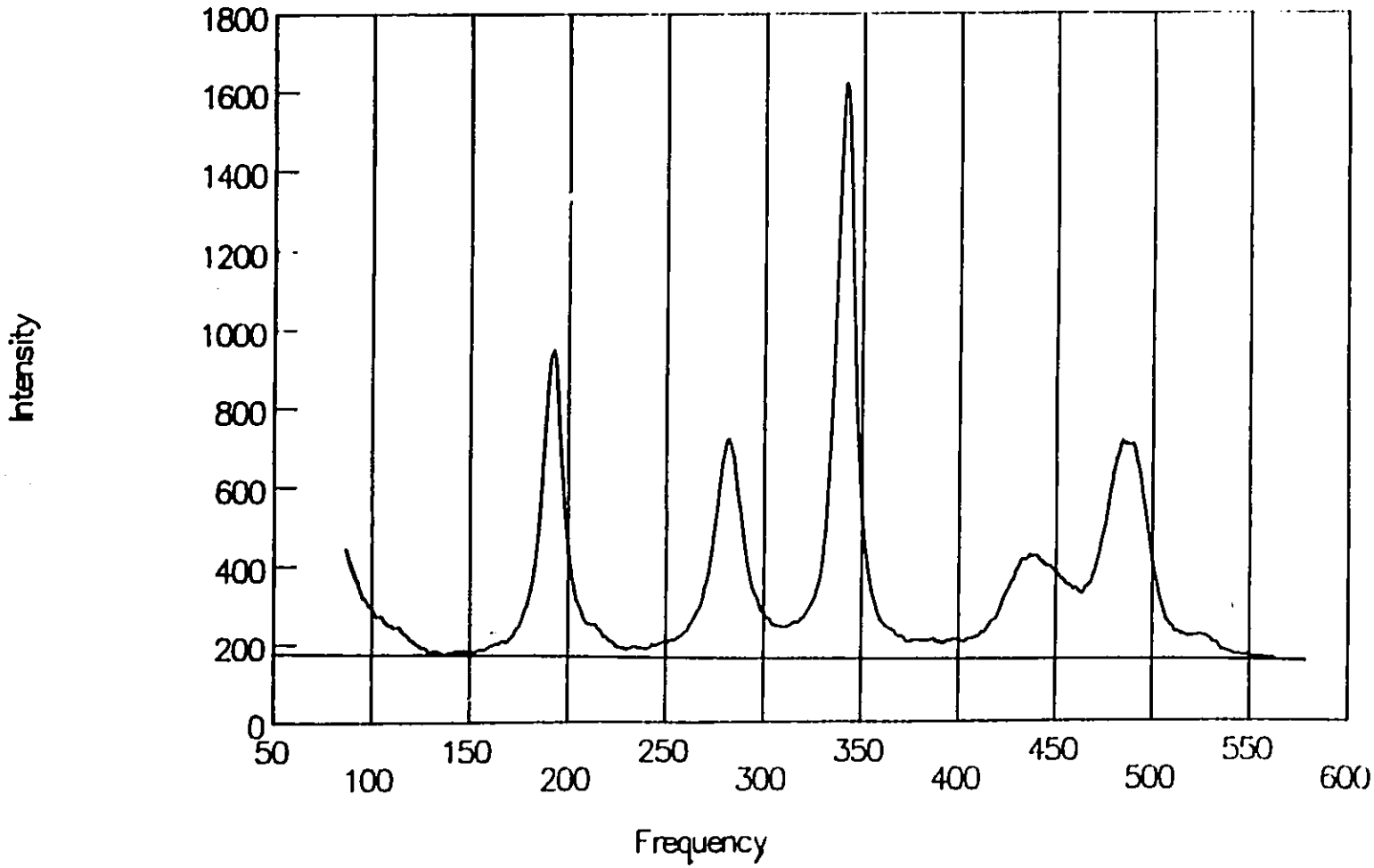

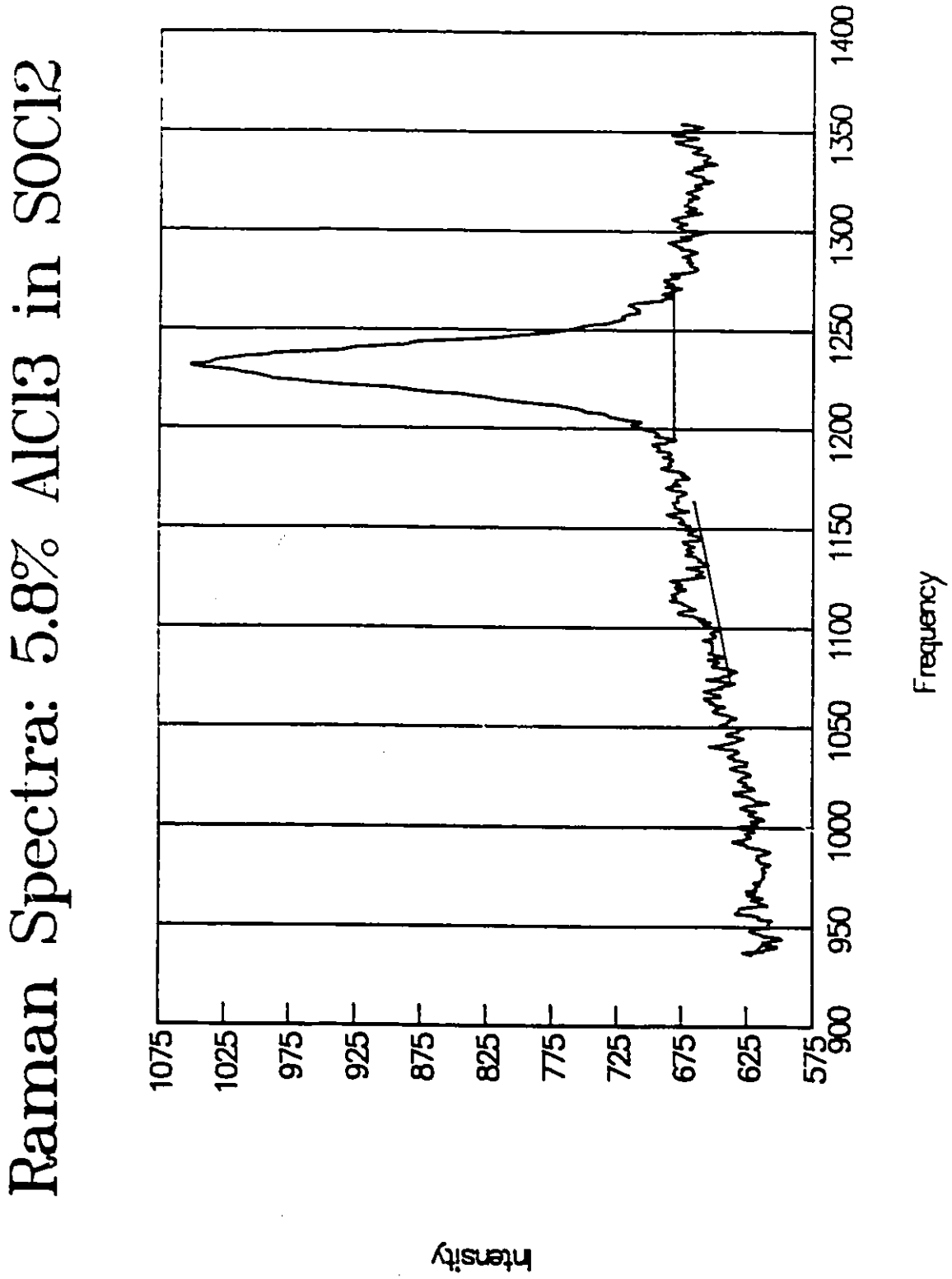
Raman Spectra: 5.8% AlCl3 in SOCl2
Intensity
1075
1025
975
925
875
825
775
725
675
625
575
900
950
1000
1050
1100
1150
1200
1250
1300
1350
1400
Frequency

Raman Spectra: 26.4% AlCl3 in SOCl2

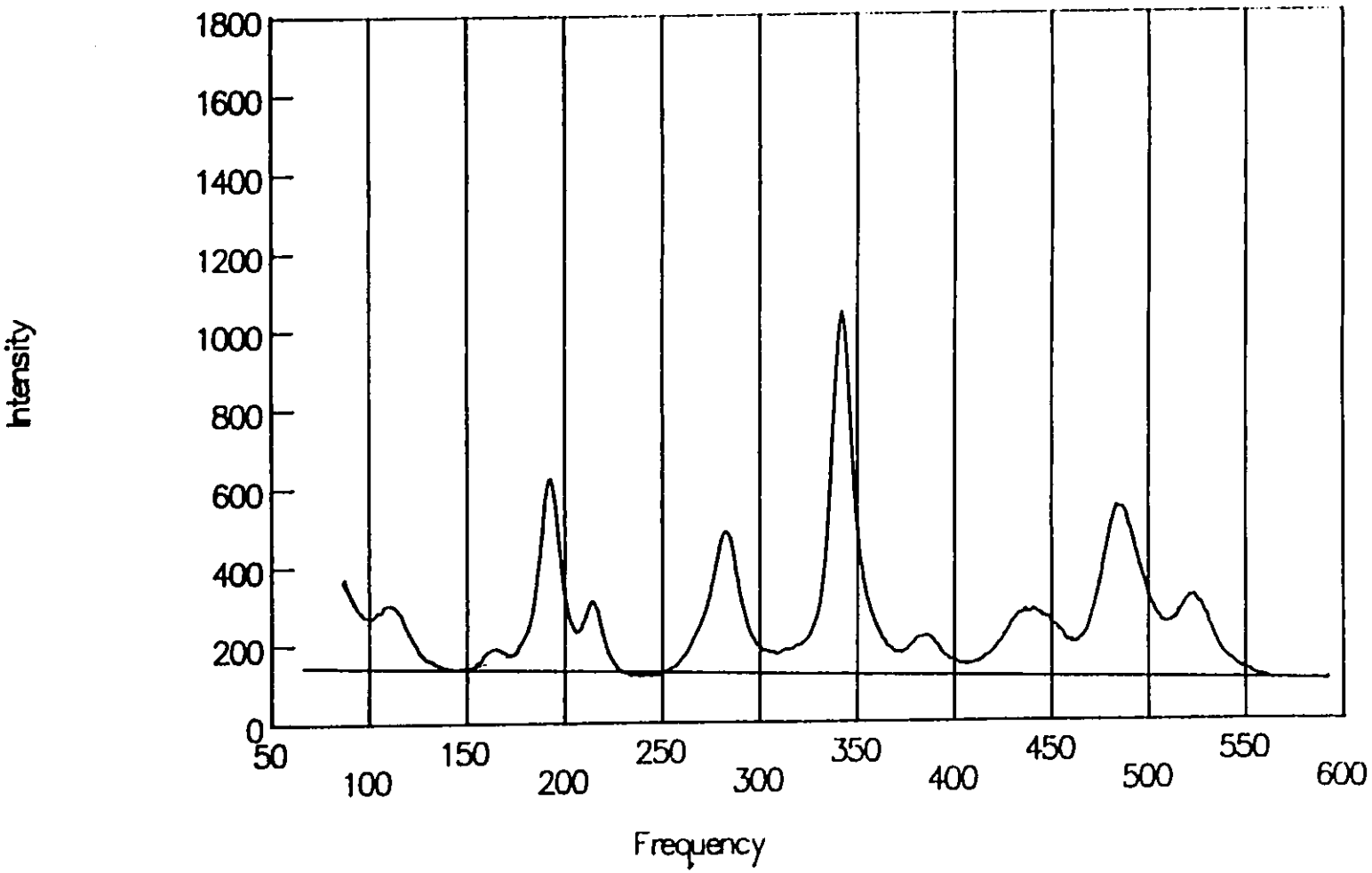

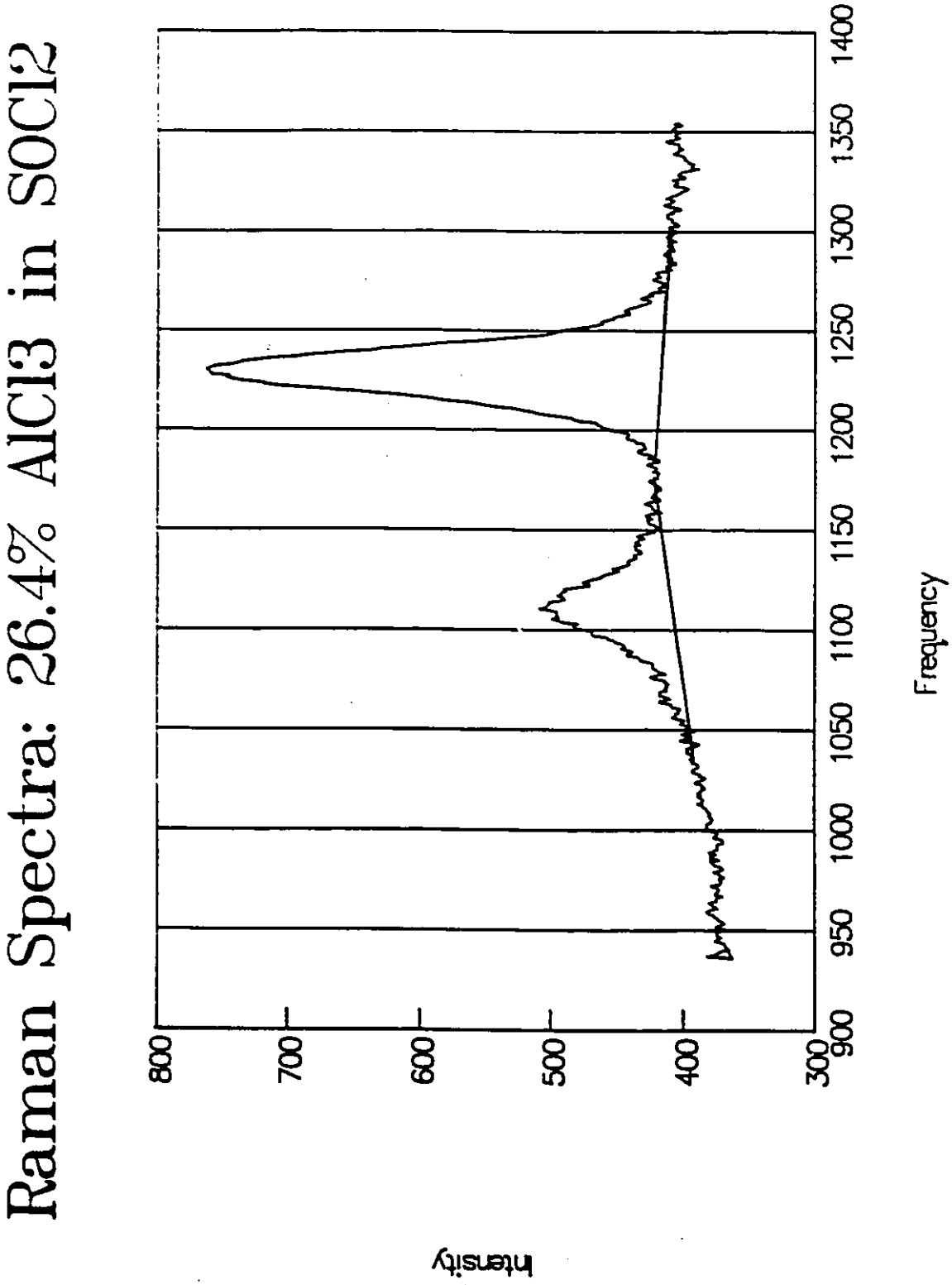
Raman Spectra: 26.4% AlCl3 in SOCl2
Intensity
800
700
600
500
400
300
900
950
1000
1050
1100
1150
1200
1250
1300
1350
1400
Frequency

Appendix D

Glossary of Battery Terminology

Anode: The negative electrode, on discharge, oxidation occurs at this electrode.

Cathode: The positive electrode, on discharge, reduction occurs at this electrode.

Cell Reversal: This is equivalent to the charging configuration, (anode becomes the cathode and cathode becomes the anode). This is be a safety problem for non-rechargeable systems.

Depth of Discharge: Discharge to specified cut-off voltage will represent a certain percentage of the maximum depth of discharge. The maximum depth of discharge is determined by the system chemistry and design.

Electrolyte: Ionically conductive, but electronically neutral material contained in the battery - allows the transfer of ions from the anode to the cathode.

Energy Efficiency: The ratio of energy realized from the system to energy input to the system.

Passivating Film: On storage, a film can develop on one or both electrodes preventing or limiting the discharge of the cell or causing a delay when the external circuit is closed before current can flow through the battery.

Power Density: Amount of power for a given mass or volume of a practical system (W/kg).

Practical Energy Density: Amount of useable energy stored in given volume or weight of a practical battery system (Wh/l or Wh/kg).

Primary Battery: A non-rechargeable battery.

Secondary Battery: A rechargeable battery.

Shelf-life: Period of time in which a battery can be stored and still maintain a specified capacity.

Theoretical Energy Density: Amount of energy stored in a given system when the total mass of the system is occupied by active material (Wh/kg).

Voltaic Efficiency: Ratio of the discharge voltage to the theoretical voltage for the system.

Appendix E

Abstracts of Works Presented While Attending The University of Ottawa, 1988 - 1990.

RAMAN INVESTIGATIONS OF $AlCl_3/SOCl_2$ INTERACTIONS

J.LEDUC, W.PELL, W.A.ADAMS and L.R.HILL
Electrochemical Science and Technology Centre,
University of Ottawa, Ottawa, Ont., K1N 6N5 Canada

The existence of 1:1 and 2:1 adducts of $AlCl_3$ and $SOCl_2$ (thionyl chloride) was proposed about 40 years ago (1,2). Since then, Raman spectroscopy has indicated that the 1:1 adduct is present in the solution, from the number of new bands produced (3); however, the solid that crystalizes from these solutions is $SOCl_2 \cdot 2AlCl_3$ (3) and the Raman spectra of these two species are very similar. One assumes that the 1:1 adduct is present in such solutions but, in the present investigation, we have proven that a 1:1 adduct is formed using relative Raman intensities. The approach is simple but novel.

Raman spectra were obtained from successively more concentrated solutions of $AlCl_3$ in $SOCl_2$. The intensities of the unshifted ("free") bands of $SOCl_2$ were monitored. These intensities were termed the "experimental" intensities. A series of "hypothetical" intensities was then determined. These are intensities that would be expected due to dilution of the $SOCl_2$ by $AlCl_3$, but assuming that no adduct were formed. A plot of "hypothetical" vs "experimental" Raman intensities should yield a straight line of slope=2, for a 1:1 complex, and slope=1 for a 1:2 complex. If a mixture of both complexes were present at higher concentrations then the plot would not be linear.

Results of this work will be presented and further details from spectra obtained at different temperatures will be discussed.

REFERENCES

(1) H.Hecht, Z. Anorg. Chem. 254 (1947) 44.
(2) H.Spandau and E.Brunneck, Z. Anorg. Chem. 270 (1952) 201.
(3) D.A.Long and R.T.Bailey, Trans.Faraday Soc. 59 (1963) 594.

Presented at the XXI International Conference on Solution Chemistry, Ottawa, Ontario, August 5 - 10, 1990.

Zn/Br_2 FLOW BATTERIES - AN EXAMPLE IN A SOLAR/ELECTRIC CAR

W. A. Adams, W. Pell and G. Song
Electrochemical Science and Technology Centre
University of Ottawa

ABSTRACT

Zinc/bromine flow battery technology developed by Johnson Controls for EV applications has been adapted for use in a solar powered racing vehicle for the General Motors Sunrayce USA (July 1990). Charging of the battery is provided from an 8 m^2 photovoltaic panel and from regenerative braking. The useful battery capacity is 5 kWh with stack operating voltage of approximately 72 volts. Electrolyte storage and flow, and stack thermal management were accomplished by a pumping system and heat exchanger optimized to provide the highest overall batery speciric energy and efficiency while maintaining reliable operation under race conditions. Various options considered in the design process and the performance of the vehicle will be presented.

Presented at The Fall Symposium, Canadian Section, The Electrochemical Society, Inc., Ottawa, November, 1990.

Design and Performance of a Photovoltaic Zinc/Bromine Battery Propulsion System for a Solar Powered Electric Racing Vehicle

W. A. Adams*, E. Bernard, A. Fahim**, A. R. Hicks,
D. Ladd, S. Lines, L. Nash, J.C.T. Oliveira, W. Pell and G. Song
University of Ottawa
Ottawa, Ontario, Canada

P. A. Eidler
Johnson Controls, Inc.
Milwaukee, Wisconsin, U.S.A.

ABSTRACT

Zinc/bromine flow battery technology developed by Johnson Controls for EV applications has been adapted for use in a solar powered racing vehicle for the General Motors Sunrayce USA (July 1990). Charging of the battery is provided from an 8 m^2 photovoltaic panel and from regenerative braking. The useful battery capacity is 5 kWh with stack operating voltage of approximately 72 volts. Electrolyte storage and flow, and stack thermal management were accomplished by a pumping system and heat exchanger optimized to provide the highest overall battery specific energy and efficiency while maintaining reliable operation under race conditions. Various options considered in the design process and the performance of the vehicle will be presented.

Presented by Dr. W. Adams at the 10th International Electric Vehicle Symposium, Hong Kong, December, 1990.

Appendix F

Sample Error Calculations

1. Viscosity

The expression relating the experimentally determined parameter (time) to the viscosity of the sample is:

$$\eta = \frac{(Time for sample)}{(Time for methanol)} x \eta_{methanol} x \frac{\rho_{sample}}{\rho_{methanol}}$$

For pure $SOCl_2$ at 0.0°C:

$$\eta = \frac{123.7 \pm 0.3 s}{247.4 \pm 0.3 s} x\ 0.8200 cP\ x\ \frac{1.674 \pm 0.002 g/ml}{0.8010 g/ml}$$

$$\eta = 0.857 \pm (0.24\% + 0.12\% + 0.07\%)$$

$$\eta = 0.857 \pm 0.43\%$$

$$\eta = 0.857 \pm 0.004\ cP$$

2. Error on value obtained from fitted equation

The fitting procedure assumes that the error in the independent variable is zero. For the polynomial equation below:

$$F(x) = A + A_2x + A_3x^2 + \ldots + A_nx^{n-1}$$

the error in F(x) is:

$$d(F(x)) = dA + dA_1x + dA_2x^2 + \ldots + dA_nx^{n-1}$$

Curve fitting program Asystant (TM Asyst, 1989) determines the parameter errors.